

**TOWARDS A UAV BASED STANDALONE SYSTEM  
FOR ESTIMATING AND MAPPING ABOVEGROUND  
BIOMASS/ CARBON STOCK IN BERKELAH  
TROPICAL RAIN FOREST, MALAYSIA**

TIEGSTI HADUSH BERHE

February, 2018

SUPERVISORS:

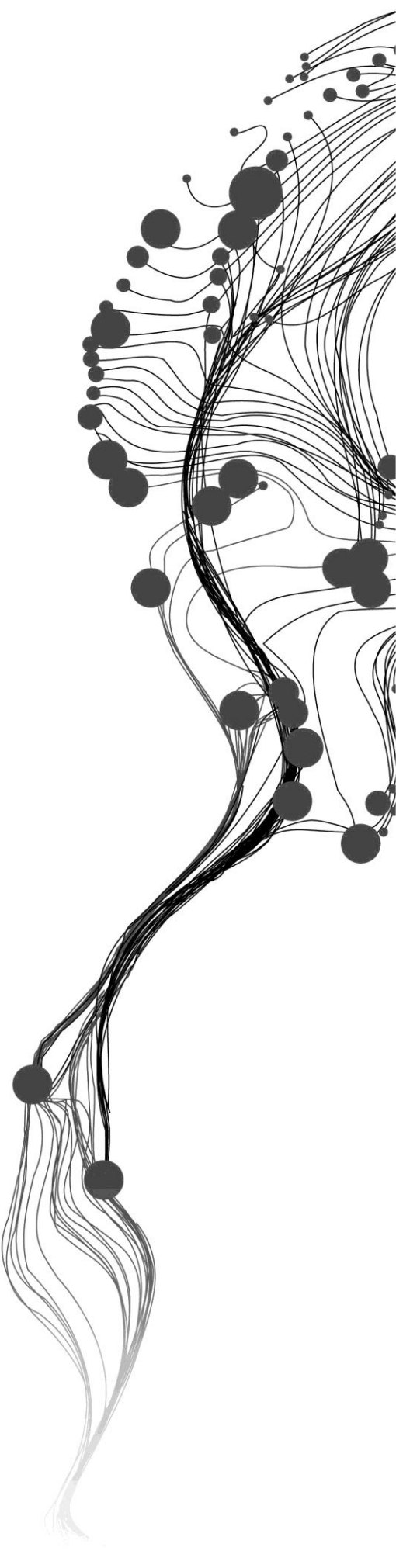
Drs. E. H. Kloosterman

Dr. Y. A. Hussin

ADVISOR:

Dr. Zulkiflee Abd Latif





# **TOWARDS A UAV BASED STANDALONE SYSTEM FOR ESTIMATING AND MAPPING ABOVEGROUND BIOMASS/ CARBON STOCK IN BERKELAH TROPICAL RAIN FOREST, MALAYSIA**

**TIEGSTI HADUSH BERHE**

Enschede, The Netherlands, February, 2018

Thesis submitted to the Faculty of Geo-Information Science and Earth Observation of the University of Twente in partial fulfilment of the requirements for the degree of Master of Science in Geo-information Science and Earth Observation.

Specialization: Natural Resources Management

**SUPERVISORS:**

Drs. E. H. Kloosterman

Dr. Y. A. Hussin

**ADVISOR:**

Dr. Zulkiflee Abd Latif

**THESIS ASSESSMENT BOARD:**

prof.dr. A.D. Nelson (Chair)]

Dr. T. Kauranne (External Examiner, Lappeenranta University of Technology, Finland)

#### DISCLAIMER

This document describes work undertaken as part of a programme of study at the Faculty of Geo-Information Science and Earth Observation of the University of Twente. All views and opinions expressed therein remain the sole responsibility of the author, and do not necessarily represent those of the Faculty.

# ABSTRACT

Forest ecosystem plays a crucial role in climate change reduction through their exceptional nature of carbon sequestration which regulates the global temperature. The tropical rainforest is one of the forest ecosystems which can store and release a vast amount of carbon dioxide depending on the status of forest management. Around 78.14% of sequestered carbon in the tropical rainforest is stored in aboveground biomass. Tropical deforestation and forest degradation contribute about 20%, the highest global carbon dioxide emission next to fossil fuels which contribute to climate change. The UNFCCC was established for GHG emission reduction. Following the convention REDD+ initiative was established aiming to follow up emission reduction activities. MRV of carbon stock is REDD+ mechanism to measure the status of the forest and to monitor the emission balance of REDD+ adopted countries such as Malaysia. Accurate measurement of forest inventory parameters has a relationship with accurate aboveground biomass estimation which is a major concern of REDD+MRV program as it assists computing accurate carbon estimation. However, accurate measurement of these parameters in the multilayered tropical rainforest is challenging due to occlusion.

This study aimed to investigate possibilities for accurately assessing the aboveground biomass/carbon stock of multilayered tropical rainforest canopy structure using UAV imagery. A circularity measured CPA adjustment, and the relationship with DBH as well as the accuracy of tree height extracted from UAV derived CHM achieved reasonable results.

DTM, DSM, and Orthophoto were generated in Agisoft photo scan professional by photogrammetric image processing from UAV high-quality, dense point cloud and CHM was calculated in Arc GIS raster calculator by subtracting DTM from DSM. Orthophoto segmentation and incomplete CPA adjustment after segmentation as well as tree height extraction from UAV derived CHM were performed. DBH was estimated through regression using the adjusted CPA as independent and field DBH as the dependent variable. The estimated DBH achieved  $R^2$  of 80% with power model. Airborne LiDAR-derive height validated the tree height from UAV-CHM, and there was no significant difference between airborne LiDAR and UAV derived CHM) with RMSE of 17% in the study area.

The adjusted CPA as a proxy to DBH and tree height from UAV derived CHM was used to assess AGB/carbon stock. The estimated AGB/carbon stock was validated using t-test, and the result is not significant due to error multiplication during DBH prediction, and UAV derived CHM generation.

Therefore, a UAV-based AGB/carbon stock estimation in vertically multilayered forest canopy structure using generic allometric equation needs integration with other remote sensing tools to achieve REDD+ MRV program. However, incomplete tree crowns adjustment using circularity measure achieved a robust CPA-DBH relationship.

**Keywords:** Tropical rainforest, Climate change, REDD+ MRV, UAV, LiDAR, AGB/Carbon stock

# ACKNOWLEDGEMENTS

First and for most I would like to thank the almighty God who helped me to accomplish this MSc work with his power and love and I glorify his name.

I would like to take this opportunity to thank the Netherlands Government and the Netherlands organization for international cooperation in higher education (NUFFIC) who granted me a scholarship to pursue the MSc degree in The Netherlands.

I am very grateful to express my sincere gratitude and appreciation to my first supervisor Drs. Henk Kloosterman for his continuous encouragement, massive field support, constructive feedback and comments from the beginning till the completion of this research. It was a good opportunity and pleasure to work under his supervision. To my second supervisor, Dr. Yousif Ali Hussin, I am humbled to extend my sincere and deepest thanks for his supervision, productive responses, advice and field work support. Without the guidance of my supervisors', this research would hardly have come to fruition.

My sincere thanks go to Prof. Dr. A.D. Nelson for his constructive comments and suggestions during the proposal and mid-term defense which help me to improve my research method.

I am also glad to express my thanks and appreciations to the entire staff of Faculty of Geo-Information Science and Earth Observation (ITC) from whom I had a privilege of acquiring sustainable Knowledge and skills during my study period.

I would like to acknowledge and express my thanks and appreciations for The University Technology Mara, Malaysia for their help to get airborne LiDAR data and support throughout the fieldwork period. Special thanks to Dr. Zulkiflee Abd Latif, Associate Professor at University Technology Mara Malaysia (UiTM) and Ms. Syaza Rozali, PhD Candidates at University Technology Mara Malaysia (UiTM) for all their support and guidance during fieldwork (logistics, transportation, accessing Berkelah Forest, etc.) when I was in Malaysia.

I would like to extend genuine thanks to my fieldwork mates Solomon Birhanu, Agerie Nega, Edward Justine, Exavery Kigosi, Robert Moselele and Belinda Odia. Many thanks to NRM 2016/18 batch classmates for fruitful time and joyfulness throughout the study period.

Finally, deepest appreciation goes to my lovely mother (Tsadikan Gebremeskel) for her tireless support and prayers to me.

Tiegsti Hadush Berhe  
Enschede, The Netherlands  
February, 2018

# TABLE OF CONTENTS

---

1. INTRODUCTION .....	1
1.1. Background information.....	1
1.2. Statement of the problem and Justification.....	3
1.3. Research Objective, Questions and Hypothesis.....	6
1.3.1. General Objective .....	6
1.3.2. Specific objectives .....	6
1.3.3. Research questions.....	6
1.3.4. Research Hypothesis.....	6
1.4. Theoretical framework of the study .....	7
2. LITERATURE REVIEW .....	8
2.1. Tropical Rainforest Biomass and Carbon.....	8
2.2. Allometric Equation .....	8
2.3. Overview of UAV and Photogrammetry .....	9
2.4. Application of UAV in forestry.....	10
2.5. Advantage and disadvantage of UAV imagery .....	10
2.6. Airborne LiDAR and its Application in forestry.....	11
2.7. Crown projection area.....	12
2.8. Object-based image analysis.....	13
3. MATERIALS AND METHODS.....	14
3.1. Study Area .....	14
3.2. Materials.....	15
3.3. Methods .....	15
3.3.1. Pre-fieldwork .....	17
3.3.2. Sampling Method .....	17
3.3.3. Field Data Collection.....	18
3.3.4. Airborne LiDAR Data Processing .....	19
3.3.5. UAV Image Processing.....	20
3.3.6. CPA manual delineation and circularity measure.....	21
3.3.7. Multiresolution segmentation.....	23
3.3.8. CPA adjustment .....	26
3.3.9. Tree Height extraction from UAV and airborne LiDAR-CHM.....	26
3.3.10. Individual tree Matching.....	27
3.3.11. Data analysis .....	27
3.3.11.1. Comparison of actual and circularity measured CPA .....	27
3.3.11.2. Delineated and circularity measured CPA and DBH relationship.....	28
3.3.11.3. Relationship between DBH and CPA.....	28
3.3.11.4. Comparison of UAV and airborne LiDAR-derived tree height .....	28
3.3.11.5. Aboveground Biomass estimation .....	29
3.3.11.6. Regression and model validation.....	29
3.3.11.7. Comparison of AGB-UAV and AGB-field.....	29
3.3.11.8. Carbon stock mapping.....	30
4. RESULTS.....	31
4.1. DTM, DSM and CHM generation from airborne LiDAR data .....	31

4.2. DSM, DTM , CHM, and orthophoto generation from photogrammetric image processing .....	32
4.3. Multiresolution segmentation.....	33
4.4. segmentation accuracy .....	34
4.5. Descriptive statistics of field data.....	35
4.6. Circularity measured CPA accuracy.....	35
4.7. Relation DBH and manual delineated CPA.....	37
4.8. Relation segmented CPA and DBH .....	39
4.9. Relation adjusted CPA and DBH .....	41
4.10. UAV derived CHM accuracy.....	44
4.11. Comparison of AGB-UAV and AGB-field .....	47
4.12. Carbon stock map .....	49
5. DISCUSSION .....	50
5.1. Distributions of DBH data.....	50
5.2. Accuracy of circularity measured CPA .....	50
5.3. Relationship of delineated and circularity measured CPA and DBH .....	50
5.4. Relationship of adjusted CPA and DBH .....	52
5.5. Accuracy of UAV derived tree height.....	54
5.6. AGB/ Carbon stock accuracy .....	57
5.7. AGB/Carbon stock of the study area .....	58
6. CONCLUSION AND RECOMMENDATION.....	59
6.1. Conclusion.....	59
6.2. Recommendation .....	60
LIST OF REFERENCES .....	61
APPENDICES.....	71



## LIST OF FIGURES

---

Figure 1: The problem and objective trees of the study.....	5
Figure 2: Theoretical framework of the study.....	7
Figure 3: Illustration of tropical rainforest layers. ....	8
Figure 4: major types of UAV .....	9
Figure 5: Illustration of structure from motion .....	10
Figure 6: Illustration of Airborne LiDAR. ....	11
Figure 7: Illustrations of discreet-return and waveform LiDAR devices conceptual differences .....	12
Figure 8: Demonstration of crown projection area .....	13
Figure 9: Study area location map.....	14
Figure 10: Flowchart of the research methods.....	16
Figure 11: 45 cm X 60 cm Marker and plastic tube inserted at centre. ....	17
Figure 12: Sample plot distribution and UAV flight covered blocks.....	18
Figure 13: Flight planning and settings for the DJI Phantom-4 UAV. ....	19
Figure 14: Illustration of the main UAV image processing in Agisoft photo scan pro. ....	21
Figure 15: Illustration of fitting circularity on manually delineated CPA.....	22
Figure 16: Illustration of multi-resolution segmentation process.....	23
Figure 17: Illustration of the watershed transformation principle.....	24
Figure 18: Matching cases of an extracted object .....	25
Figure 19: Illustration of CPA adjustment after segmentation. ....	26
Figure 20: Airborne LiDAR-derived images.....	31
Figure 21: Agisoft UAV image processing results.....	32
Figure 22 : Small part of orthophoto generated from UAV image.....	33
Figure 23: Orthophoto before and after segmentation.....	34
Figure 24: Manually delineated and segmented crowns for accuracy assessment.....	34
Figure 25: Histogram and normal distribution curve of DBH data.....	35
Figure 26: Scatter plot of actual and adjusted CPA (intermediate, inner & outer circles).....	36
Figure 27: Histogram and normal distribution curve of actual CPA, adjusted CPA and DBH.....	38
Figure 28: scatter plot of relationship between delineated CPA (actual CPA), adjusted CPA and field DBH.....	38
Figure 29: Histogram and normal distribution curve of CPA and DBH data.....	40
Figure 30: scatter plot of relationship between segmented CPA and observed DBH.....	41
Figure 31: scatter plot that shows relationship between adjusted CPA and DBH.....	42
Figure 32: scatter plot of predicted and Observed DBH.....	43
Figure 33: scatter plot UAV DM, airborne LiDAR DTM and DGPS altitude.....	45
Figure 34: Scatter plot of UAV and airborne LiDAR CHM.....	46
Figure 35: scatter plot between AGB-UAV and AGB-field.....	48
Figure 36: Carbon stock map of UAV flight block 2 based on UAV imagery.....	49
Figure 37: Graphs showing data skewness position[source.....	50
Figure 38: Relationship between field DBH and CPA.....	51
Figure 39: Scatter plot of a relationship between CPA and DBH in compare to another research result. .	53
Figure 40: Illustration of UAV point cloud andairborne LiDAR point cloud in the forest canopy.....	56
Figure 41: Illustration of open land surface location effect in DTM interpolation.....	57

## LIST OF TABLES

---

Table 1: Field measurement tools and equipment. ....	15
Table 2: Required soft ware. ....	15
Table 3: Segmentation accuracy assessment result. ....	34
Table 4: Descriptive statistics of field DBH. ....	35
Table 5: Descriptive statistics of actual and adjusted CPA (inner, outer and intermediate circles). ....	35
Table 6: Result summary of paired t-test between actual and adjusted CPA (inner, outer and intermediate circles).....	37
Table 7: Descriptive statistics of delineated and adjusted CPA and field DBH. ....	37
Table 8: Result summary of regression analysis between manually delineated CPA and Observed DBH. .	39
Table 9: Descriptive statistics of segmented CPA and field DBH. ....	39
Table 10: Result summary of regression analysis between segmented CPA and Observed DBH. ....	41
Table 11: Descriptive statistics of the adjusted CPA and observed DBH. ....	42
Table 12: Result summary of regression analysis between adjusted CPA and Observed DBH.....	42
Table 13: Summary statistics of data used for validation. ....	43
Table 14: Result summary of two-sample t-test between predicted and observed DBH of power model. .	44
Table 15: Descriptive statistics of UAV-DTM, airborne LiDAR-DTM and ground truth DTM. ....	44
Table 16: Result summary of RMSE of UAV DTM, LiDAR DTM, and altitude from DGPS. ....	45
Table 17: Descriptive statistics of tree heights derived from UAV-CHM and airborne LiDAR-CHM. ....	46
Table 18: Two-sample assuming equal variances t-test for means of tree heights from UAV and airborne LiDAR CHM. ....	47
Table 19: Descriptive statistics of CPA, tree height and DBH data for AGB/carbon stock estimation. ....	47
Table 20: Results summary of UAV-based and field-based AGB .....	48
Table 21: Result summary of two sample t-test assuming equal variance between AGB-UAV and AGB-field. ....	48

## LIST OF EQUATIONS

---

Equation 1: Area of adjusted CPA .....	23
Equation 2: Over segmentation equation model.....	25
Equation 3: Under segmentation equation model .....	25
Equation 4: Measures of goodness .....	25
Equation 5: Equation of RMSE computation .....	27
Equation 6: Equation of %RMSE computation .....	27
Equation 7: Allometric equation model.....	29
Equation 8: Carbon stock estimation.....	29
Equation 9: Regression model.....	43

# LIST OF APPENDICES

---

Appendix 1: Field data collection sheet form.....71  
Appendix 2: Sample calculated adjusted CPA using intermediate circle.....72  
Appendix 3: Correlation between CPA and DBH results.....73  
Appendix 4 : Field photos .....74

## LIST OF ACRONYMS

---

AGB:	Above Ground Biomass
ALS:	Airborne Laser Scanner
ANOVA	Analysis of Variance
Cm	Centimetres
CF:	Carbon Fraction
CHM:	Canopy Height Model
CO <sub>2</sub> :	Carbon Dioxide
CPA:	Canopy Projection Area
DBH:	Diameter at Breast Height
DEM:	Digital Elevation Model
DGPS:	Differential Global positioning System
DSM:	Digital Surface Model
DTM:	Digital Terrain Model
GCP:	Ground Control Points
GHG:	Green House Gases
GPS:	Global Positioning System
IMU:	Inertia Measuring Unit
IPCC:	Intergovernmental Panel on Climate Change
LiDAR:	Light Detection and Ranging
Mg	Mega-gram
MRV:	Measurement Report and Verification
OBIA:	Object Based Image Analysis
REDD:	Reduce Emission from Deforestation and forest Degradation
RGB:	Red, Green and Blue
RMSE:	Root Mean Square Error
SAGA	System for Automated Geo-scientific Analysis
SfM:	Structure from Motion
TLS:	Terrestrial LiDAR Scanning
UAV:	Unmanned Aerial Vehicle
UNFCCC:	United Nations Framework Convention on Climate Change



**TOWARDS A UAV BASED STANDALONE SYSTEM FOR ESTIMATING AND MAPPING  
ABOVEGROUND BIOMASS/ CARBON STOCK IN BERKELAH TROPICAL RAIN FOREST,  
MALAYSIA**

# 1. INTRODUCTION

## 1.1. Background information

Forest ecosystem plays a crucial role in climate change reduction through carbon sequestration which regulates the global temperature (Pan et al., 2011). Forest covers about 30% of Earth's land surface and stored 45% of the carbon stored on land (Saatchi et al., 2011). Forests store more carbon than any other terrestrial ecosystems and serves as the best carbon bank and natural mitigation of climate change (Gibbs et al., 2007). According to Saatchi et al., (2011) researchers found that around 247 billion tons of carbon is sequestered in tropical forests, of which 78.14% is stored in aboveground biomass (trunks, branches, and leaves) and 21.86% is stored in the roots. Forest ecosystem destruction releases a vast amount of carbon back to the atmosphere as carbon dioxide (CO<sub>2</sub>) (Gibbs et al., 2007; Mohren et al., 2012). The tropical rainforest is one of the forest ecosystems which can store and release a vast amount of carbon dioxide (Soares Filho et al., 2010). Nowadays, tropical rainforests are declining due to deforestation and forest degradation (Jungle Boy, 2013). Tropical deforestation and forest degradation contribute around 20%, the highest global carbon dioxide emission next to fossil fuels (Hirata et al., 2011). Carbon dioxide is a Green House Gas (GHG) which causes climate change (Paustian et al., 2000). The intergovernmental panel on climate change (IPCC) third assessment report (2001) mentioned that Carbon dioxide emission due to tropical forest destruction has a serious impact on climate change (Houghton et al., 2001)

The United Nation Framework Convention on Climate Change (UNFCCC) was established in 1992 for the purpose of greenhouse gas (GHG) emission reduction, and countries agreed on the Convention to stabilize the GHG emission. Monitoring and reporting the forest carbon emission status is needed by the Convention (Peltoniemi et al., 2006). Following the convention, Reducing Emission from Deforestation and forest Degradation (REDD+) including sustainable forest management for carbon stock enhancement has been initiated to follow-up on emission reduction activities (Graham et al., 2017). The REDD+ needs an accurate measurement, reporting, and verification (MRV) mechanism of forest carbon stock balance monitoring to offer result based reimbursement for REDD+ adopted countries (Goetz et al., 2012).

Accurate forest biomass estimation is crucial for accurate carbon stock assessment since 47-50% of the dry forest biomass is carbon (Drake et al., 2002; IPCC, 2007). The assessment of aboveground biomass is a major concern to REDD+ MRV mechanism (Phua et al., 2016). The most accurate method of aboveground biomass estimation is cutting, drying and weighing all parts of the tree but, this method is destructive, labour-intensive and covers a small area only (Basuki et al., 2009). This destructive method of biomass estimation can underpin other nondestructive methods to estimate carbon stock, using allometric equation (Clark et al., 2001). The allometric equation needs forest parameters such as tree height, diameter at breast height (DBH), Crown projection area (CPA) and wood density as an input (Basuki et al., 2009; Ketterings et al., 2001; Sampaio et al., 2010).

The use of remote sensing technology to extract forest inventory parameters is a nondestructive method to estimate aboveground biomass (Ahamed et al., 2011). Numerous studies have been carried to estimate or measure these forest inventory parameters, using different types of remote sensing techniques (Brovkina et al., 2017; Ene et al., 2016; Kankare et al., 2013; Liang et al., 2014; Nelson et al., 2017). In simple forest modelling diameter at breast height from LiDAR data by making a relationship with other forest parameters is feasible (Andersen et al., 2005; Drake, Dubayah, Clark, et al., 2002; M. A. Lefsky et al., 2005; Naesset et al., 2005). Terrestrial LiDAR can scan the stem of trees and estimate DBH comparable to

**TOWARDS A UAV BASED STANDALONE SYSTEM FOR ESTIMATING AND MAPPING  
ABOVEGROUND BIOMASS/ CARBON STOCK IN BERKELAH TROPICAL RAIN FOREST,  
MALAYSIA**

DBH measured in the field (Hopkinson et al., 2004; Pfeifer et al., 2004). Scanning forests using Terrestrial LiDAR for DBH measurement needs multiple scans to extract 3-D point clouds of the maximum number of individual trees and of sufficient quality. A solitary scan in the dense tropical forest using Terrestrial LiDAR is subjected to occlusion (Pfeifer et al., 2004; Yao et al., 2011).

Various studies have been carried out in retrieving tree height using different LiDAR types with different point densities (Harding et al., 2001; Harding & Carabajal, 2005; Lefsky et al., 2005; Næsset & Økland, 2002). Terrestrial LiDAR cannot detect upper canopy of tropical rainforest as it cannot perceive long distance vertically. Mostly airborne and spaceborne LiDAR detects the forests upper canopy accurately, but it needs canopy openings to record data from the forest floor (Magnussen & Boudewyn, 1998; Næsset, 1997). Even though researchers acknowledge the potential of LiDAR in forest inventory parameter estimation, but in a dense tropical rainforest are faced with challenges due to occlusion (Coops et al., 2007; Lovell et al., 2003). In addition to the DBH and tree height, crown dimension provides an estimation of aboveground biomass and carbon stock, since they serve as input for the allometric equation (Brown et al., 2005; Popescu et al., 2003).

Unmanned Aerial Vehicles (UAV) a relatively new tool which can able to supply imagery at high spatial and temporal resolution (Turner et al., 2012). According to Turner et al., (2012) there are two kinds of UAVs; fixed wing and multi-rotors UAV design. The fixed-wing UAV flies faster and can cover a larger space, while multi-rotors can fly slowly and can capture images with any required overlap. The fixed-wing UAV needs a larger area for takeoff and landing compared to the multi-rotor (Nonami et al., 2010). Even though different UAVs have a different performance when it comes to payload, they can potentially carry any camera or sensor. UAV technology can be used for sustainable forest management issues, as it assists observation, assessment and mapping forests (Remondino et al., 2011). UAV application in sustainable forest management program is crucial because of its applicability in harsh inaccessible places. According to Grenzdörffer et al., (2008) the application of this new technology in forest management can facilitate estimation of forest inventory parameters and the achievement of aims of REDD+ strategy.

There are possibilities and advantages in assessing tropical rainforest aboveground biomass and carbon stock using UAV since it has a potential to provide a high-resolution image at any moment in time if the weather allows (Messinger et al., 2016). UAV image users have the chance to plan the flight mission time and minimize the impact of weather on image quality. The advantages of UAV in the forest carbon stock assessment are light-weight, low-cost, frequent image acquisition and minimal atmospheric correction, which are essential to achieving REDD+ MRV goals (Getzin et al., 2012). UAV imagery can supplement LiDAR and labour intensive (field-based) forest inventory methods (Messinger et al., 2016b). In spite of open space requirement for GCPs, UAV imagery has a potential to capture multi-view images and can reduce shadow effect, as it can capture the object from different directions.

Structure from motion (SfM) is a photogrammetric processing technique for estimating three-dimensional structures (point clouds) from two-dimensional image sequences. SfM image processing approximates camera position and scene geometry automatically by matching a series of 2-D overlapping images (Westoby et al., 2012). The use of UAV imagery for extracting tree height and the estimated tree height can be used as an input for the allometric equation for biomass estimation (Magar, 2014; Reuben, 2017 including previous ITC thesis).

The retrieving of forest parameters using remote sensing can be achieved through object-based image analysis (OBIA). Object-based image analysis is a type of image analysis which has been successfully applied to crown projection area image segmentation in forests with a simple canopies structure, using high-resolution images as an input (Hay et al., 2005; Kim et al., 2009). In object-based image analysis, the CPA's are generated using image segmentation algorithm which portions a large image into the non-overlapping unit (Chubey et al., 2006). Object-based image segmentation uses spectral and other information such as shape, texture and contextual relationships (T. Blaschke, 2010).



**TOWARDS A UAV BASED STANDALONE SYSTEM FOR ESTIMATING AND MAPPING  
ABOVEGROUND BIOMASS/ CARBON STOCK IN BERKELAH TROPICAL RAIN FOREST,  
MALAYSIA**

## **1.2. Statement of the problem and Justification**

The main element of the agreement reached in Paris at the UNFCCC COP21 in December 2015 for climate change mitigation was about the implementation of REDD+ (Pasgaard et al., 2016). The aim of the initiative is to encourage sustainable forest management activities leading to the reduced emission of greenhouse gases. The REDD+ program provides an incentive for rehabilitation and sustainable management of degraded forests (Ansell et al., 2011). Measurement, Reporting, and Verification (MRV) of carbon stock is a REDD+ mechanism to measure the status of the forest and to monitor the emission balance of REDD+ adopted countries such as Malaysia (Köhl et al., 2009). Also, regular carbon stock assessment in tropical rainforest needs a low-cost, accessible and simple method of carbon estimation.

Accurate measurement of forest inventory parameters has a relationship with accurate aboveground biomass estimation, which is a major concern of REDD+MRV program as it assists computing accurate carbon estimation (Phua et al., 2016). However, accurate measurement of these parameters in the multilayered tropical rainforest is a challenging task due to various uncertainties (Lu, 2005).

Most of the allometric equations are developed based on forest parameters such as wood density, tree height and DBH (Bragg, 2001; Chave et al., 2014). Among those parameters, DBH explains about 95% of the variation in aboveground biomass (Brown, 2002). Tree height is a supplementary input into the biomass estimation equations (Chave et al., 2014). Measuring DBH and tree height in the field is a labour-intensive and a time-consuming (Brown, 2002; Kwak et al., 2007). Moreover, these parameters are tree-based and not applicable to large areas.

In order to quantify the aboveground biomass timely and efficiently, remote sensing technology is vital, as it reaches inaccessible areas and covers large surface (Calders et al., 2011). Although remote sensing can repeat identical measurements over time hence fits the aim of REDD+ strategy, measuring DBH from remotely sensed data is impossible (Sium, 2015) except near distance measurements through TLS.

Forests canopy height extraction and mapping are mainly achieved using LiDAR and Digital Photogrammetry (Lim & Treitz, 2004).

Unmanned Aerial Vehicle(UAV) is an elating technology which has a potential to supply high spatial and temporal resolution images (Turner et al., 2012). Photogrammetric UAV image processing is a promising cost-effective technique, since it yields a 3-D point cloud, comparable to LiDAR data, for estimating aboveground biomass (Magar, 2014). The success of LiDAR-based forest inventory parameter estimation increases with increasing the point cloud density of LiDAR data but, increasing LiDAR data point cloud density is expensive (Gibbs et al., 2007). Compared to LiDAR, UAV images are cheap, and the technique is readily available, and a 3-D point cloud obtained through a photogrammetric processing of UAV image potentially can replace LiDAR data (Leberl et al., 2010). UAV can collect data over areas of a few hundred or few thousand hectares, with a density of 400 points per m<sup>2</sup> at a ground sampling distance of 5cm, whereas airborne LIDAR has a density of 5 to 6 points per m<sup>2</sup>.

In addition, UAV low flight altitude allows an overcast sky. A disadvantage of current UAV systems is that they require accurate Ground Control Points (GPS) for geo-referencing, which means sufficient, well distributed, large enough open spaces, with markers with known coordinates.

The Crown Projection Area is the surface of the vertical projection of the outer boundary of the crown. This parameter can be detected using object-based remote sensing image processing and can result in a segmented image approaching the shape and size of the crowns(CPA) (Gartner et al., 2010; Song et al., 2010). Object-based image segmentation uses spectral and contextual information and has proven to yield good results is with and simple structure and open canopy cover (Baral, 2011; Karna, 2012; Tsendbazar, 2011).

Research shows that CPA has a relationship with DBH (Hirata et al., 2009; Shimano, 1997). Numerous researchers showed a significant relationship between DBH and tree CPA (Hemery et al., 2005; Lefsky et al., 2002; Sium, 2015; Song et al., 2010). Since DBH play a crucial role in the assessment of AGB using an

**TOWARDS A UAV BASED STANDALONE SYSTEM FOR ESTIMATING AND MAPPING  
ABOVEGROUND BIOMASS/ CARBON STOCK IN BERKELAH TROPICAL RAIN FOREST,  
MALAYSIA**

allometric equation, estimating the DBH through the CPA is a promising approach for the measurement, monitoring, reporting and verification (MRV) program within the framework of REDD+. The CPA can be used as a proxy for DBH in more simple forests, but in multilayer tropical rainforest this is more cumbersome, since the CPA cannot be successfully extracted due to occlusion.

The effect of vertical canopy structure complexity on segmentation for biomass estimation is not much studied and has not obtained a solution yet. segmentation of temperate forest Ortho-photo has been successfully used to delineate CPA (Magar, 2014; Okojie, 2017) but limited studies in the tropical rainforest. In this study, object-based image analysis and CPA adjustment technique were applied to complete the lower incomplete crowns of multilayer forest canopies using high-resolution UAV image for aboveground forest carbon-stock estimation in Berkelah tropical rainforest, Malaysia.

This research aims to investigate possibilities of AGB and carbon-stock estimation using adjusted CPA, tree height and forest inventory parameters relationship from UAV images within the context of REDD+MRV program in Berkelah part of the tropical rainforest, Malaysia(Figure 1).

**TOWARDS A UAV BASED STANDALONE SYSTEM FOR ESTIMATING AND MAPPING ABOVEGROUND BIOMASS/ CARBON STOCK IN BERKELAH TROPICAL RAIN FOREST, MALAYSIA**

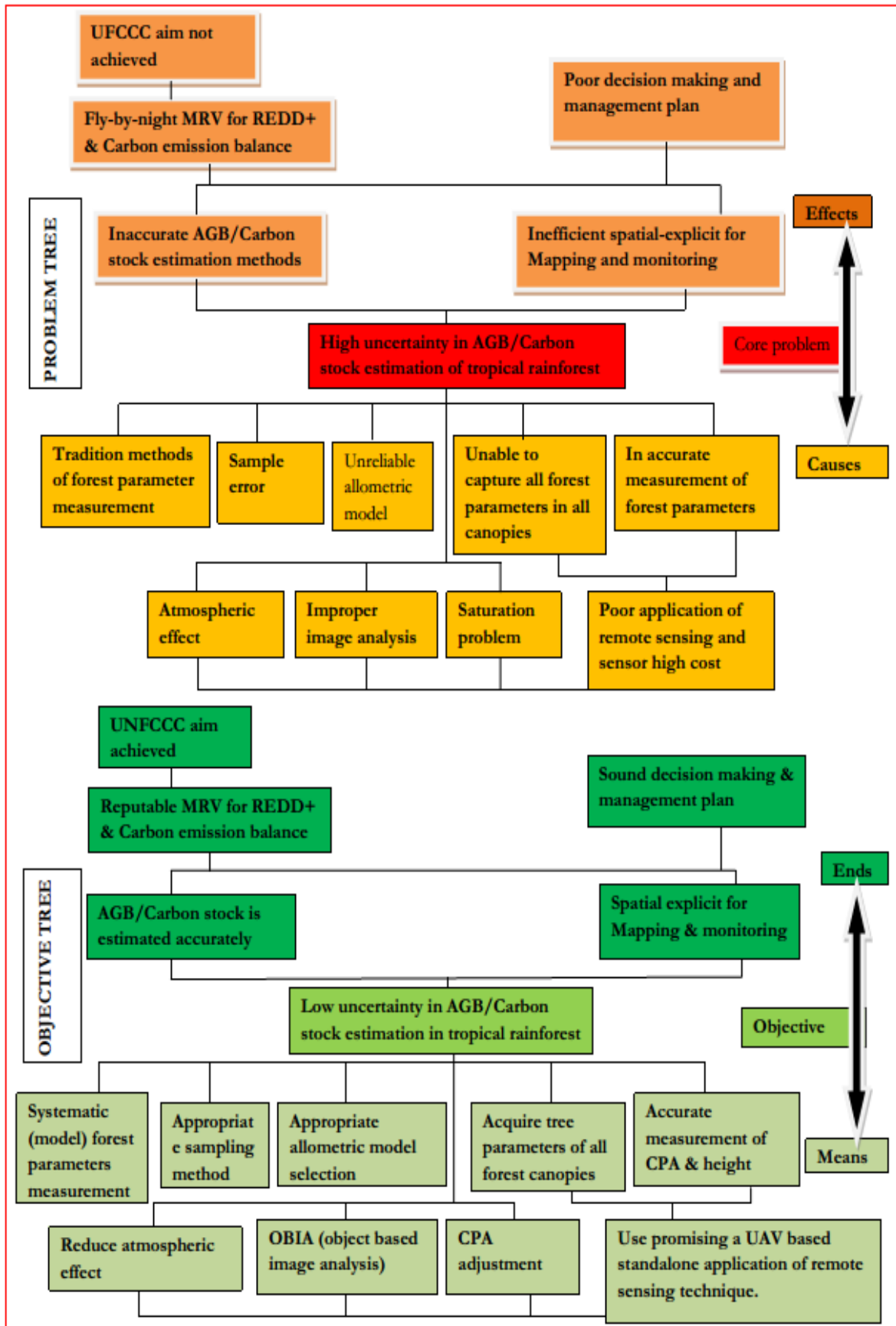


Figure 1: The problem and objective trees of the study.

**TOWARDS A UAV BASED STANDALONE SYSTEM FOR ESTIMATING AND MAPPING  
ABOVEGROUND BIOMASS/ CARBON STOCK IN BERKELAH TROPICAL RAIN FOREST,  
MALAYSIA**

### **1.3. Research Objective, Questions and Hypothesis**

#### **1.3.1. General Objective**

The main objective of this study is to investigate possibilities to assess AGB/carbon stock using adjusted CPA as a proxy for DBH and, tree height derived from UAV imagery in Berkelah tropical rainforest, Malaysia.

#### **1.3.2. Specific objectives**

1. To assess the relationship between adjusted CPA (after segmentation) and DBH measured in field in tropical rainforest
2. To assess the accuracy of tree height estimated from UAV 3-D point cloud compared to airborne LiDAR data in tropical rainforest
3. To assess the accuracy of AGB/Carbon stock-UAV compared to AGB/Carbon stock-field/airborne LiDAR.
4. To estimate and map total aboveground carbon stock using CPA and height from UAV imagery

#### **1.3.3. Research questions**

1. Is there a significant relationship between adjusted CPA (after segmentation) and DBH measured in the field in tropical rainforest?
2. Is there a significant difference between tree heights derived from UAV 3-D point cloud compared to tree height derived from airborne LiDAR in a tropical rainforest forest?
3. Is there a significant difference between AGB/carbon stocks-UAV based and field-based/airborne LiDAR?
4. What is the estimated amount of AGB/ carbon stock from UAV imagery in the study area?

#### **1.3.4. Research Hypothesis**

1. Ho: There is no a significant relationship between adjusted CPA and DBH measured in the field  
Ha: There is a significant relationship between adjusted CPA and DBH measured in the field
2. Ho: There is no a significant difference between tree heights derived from UAV 3-D point cloud compared to tree height derived from airborne LiDAR data  
Ha: There is a significant difference between tree heights derived from UAV 3-D point cloud compared to tree height derived from airborne LiDAR data
3. Ho: There is no a significant difference between AGB/carbon stock-UAV-based and AGB/carbon stock field/airborne LiDAR  
Ha: There is a significant difference between AGB/carbon stock-UAV-baesd and AGB/carbon stock field/airborne LiDAR

**TOWARDS A UAV BASED STANDALONE SYSTEM FOR ESTIMATING AND MAPPING  
ABOVEGROUND BIOMASS/ CARBON STOCK IN BERKELAH TROPICAL RAIN FOREST,  
MALAYSIA**

**1.4. Theoretical framework of the study**

In order to accomplish this study, relevant literature was reviewed, the research problem was identified and subsequent questions and research objectives were formulated. Secondary data and required tools were requested and fieldwork was carried out. The collected data were processed and analysed and the result was discussed, comparing them to literature. Finally, the research was summarized in conclusion and recommendation. The general description of the process is illustrated in Figure 2.

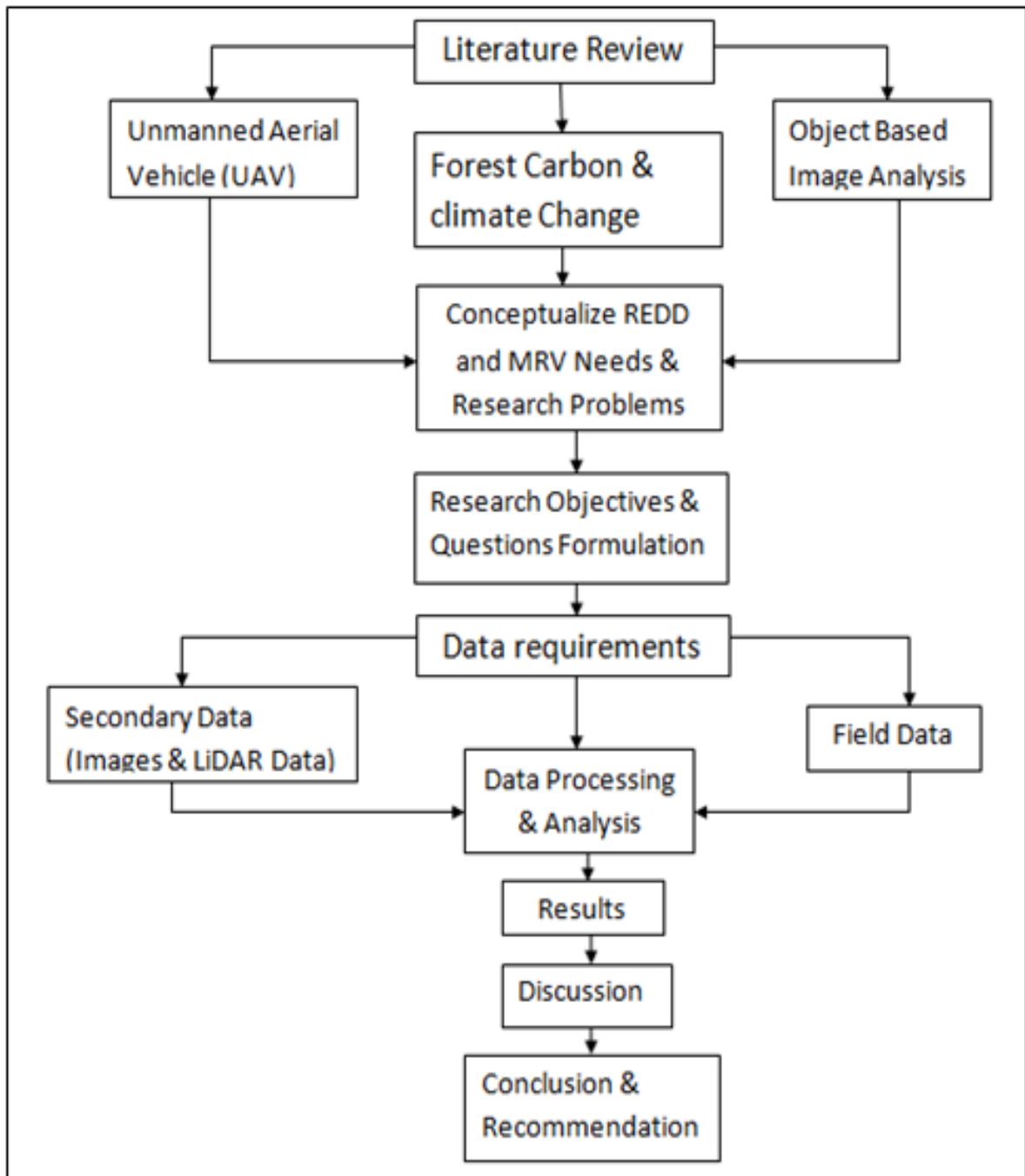


Figure 2: Theoretical framework of the study.

## 2. LITERATURE REVIEW

### 2.1. Tropical Rainforest Biomass and Carbon

The tropical rainforest or low land equatorial evergreen rainforest is, generally composed of broad-leaved trees in hot and moist areas near the earth's equator (Smith, 2015). Tropical rainforests are fundamental to carbon storage and carbon sequestration on a global scale. Tropical rainforest includes four layers (emergent, canopy, understory and forest floor). The emergent layer is formed by the tallest trees, the canopy is the thickest layer, consisting of trees shorter than the emergent layer, the understory tree layer is below canopy layer and receives less sunlight and the floor of the forest is full of litterfalls (Figure 3).

Tree biomass is defined as the total dry weight of the trees per unit area. It includes the above and below-ground dry weights (Dengsheng Lu, 2006). Below-ground biomass refers to the total mass of live plant roots (Ravindranath & Ostwald, 2008). Conversely, the above-ground biomass refers to the dry weight of stem, branches and leaves (Gschwantener et al 2009). For this study Above Ground Biomass (AGB) is considered, since the main cause of carbon emission is AGB destruction and depletion (Gibbs. et al 20027). The most appropriate and direct means of quantifying aboveground biomass is through harvesting all above-ground parts of the trees, oven-drying and weighting them (Gibbs, 2007). Some authors state the approximately 50% of the biomass is carbon (Brown, 1997; Drake, et al, 2002). The IPCC (2007) report suggests that around 47% of the forest biomass is carbon; considering the different density of various species. The forest biomass is a vital biophysical parameter for different ecological and biophysical models hence, the accurate estimation of biomass is crucial for improving the applicability of those models (Luo et al., 2017).

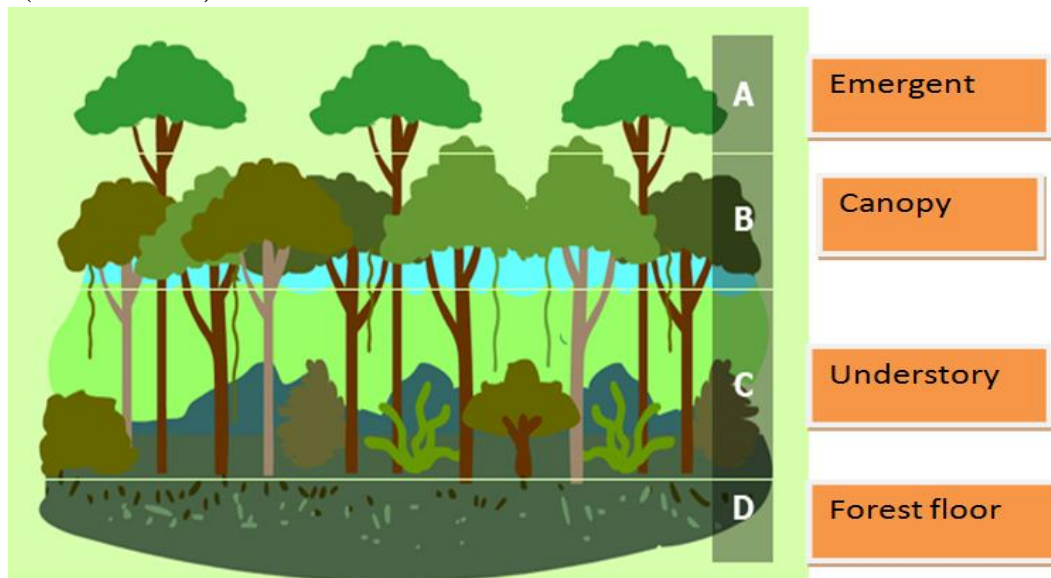


Figure 3: Illustration of tropical rainforest layers (www.ace geography (modified)).

### 2.2. Allometric Equation

According to Bujotzek, (2007) allometry is “measuring and comparing the relation of body mass to different biological parameters”. The allometric equation in forest biomass estimation is the most reliable and non-destructive approach once the relationship with structural tree parameters (DBH, height, CPA, etc) is developed (Ketterings et al., 2001; Wang, 2006). Estimation of AGB should consider the forest structure and climatic conditions so as to reduce the generalization of field allometric equations which lead

**TOWARDS A UAV BASED STANDALONE SYSTEM FOR ESTIMATING AND MAPPING  
ABOVEGROUND BIOMASS/ CARBON STOCK IN BERKELAH TROPICAL RAIN FOREST,  
MALAYSIA**

to uncertainty (Drake et al., 2003; Yuen et al, 2016). Basuki. et al (2009) suggested that site specific allometric equation selection for accurate biomass estimation is essential.

**2.3. Overview of UAV and Photogrammetry**

Unmanned Aerial Vehicle (UAV) also known as drones or unmanned aircraft was deployed for the first time by Americans Lawrence and Elmer Sperry in 1916 (Nonami, 2007). It was initially fashioned for a military purpose without any risk for pilots and later applied for civil and geomatics at the end of the 1970s (Colomina & Molina, 2014). Currently, “the use of UAVs in the civilian domain, as remote sensing tool, presents new and stimulating opportunities (Turner et al., 2012). The increased demand UAV’s by civilians has to do with its low-weight, low-cost, availability of accurate and miniature Global Positioning System (GPS) as well as Inertial Measurement Units (IMUs) (Colomina & Molina, 2014; Fritz et al, 2013, Zhang et al., 2016). Generally, UAV types are classified based on their area requirement to takeoff; as fixed-wing aircraft (large area needed) and rotary-wing (small area needed) (Figure 4). The flight speed and area coverage is smaller in rotary-wings than in fixed-wings (Nonami et al., 2010).

A UAV photogrammetry is a 3D footage of ground information as a valid complementary solution of terrestrial acquisition (Colomina et al, 2008). According to Mayr, (2011) appropriate design of the UAV trajectory and a real-time task management capacity are significant in achieving fruitful and secure acquisition missions. UAV data can be acquired under an overcast sky, but the platform is susceptible to wind and should not be during high-wind or wind bursts. The UAV flight instability can to some extent be compensated by 90% forward and 60-80% cross overlap for proper application of photogrammetry and remote sensing (Colomina & Molina, 2014).



a) Rotor-wing UAV



b) Fixed-wing UAV

Figure 4: major types of UAV (source: [www.questuav.com](http://www.questuav.com)).

Photogrammetry is a method of estimating structural parameters of topographic features in a 3-dimensional way from photographs. The basic principle used by Photogrammetry is triangulation using photographs of an object that captured from its different sides based on lines of sights from the camera location to points on the object (Figure 5). These lines of sight are scientifically intersected to produce the 3-D coordinates of the points of interest. Photogrammetry was established for topographic mapping. Photogrammetry deals with the precise measurements regarding the size, shape, and position of objects, next to recognition and identification of feature visible on the image. Photogrammetry is a structure-from-motion technique to solve feature positions within a defined coordinate system (Westoby et al., 2012).



**TOWARDS A UAV BASED STANDALONE SYSTEM FOR ESTIMATING AND MAPPING  
ABOVEGROUND BIOMASS/ CARBON STOCK IN BERKELAH TROPICAL RAIN FOREST,  
MALAYSIA**

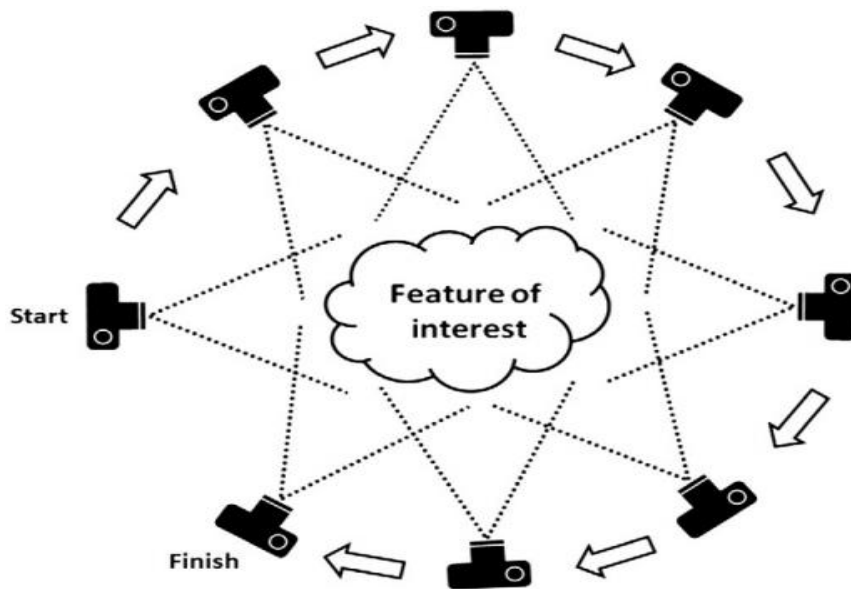


Figure 5: Illustration of structure from motion (source: (Westoby et al., 2012)).

#### **2.4. Application of UAV in forestry**

A UAV delivers very high-resolution imagery which can play an important role in forest management through its contribution to assessment, mapping and modelling issues (Remondino et al., 2011). The UAV application in forestry is very promising, not only because of its low-cost, but also its ability to minimize the accident to pilot in a harsh environment in comparison to traditional airborne platforms. According to Grenzdörffer et al., (2008) UAV imagery is a valuable tool in different forest inventories activities as well as to perform precision silviculture. Forest production and growth rate research require a platform that can be deployed frequently and is readily available (Horcher & Visser, 2004), both requirements are strong points of a UAV. Forest monitoring in tropics can be successfully performed using the UAV very high-resolution image which is advantageous over the established remote sensing techniques (Messinger et al., 2016b). The effect of unfavourable atmospheric conditions, (like clouds and rain showers) can be circumvented, since a UAV flight mission can be scheduled and executed on very short notice and with an overcast sky. In addition, reduced time and effort for atmospheric correction and the relatively low purchase amount guarantees a UAV to be a valuable tool in the framework of REDD+ MRV (Getzin et al., 2012).

#### **2.5. Advantage and disadvantage of UAV imagery**

Different shapes and sizes of UAV have both advantages and disadvantages which eventually leads to the operator's decision which platform will best fit the application (Remondino et al., 2011). Phantom 4 DJI UAV is a helicopter with 4 rotor blades that revolve around a fixed mast. Opposed to fixed-wing, rotor blades UAV's do not need constant forward movement and can land vertically which allows small takeoff and landing space. Disadvantages are limited battery power, directly affecting the duration of a mission and the weight of the payload. Currently, the ability of UAV to stay in the air with a small camera is not more than a half hour per single flight mission (Remondino et al., 2011; Torresan et al., 2017) and this limits the area which can be covered in one mission (Matese et al., 2015). Geo-referencing of UAV images needs additional ground control points, since the quality of the onboard GPS is limited and GPS and camera are not aligned to the same point in the ground. Due to the high spatial resolution a UAV mission results in a large amount of data per hectare surveyed, which subsequently requires powerful data processing capability (Torresan et al., 2017).



**TOWARDS A UAV BASED STANDALONE SYSTEM FOR ESTIMATING AND MAPPING  
ABOVEGROUND BIOMASS/ CARBON STOCK IN BERKELAH TROPICAL RAIN FOREST,  
MALAYSIA**

**2.6. Airborne LiDAR and its Application in forestry**

Airborne LiDAR (Light Detecting and Ranging), is an active remote sensing technology which uses airplane and helicopter platforms (Figure 6) and produces high accuracy 3-dimensional topographic data (Lafsky et al, 2002). LiDAR uses a medium power laser and generates point clouds with X, Y, Z positions, based on measurement of the distance between the sensor and targeted objects. It determines the elapsed time between emission of the laser pulse and detection of returned (reflected) laser signals at the receiver. An air born LiDAR system carries; a Laser device, an inertial navigational Measurement Unit (IMU) which records aircraft orientation, an airborne global positioning system (GPS) unit, which records the X, Y, Z positions of the aircraft and a computer interface that manages the communication among devices and data storage(Figure 6).

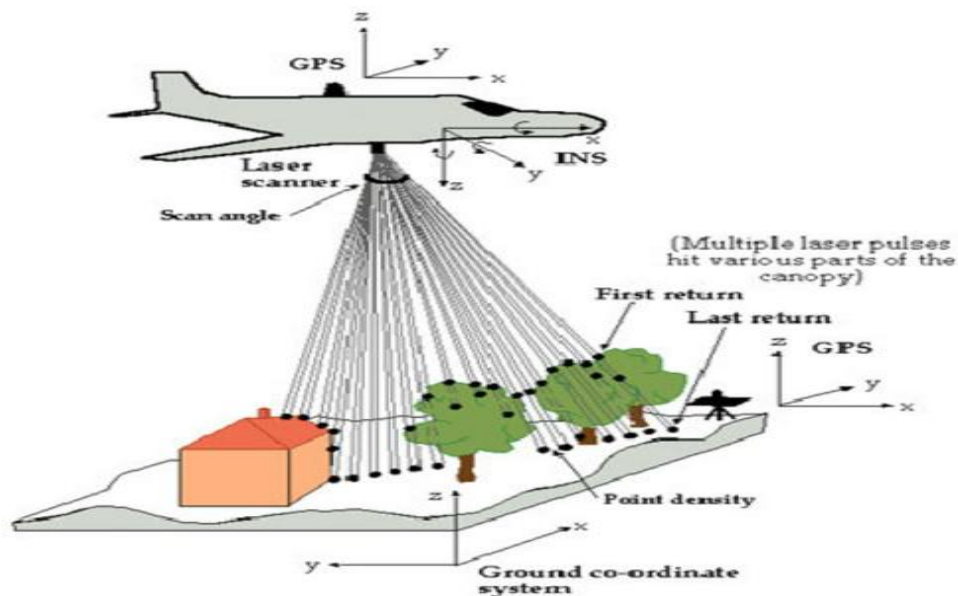


Figure 6: Illustration of Airborne LiDAR (Dowman, 2004).

The laser pulse emitted from the device is reflected back from the forest canopy, leaves, branches and bare surface (Evans et al., 2009). Airborne LiDAR systems for forest application and topographic mapping uses eye-safe near-infrared laser light, mostly at 1064 nm. This technology has proven its use for forestry purposes, due to its ability to assess the 3-D canopy structure and provide high precision data (Patenaude et al., 2005; Balzter et al., 2007). Airborne LiDAR plays role in the study of tree height and forest stand volume (Nilsson, 1996).

There are two LiDAR laser pulse recording systems; discreet-return, which records the data as separate returns and full waveform system, which records the whole return as one continuous wave (figure 7). When used for a forest area, the discreet-return system records several returns from many parts of the trees. The first return represents the canopy height, while the last return reveals the terrain height. The data used in this study has 4 returns and the fourth one is the last return which was used to generate the DTM. The waveform system has lower spatial resolution and hence a larger 'footprint' and continuously records the amount of energy returned back to the receiver (Evans et al., 2009). Terrestrial LiDAR (Terrestrial Laser Scanner) allows for accurate 3D measurement of biophysical parameters in the field (Lafsky et al, 2002), basically using the same technology as airborne systems.

**TOWARDS A UAV BASED STANDALONE SYSTEM FOR ESTIMATING AND MAPPING ABOVEGROUND BIOMASS/ CARBON STOCK IN BERKELAH TROPICAL RAIN FOREST, MALAYSIA**

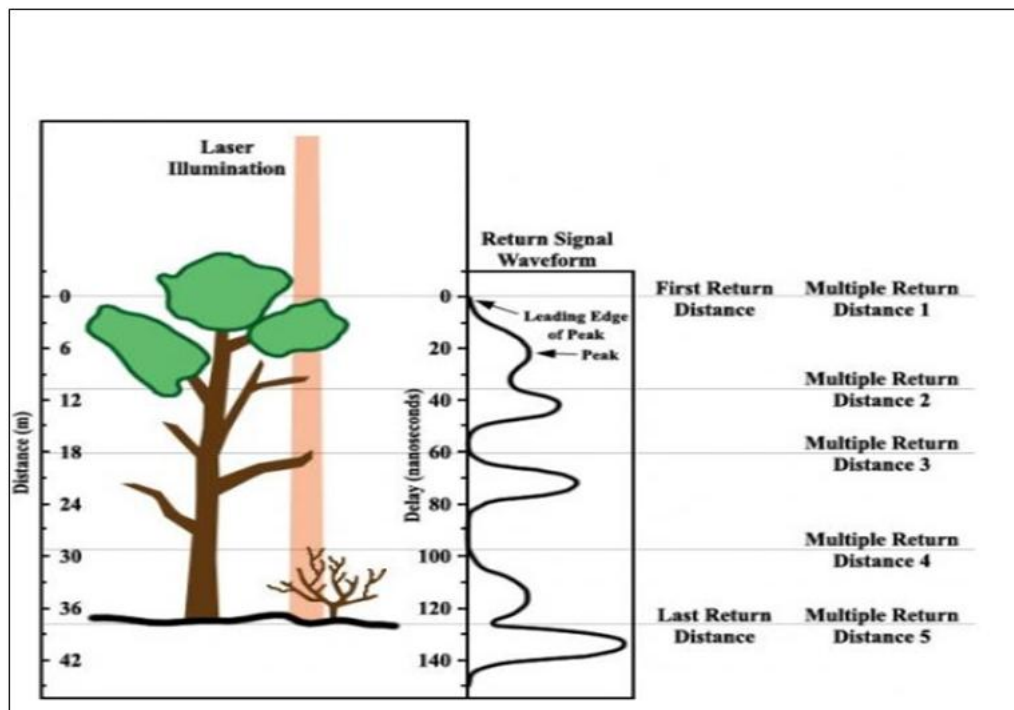


Figure 7: Illustrations of discrete-return and waveform LiDAR devices conceptual differences

(Source: Lefsky et al, 2002).

### 2.7. Crown projection area

The crown projection area (CPA) of a tree is the area covered by the projection of the outer border of the crown on the horizontal plane (Gschwantner et al., 2009) (see figure 8). The relationship of crown projection area and DBH (see section 1.2) can be influenced by the sensor view angle, sun elevation and topography (Pouliot et al., 2005). According to Culvenor (2002), a small off-nadir view angle and higher solar zenith angle can help to discriminate the real geometric and radiometric properties of tree crown in very high-resolution images. The influence of geometric and radiometric properties of trees can be minimized using UAV imagery, since the time of image acquisition and view angle can be managed, in combination with high image overlap. Most probably, at the nadir view and solar zenith angle, a regular circular crown shape could be seen but such perfect situation can be hardly ever found (Pollock, 1996). Erikson (2004) suggested that CPA delineation is tricky when the imagery is recorded at low sun angle due to a shade side effect of the trees.

The CPA of individual trees can be extracted through crown delineation from very high resolution optical and LiDAR imagery (Song et al., 2010). Various studies show a significant relation between CPA and DBH (Hermery et al, 2005; Song et al, 2010; Lefsky et al., 2002). The UAV image photogrammetry can provide height and canopy structure with less-cost and at appropriate solar zenith angle. Since DBH and CPA have a relationship (Hirata et al., 2009), it is reasonable to assume that CPA and height could provide a better estimate of aboveground forest biomass and carbon stock. In a multilayered tropical forest the CPA of the lower trees is not fully visible and due to that, complete crown segmentation is a difficult task. Incomplete crowns need adjustment to minimize CPA under segmentation problem. CPA calculation assumes circularity from the maximum crown diameter (Kuuluvainen, 1991)

**TOWARDS A UAV BASED STANDALONE SYSTEM FOR ESTIMATING AND MAPPING  
ABOVEGROUND BIOMASS/ CARBON STOCK IN BERKELAH TROPICAL RAIN FOREST,  
MALAYSIA**

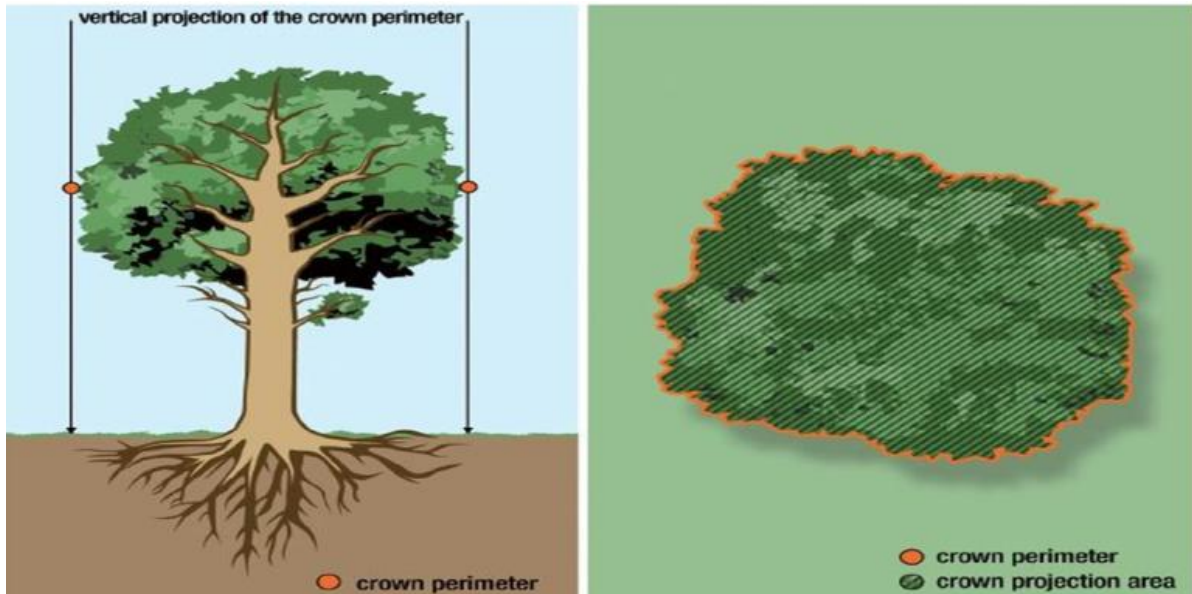


Figure 8: Demonstration of crown projection area (Gschwantner et al., 2009).

### 2.8. Object-based image analysis

Object-based image analysis (OBIA) has the ability to incorporate contextual information of an object instead of depending on pixel information only. This method received increasing attention with the development of high-resolution remote sensing data. High-resolution imagery creates an opportunity to derive objects of interest based on the information from several pixels (Blaschke, 2010). OBIA results in a segmented image. The OBIA process includes portioning of an image into meaningful separable objects, feature set building and optimization to remove undesired objects and classification of objects into meaningful categories. OBIA technique differs from the traditional pixel-based image classification processes as it works through aggregating of neighbouring pixels into meaningful image objects within designated parameters (Riggan & Weih, 2009). Image segmentation is the start of object-based image analysis. Segmenting an image is the process of subdividing an image of groups of homogenous pixels to build meaningful image objects. The segmented image object needs further classification based on textural, spectral, shape and contextual information to make object-based image analysis complete (Hay et al., 2005; Li. & Zhang, 2009).

**TOWARDS A UAV BASED STANDALONE SYSTEM FOR ESTIMATING AND MAPPING  
ABOVEGROUND BIOMASS/ CARBON STOCK IN BERKELAH TROPICAL RAIN FOREST,  
MALAYSIA**

### 3. MATERIALS AND METHODS

#### 3.1. Study Area

Berkelah, tropical rainforest is one of the tropical rainforest forest areas in Malaysia. The forest area has undulated topography and diverse tree density with various canopy density and structure. It is around 25 kilometers far from Kuantan city to North West direction. The forest was logged before 40 years ago and now it is rehabilitated secondary forest type of tropical rainforest (Barizan, et al. 1997).

The geographical location of Berkelah tropical rainforest is in Kuantan district-Pahang region, Northeast of Peninsular Malaysia, and is located between 3°57' 43" N and 102°41' 47" E (Figure 9).

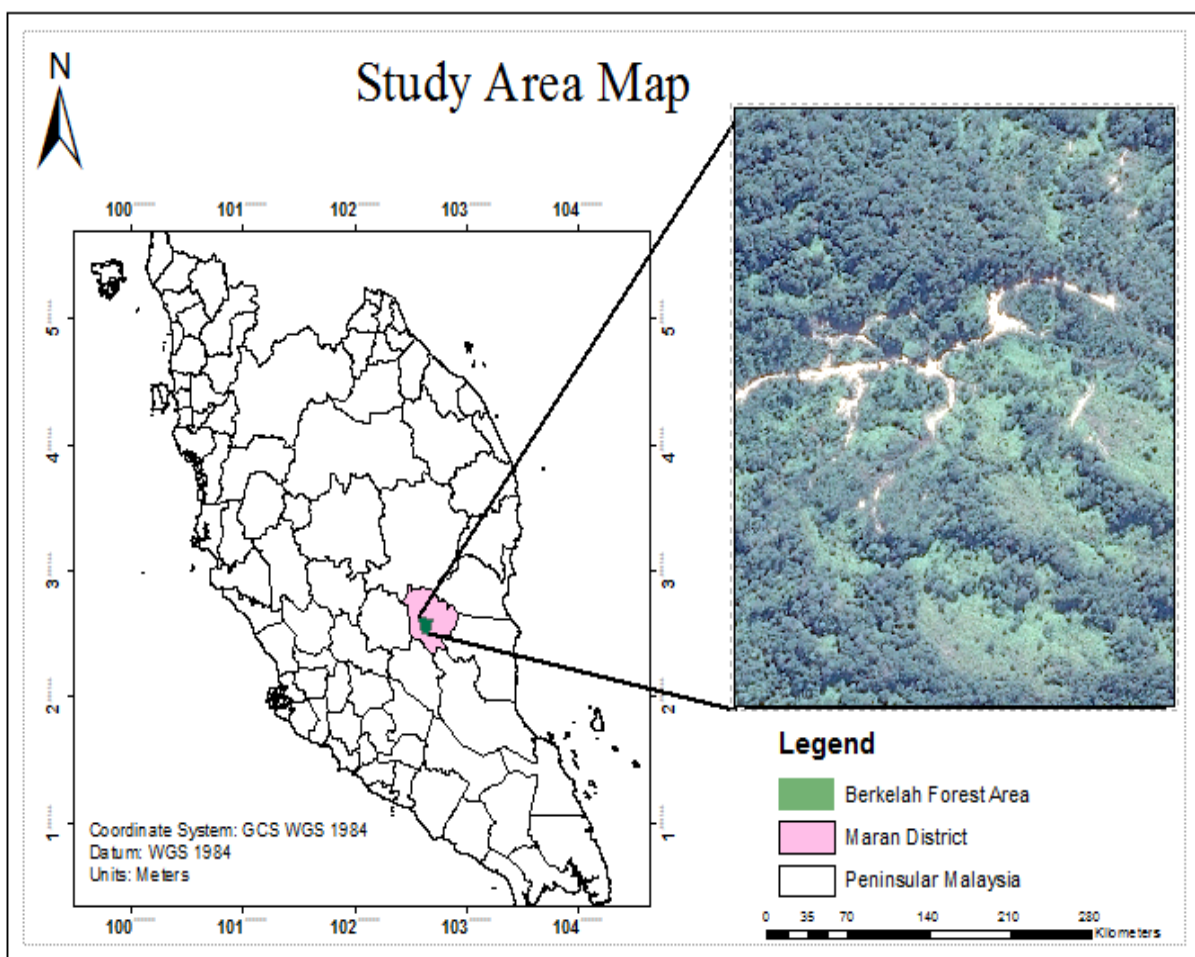


Figure 9: Study area location map.

Berkelah tropical rainforest has a humid tropical climate which characterized by high-temperature, high relative humidity and abundant year-round rainfall. The average temperature is around 30°C and the mean annual rainfall is 2,540 mm (Barizan et al., 1997).

The vegetation of Berkelah forest reserve consists of a mixed Dipterocarp hill forest. The forest is characterized by a high proportion *Shorea* species which is categorized under red meranti group. The area was logged and after that, the vegetation can be classified as a mixed hill Dipterocarpaceae forest dominated by *Dipterocarpaceae* which is the dominant timber producing tree family (Barizan et al., 1997).

**TOWARDS A UAV BASED STANDALONE SYSTEM FOR ESTIMATING AND MAPPING  
ABOVEGROUND BIOMASS/ CARBON STOCK IN BERKELAH TROPICAL RAIN FOREST,  
MALAYSIA**

**3.2. Materials**

The tools and equipment in Table 1 have been used to measure and collect the necessary field data in this study.

Table 1: Field measurement tools and equipment.

<b>Tools and equipment</b>	<b>Specific function</b>
Measuring tape (50m)	Plot layout and measurement
Diameter tap (5)	Tree girth measurement
GPS	Navigation and X Y coordinate reading
Densitometer	Measuring canopy density

In this study, airborne LiDAR, UAV imagery and field-based biometric data were used. The UAV imagery and biometric data was acquired and collected during the fieldwork. Airborne LiDAR dataset of the study area, with average point density of 6 points/m<sup>2</sup> from 2014 was obtained from University Technology Mara Malaysia (UiTM). The required software and specific function were as shown in Table-2.

Table 2: Required soft ware.

<b>Soft wares</b>	<b>Specific Function</b>
e-Cognition 9.2.1 developer	Image segmentation
Arc map 10.5	GIS analysis
SPSS v. 20 software	Statistical analysis
AGISOFT photo scan professional	UAV image processing
Erdas imagine	image analysis
Microsoft Excel	Data analysis
Arcscene 10.5	for 3-D visualization of images

**3.3. Methods**

The methods which were applied in this study have four main parts; field data collection, remote sensing data processing, segmentation and CPA adjustment and data analysis. The main process of the methods that were applied was as shown in Figure 10.



**TOWARDS A UAV BASED STANDALONE SYSTEM FOR ESTIMATING AND MAPPING ABOVEGROUND BIOMASS/ CARBON STOCK IN BERKELAH TROPICAL RAIN FOREST, MALAYSIA**

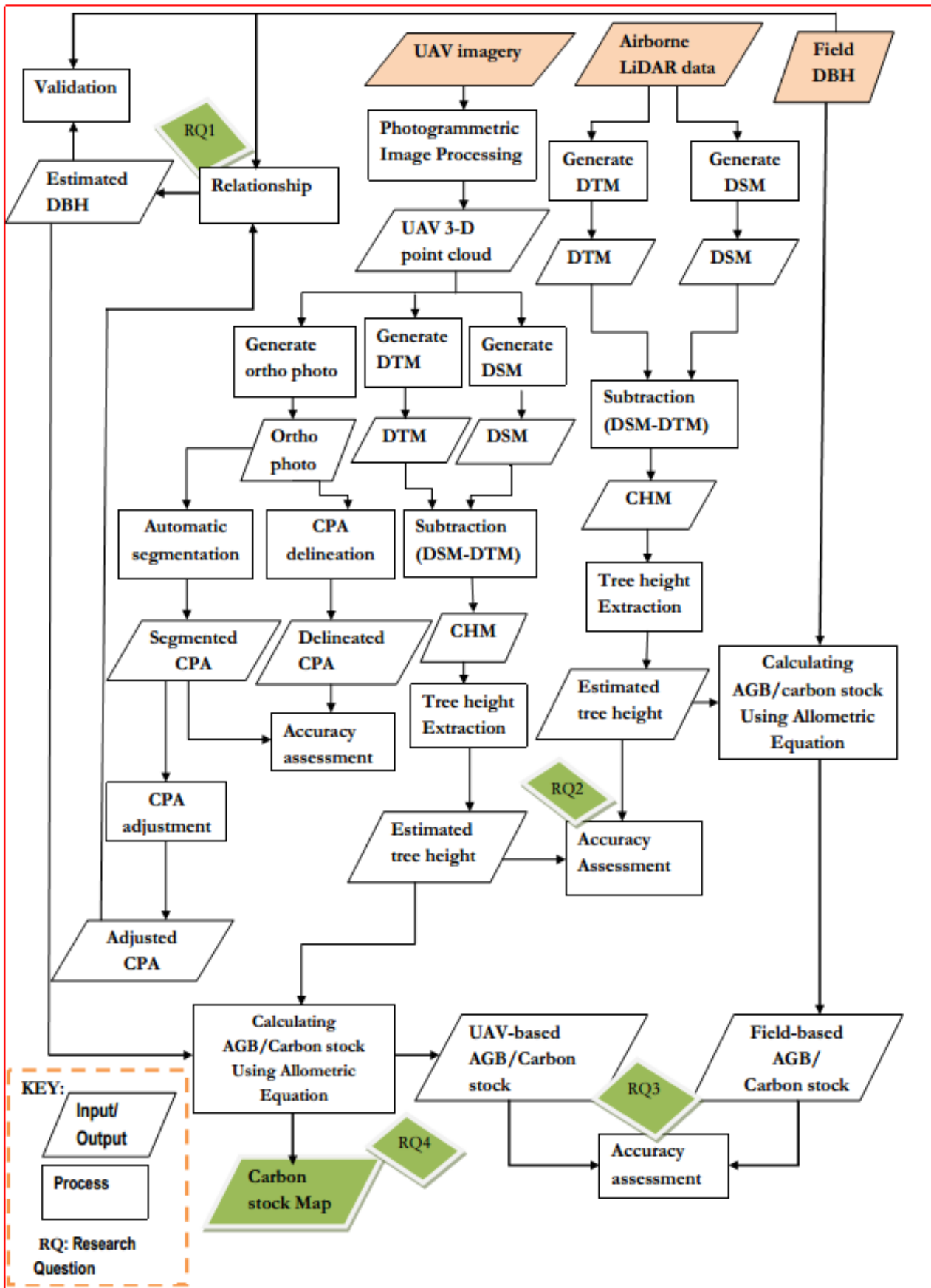


Figure 10: Flowchart of the research methods.

**TOWARDS A UAV BASED STANDALONE SYSTEM FOR ESTIMATING AND MAPPING  
ABOVEGROUND BIOMASS/ CARBON STOCK IN BERKELAH TROPICAL RAIN FOREST,  
MALAYSIA**

**3.3.1. Pre-fieldwork**

Field data collection needs pre-fieldwork activities such as field data collection sheet designing, testing of equipment and tools, practicing the different field instrument, preparing field data collection sheets (appendix1), checking GPS and UAV batteries and all those activities were conducted before fieldwork. Black and white paint, 45 cm X 60 cm white marker and plastic tubes were prepared to mark the ground control points and to provide good visibility in the UAV images (Figure 11).



Figure 11: 45 cm X 60 cm Marker and plastic tube inserted at centre.

**3.3.2. Sampling Method**

In this study, a purposive sampling method was applied because of the fieldwork time and accessibility limitation to collect the required number of plots that would take a lot of time. The technique was applied to effectively use the fieldwork time and minimize risks of inaccessible places. In the field circular plots, a radius of 12.62m (500m<sup>2</sup>) was laid out. The radius was corrected for the slope when required (Abegg et al., 2017). UAV flight plans were selected based on the open space available for marker placement. In total four flight plans were established, with 32 sample plots. In every plot, the following data were collected:

**TOWARDS A UAV BASED STANDALONE SYSTEM FOR ESTIMATING AND MAPPING ABOVEGROUND BIOMASS/ CARBON STOCK IN BERKELAH TROPICAL RAIN FOREST, MALAYSIA**

coordinates of the centre point and 1033 individual trees (Figure 12). From the 1033 trees, the DBH was measured with diameter tape.

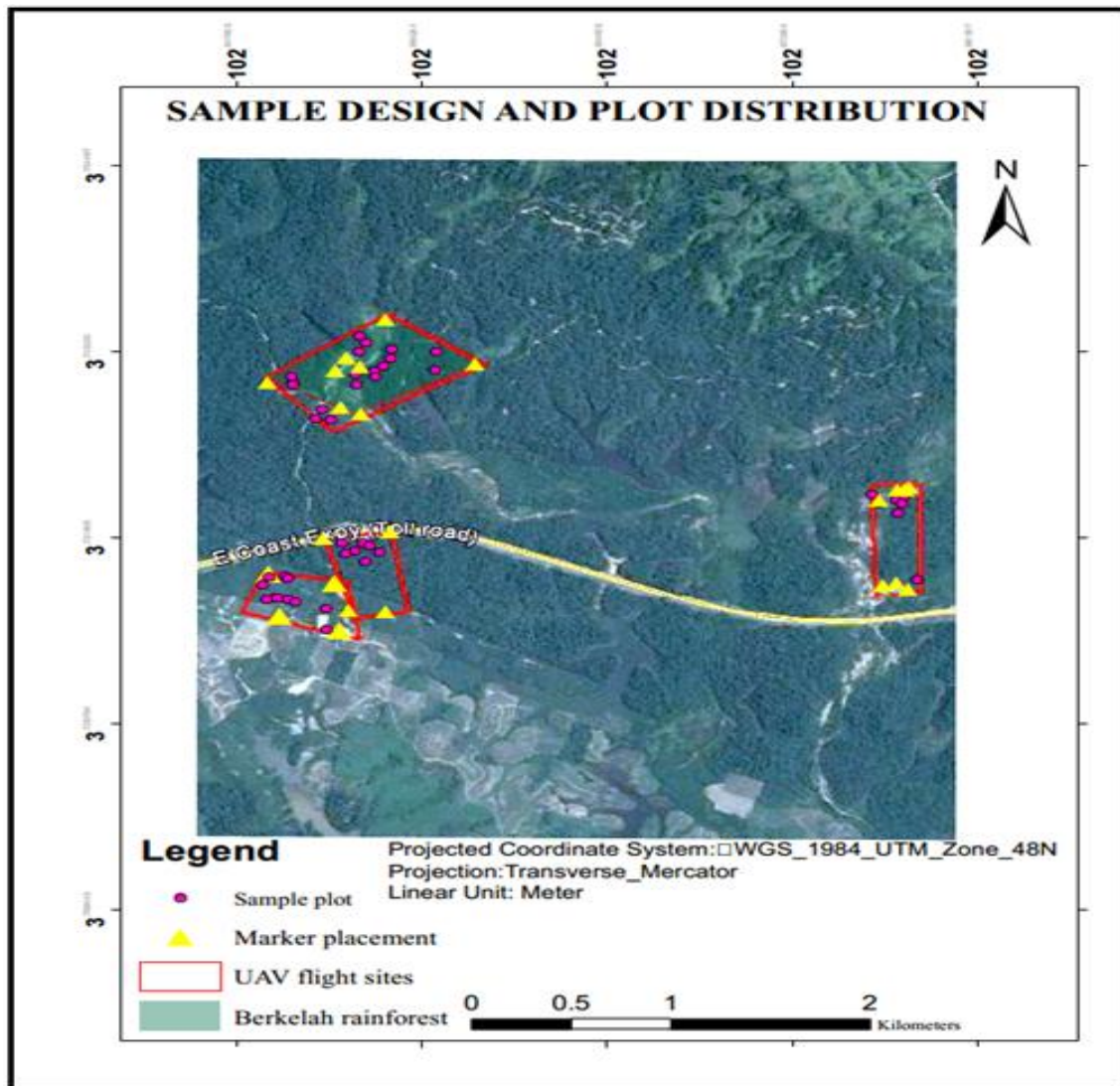


Figure 12: Sample plot distribution and UAV flight covered blocks.

### 3.3.3. Field Data Collection

#### 3.3.3.1. UAV Image Acquisition

UAV image acquisition was carried out using a Phantom 4 DJI UAV with RGB camera model FC330 (3.61mm), 4000 X 3000 resolution, 3.61mm focal length, and 1.56 X 1.56  $\mu\text{m}$  pixel size. Four areas were selected (1, 2, 3 and 4) with a slope range between 0-13.9, 0-14.5, 0-15 and 0.33-26.5 degrees respectively and covered by 8 flight missions. Based on open space availability and block area size, 4-8 markers (35 in total) were placed for ground control point recording. The Pix4D capture app was used for UAV flight plan preparation, with the following settings: moderate speed (approx. 50% of the maximum speed) 90% overlap and a flight altitude of 120m (Figure 13). The Ground Control Points (GCPS) were recorded using Differential Global Position System (DGPS). The size of the UAV flight mission was determined by the capacity of the battery (18-20 minutes).



**TOWARDS A UAV BASED STANDALONE SYSTEM FOR ESTIMATING AND MAPPING ABOVEGROUND BIOMASS/ CARBON STOCK IN BERKELAH TROPICAL RAIN FOREST, MALAYSIA**

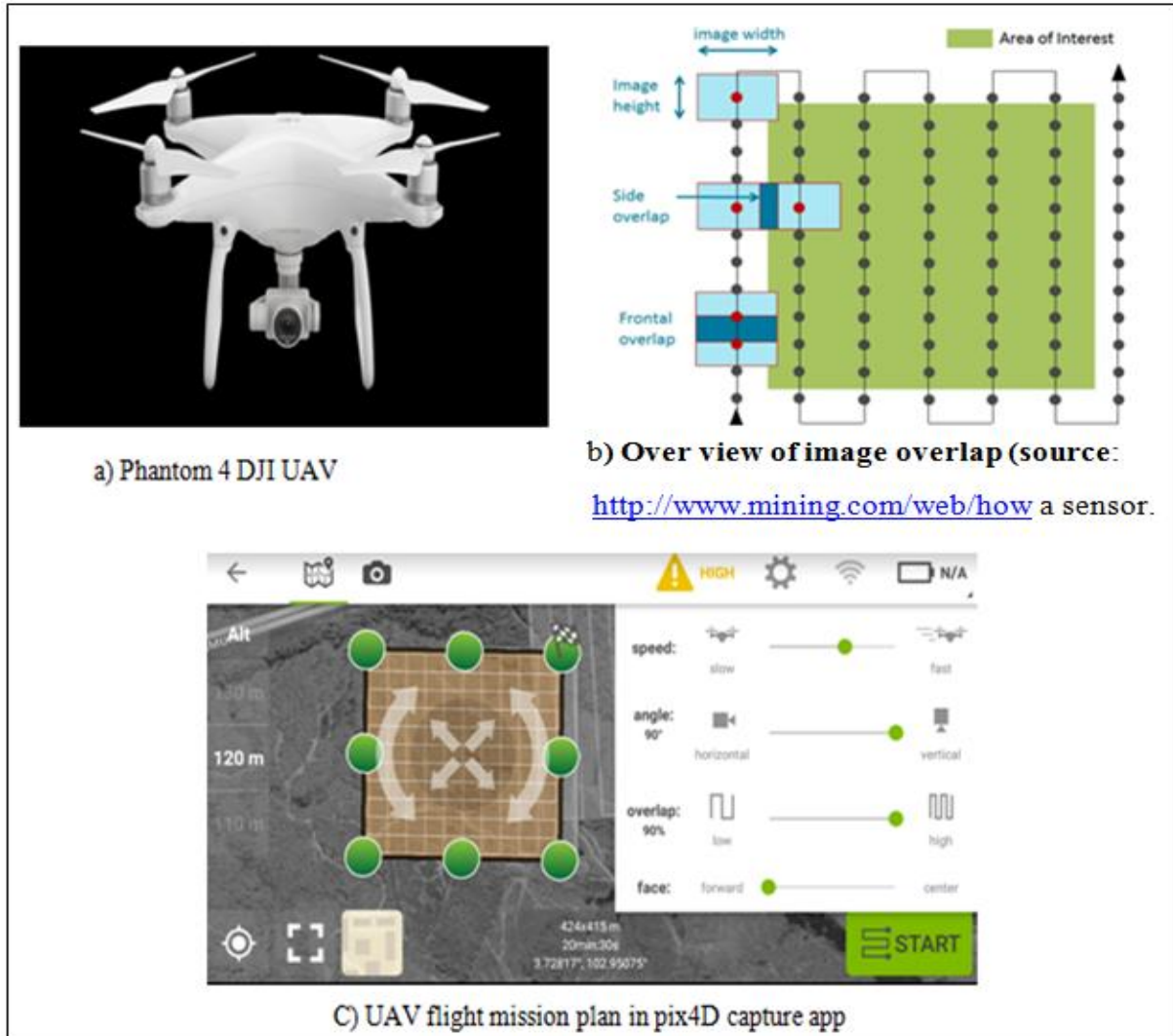


Figure 13: Flight planning and settings for the DJI Phantom-4 UAV.

### 3.3.3.2. Biometric Data Collection

The DBH was measured using diameter tape and recorded on the data collection sheet. Even though trees with less than 10 cm DBH have no significant contribution to biomass and carbon stock (Brown, 2002), in this study trees with a DBH between 5 and 10 cm were also included, since the main goal of this study is to adjust CPA and explore the relationship between DBH and CPA. Folk trees have been considered as one tree when the folk is above 1.3 m and as two trees when below 1.3 m. During the fieldwork, the coordinates of each tree were recorded to locate the tree in the image. The average tree crown diameter was estimated in the field and recorded to decide on the input value for local maxima and local minima during the object-based image segmentation process. During the fieldwork, a total of 1033 trees were measured.

### 3.3.4. Airborne LiDAR Data Processing

In this study, the airborne LiDAR data was required to extract tree height which is relatively accurate hence validate tree height derived from UAV 3-D point cloud only since tree height measurement in the tropical rainforest using handheld tools is difficult due to occlusion. The final output of the airborne

**TOWARDS A UAV BASED STANDALONE SYSTEM FOR ESTIMATING AND MAPPING  
ABOVEGROUND BIOMASS/ CARBON STOCK IN BERKELAH TROPICAL RAIN FOREST,  
MALAYSIA**

LiDAR data processing was Canopy Height Model (CHM), to extract tree height from airborne LiDAR-CHM. The airborne LiDAR data which was obtained from University Technology Mara Malaysia (UiTM) was LAS dataset file in a \*.las extension. To generate the CHM, generating Digital Surface Model (DSM) and Digital Terrain Model (DTM) was the first procedure.

#### **3.3.4.1. DSM and DTM generation from airborne LiDAR Data**

The airborne LiDAR data were used to generate a Digital Terrain Model (DTM) and a Digital Surface Model (DSM) using Arc GIS 10.5. The DSM and DTM were generated after the LAS dataset was defined using create dataset geoprocessing tool in Arc GIS and a layer was created by adding the data into Arc map. Identifying the last return and first return points were the first step of generating DSM and DTM. The last return of the airborne LiDAR data was return 4 hence DTM was generated from the fourth return while the DSM was generated from the first return. After identification of the points to process, the layer with the selected points was changed to raster in Arc Map using the LAS dataset to raster tool (rasterization) (Sumerling, 2011). The interpolation of DSM and DTM was using the same cell size with a maximum and average cell assignment respectively (in DSM result biasing to higher elevation but, in DTM average interpolation is best). The DSM represents the earth surface including objects on it while the DTM is only the bare ground surface.

#### **3.3.4.2. Airborne LiDAR canopy height model (CHM) generation**

CHM also called normalized DSM represents the heights of all objects above the ground. The CHM was generated by subtracting DTM from DSM (DSM-DTM) in Arc GIS using raster calculator. The out of the calculation is not the absolute tree height and needs noise removal (Magar, 2014). The output was inspected, and the generated CHM showed extreme heights which were not absolute tree heights in reality (since the heights of the tree in the forest were not more than 50 m). Thus, all the noise points were removed using raster calculator and kept the CHM values between zero and 50m.

### **3.3.5. UAV Image Processing**

#### **3.3.5.1. DSM, DTM and Orthophoto generation from UAV imagery**

UAV image was processed with Agisoft photo scan professional version 1.3.4. Software, which was used by Torres-Sánchez et al., (2015). Agisoft Photoscan Professional software works through the principle of structure from motion (SfM) and contains the following steps: uploading photographs in to Agisoft photo scan professional, inspecting uploaded images, removing random photos, load camera positions, photo-alignment, adding ground control points for geo-referencing, optimize camera alignment, dense point cloud generating, building a mesh, creating DTM and DSM, build ortho-mosaic and export results (Figure 14). During photo-alignment, the software searches for common points on consecutive images and reconstructs the approximate camera position based on GPS, pitch roll, and yaw data which were recorded simultaneously with the photograph. The result of this step is a sparse 3-D (x, y & z) point cloud. From this point cloud, a mesh (a 3-D surface model) is derived, which is a required intermediate step if Ground Control Points (GCP's) are being used. The next step is locating the markers of the GCP's on the images and entering the corresponding x, y and z value, which were obtained by Differential Global Positioning System (DGPS) in the field. After placing the markers, the camera orientation is re-calculated and possible distortion is corrected based on the added GCP's and a dense point cloud can be constructed. The dense point cloud is the input for the DSM and DTM. The DSM is a surface model consisting of a regular grid of height values. The DTM is also a regular grid with height values, but these values are the result of interpolation between those pixels which were classified as "ground points". The DSM in its turn the input for the Ortho-mosaic The DSM, DTM, and Ortho-mosaic were produced from

**TOWARDS A UAV BASED STANDALONE SYSTEM FOR ESTIMATING AND MAPPING  
ABOVEGROUND BIOMASS/ CARBON STOCK IN BERKELAH TROPICAL RAIN FOREST,  
MALAYSIA**

average point cloud density of 121points/m<sup>2</sup> and with ground resolution 4.57 cm/pix. The Ortho-photo, DSM, and DTM were generated with an average error of 1.7cm in the X, Y and Z using the ground control points. The main steps of UAV image processing in agisoft photo scan are illustrated in Figure 14.

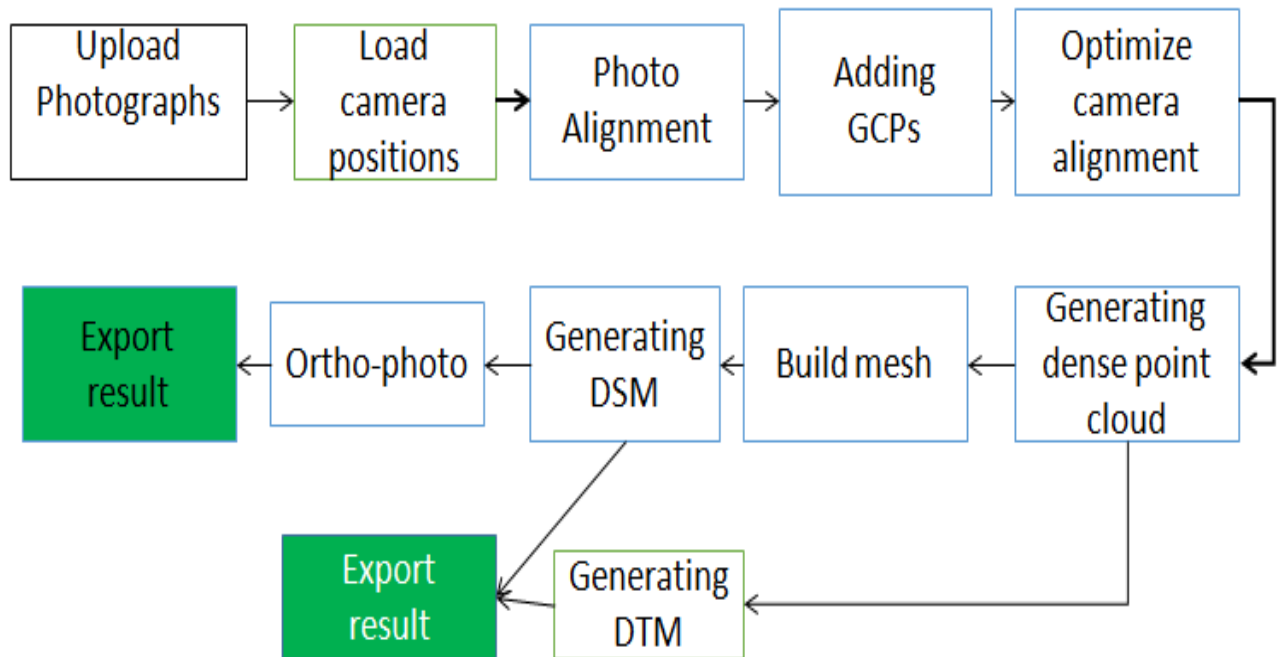


Figure 14: Illustration of the main UAV image processing in Agisoft photo scan pro.

### 3.3.5.2. UAV Canopy height model (CHM) generation

The canopy height model (CHM) of UAV 3D point cloud was generated by subtracting the DTM from the DSM in Arc-GIS 10.5 using the raster calculator similar to LiDAR CHM. The CHM was made ready for individual tree height extraction by removing the negative and more than 50 m height values (Magar, 2014).

### 3.3.6. CPA manual delineation and circularity measure

Research has shown that there exists a relation between CPA and DBH (see section 1.2) and image segmentation, based OBIA using e-Cognition software and has proven to be a successful technique to extract the CPA from a remote sensing image. However, the strength of the relationship is negatively affected when the tree crowns are interlocking or occluded, and not completely visible in a remote sensing image, which is the case in the complex canopy structure of a tropical rainforest. In this research, it is attempted to adjust incomplete tree crowns with a circularity measure and establish the relationship with the DBH. This was done in some steps:

1. Manual delineation the outer boundary by on-screen digitizing of fully visible tree crowns (CPA) on the UAV-orthophoto and assessing the relation with the corresponding DBH.
2. Applying a circularity measure in the manually digitized tree crowns (Adjusted CPA) and assesses the relation with the corresponding actual CPA and DBH.
3. Segmenting the orthophoto with object-based image analysis using e-cognition software and assessing the relation with the DBH
4. With the segmented image as input, use the circularity measure from step 2 to complete partially visible tree crowns, resulting in an adjusted CPA and assess the relationship with the corresponding DBH.

**TOWARDS A UAV BASED STANDALONE SYSTEM FOR ESTIMATING AND MAPPING  
ABOVEGROUND BIOMASS/ CARBON STOCK IN BERKELAH TROPICAL RAIN FOREST,  
MALAYSIA**

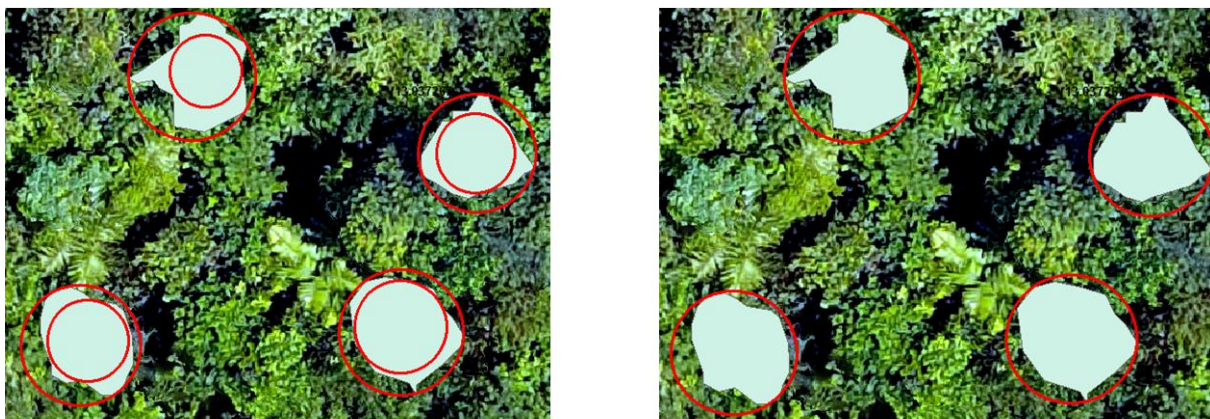
**Manual delineation of the CPA**

In this research identifying and delineating fully visible crowns is crucial for the development of CPA-DBH relationship in the study area. In this step, 55 visible tree crowns were identified in the UAV Orthophot, and the actual CPA was digitized on-screen using ArcGIS. The actual CPA's are input for the accuracy assessment of the Object-based Image Analysis (OBIA), and when combined with the corresponding DBH's was the input for linear regression.

**Circularity measure**

Object-based image analysis for tree crown delineation in the complex forest is hampered by intermingling crowns and occlusion incompleteness of crown projection area in lower forest layers. Even though roundness is a parameter in multiresolution segmentation algorithm, still it does not solve the challenge of incomplete crowns of multilayer forest canopy. For this reason, this study investigates if a circularity measure can be used to approximate the CPA of those crowns which are only partially visible on the UAV image. The word circularity in this study refers to the crown projection area of a tree assuming the shape of tree crown as circular to estimate the actual crown projection area of incompletely visible tree crowns.

Before adjusting the CPA of incomplete tree crowns (step 4), a test was done to assess the effect of a CPA circularity measure (adjusted CPA) on the relationship with the real CPA and DBH. In this test, a circle was fitted on the visible tree crowns and comparing the adjusted CPA with actual CPA. Figure 15(a) and (b) show the possibilities of fitting circles to the fully visible crowns.



a) Inner and Outer circle fitting

b) single circle fitting

Figure 15: Illustration of fitting circularity on manually delineated CPA.

The effect of fitting inner, outer and intermediate circles was tested in the fully visible tree crowns. To test the relation between the actual CPA and adjusted CPA (intermediate circle), the following procedure was applied.

1. Fit the inner circle to the arc of actual in Arc Map
2. Fit the outer circle to the arc of actual crown in Arc Map
3. Drive the radius for both circles ( $R =$  outer circle radius and  $r =$  inner circle radius)
4. Subtract inner circle radius from outer circle radius and divided by two  $(R-r)/2$  and add to the inner circle radius to arrive at the intermediate circle (Appendix 2)

*Area of inner circle*  $= \pi r^2$  (Inner circle CPA) and *Area of outer circle*  $= \pi R^2$  (outer circle CPA) were calculated in Arc Map. The area of an intermediate circle (adjusted CPA) was calculated as follows:

**TOWARDS A UAV BASED STANDALONE SYSTEM FOR ESTIMATING AND MAPPING  
ABOVEGROUND BIOMASS/ CARBON STOCK IN BERKELAH TROPICAL RAIN FOREST,  
MALAYSIA**

$$R \text{ adjusted} = [(R-r)/2] + r$$

Therefore, the area of adjusted CPA is calculated using equation 1.

Equation 1: Area of adjusted CPA

$$\text{Adjusted CPA} = \pi(R \text{ adjusted})^2 \dots\dots\dots 1$$

Where;

CPA; crown projection area

r; the radius of the inner circle

R; radius of outer circle

**3.3.7. Multiresolution segmentation**

UAV derived orthophoto was segmented using the region-based segmentation technique within e-Cognition software. This technique can extract information from the image by classifying spatially and spectrally similar pixels to a homogenous area to form an image object (tree crown). In this algorithm, segmentation starts from a single pixel and subsequently grows until a particular image object is formed. After continuous merging of a single pixel or seed pixels and image object was built, new seeds placed and a new process was repeated (Blaschke et al., 2004). Merging of smaller objects to create a bigger object were based on homogeneity criteria such as colour, smoothness and compactness parameter which determine segment heterogeneity (Carleer et al., 2005).

The region growing segmentation was implemented through multiresolution segmentation algorithm to maximize homogeneity of segmented objects (Benz et al., 2004). Watershed transformation algorithm with the aid of average crown diameter estimated in the field and expert knowledge was applied to the analysis to separate the tree crown intermingles.

The orthophoto segmentation was done using multiresolution segmentation algorithm. According to Okojie, (2017), the ortho-photo resolution was resampled to 20 cm before segmentation since the high-resolution image can create the salt-and-pepper problems during segmentation.

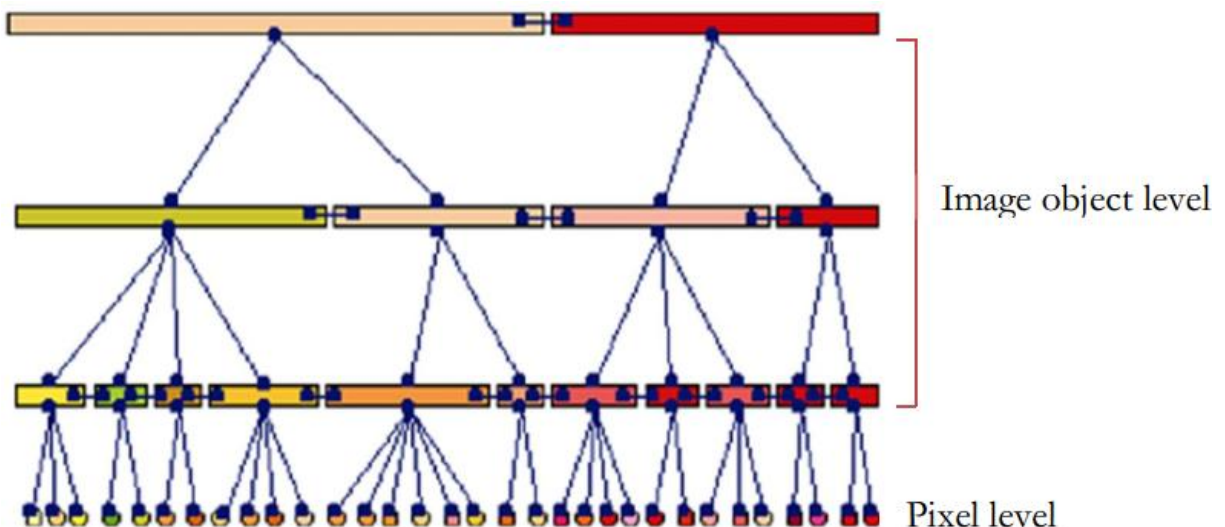


Figure 16: Illustration of multi-resolution segmentation process (Benz et al., 2004).



# TOWARDS A UAV BASED STANDALONE SYSTEM FOR ESTIMATING AND MAPPING ABOVEGROUND BIOMASS/ CARBON STOCK IN BERKELAH TROPICAL RAIN FOREST, MALAYSIA

## 3.3.7.1. Watershed Transformation

This algorithm is crucial to separate clusters into individual objects. As the watershed has a water dividing line which is important to separate one catchment area from the other; tree crowns which are intermingled each other needs like a watershed dividing ridge assuming the margin of the tree crowns as dividing line. As a watershed has a common outlet point in the topographical surface, the tree crowns have branches as the water streams and the stem of the tree as a common outlet. Individual objects can split when individual catchments touch each other so as manage sub-watersheds separately defining those dams as segmentation results Figure 17 (Derivaux et al., 2010). Based on this principle and using this algorithm intermingled cluster tree crowns were separated in the e-cognition software. The parameter which was decided in the watershed transformation algorithm as a length factor was 40 pixels since the appropriate resolution of the segmented ortho-photo was 20cm. This is based on the average size of tree crowns measured in the field, viz. 8m, which corresponds to 40 pixels. However, some of the tree crowns are split up into more than one segment and have an irregular shape. To minimize this problem refinement of some tree shapes is necessary using morphology algorithm.

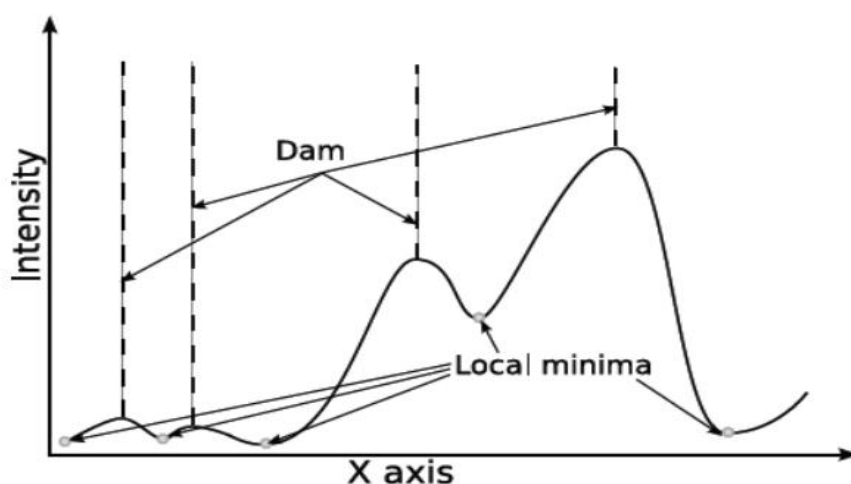


Figure 17: Illustration of the watershed transformation principle (Derivaux et al, 2010).

## 3.3.7.2. Morphology

Morphology is a mathematical algorithm applied to refine segmented objects by smoothing the boundaries of tree crowns. This refinement is either by removing pixels causing an irregular object shape or adding surrounding pixels to an image object to fill small holes inside the segmented area (Drăguț et al., 2010). Moreover the circular and square mask options in morphology are the parameters for refinement of the tree crowns. Circular mask and close image object are appropriate to refine the irregular shape since most projected tree crown shape is close to circular.

## 3.3.7.3. Removal of undesired objects

Undesired object removal was done to remove the remaining undesired objects after completing the segmentation procedure. Some very tiny objects with an area less than 20 pixels have been removed. These correspond to trees with a crown diameter of fewer than 2 meters and whose biomass would hardly contribute to the total carbon stored in the forest. In addition to this elongated features in the segmented image were removed since unlikely represent trees.

## 3.3.7.4. Segmentation Accuracy Assessment /Validation

Segmentation accuracy assessment was performed by confronting the manually segmented tree crowns with the corresponding segment in the classified image. The assessment considers the topological and

**TOWARDS A UAV BASED STANDALONE SYSTEM FOR ESTIMATING AND MAPPING  
ABOVEGROUND BIOMASS/ CARBON STOCK IN BERKELAH TROPICAL RAIN FOREST,  
MALAYSIA**

geometrical relationships of the tree crowns (Möller et al., 2007). Topological relationships of tree crowns deal with ‘containment’ and ‘overlap’, while the comparison of crown positions assesses geometric relationships.

If the automatically segmented crown areas fully enclose the manually digitized crown areas, it is a perfect segmentation. Minimum acceptable accuracy is 50% of reference and automatic segment overlap (Zhan, 2005).

There are four matching cases of segmented objects (CPA) with their manually digitized reference objects (CPA) (Figure 18). The orange part of the polygon is matching well between the automatic segment and its manually digitize reference polygon; green part is the region in the segmented object not explained by its reference whereas blue part is a region in reference object but not described by the segmented object.



Figure 18: Matching cases of an extracted object (Zhan et al., 2005).

Figure 25 (a) shows the overlap between a reference polygon and an automatic segment of more than 50%; (b) shows matching of both objects in size and shape but not location and in (c) and (d) the position of reference polygon and automatic segments matched but with variation in spatial extent. The segmentation accuracy was assessed by comparing the e-cognition results with manually delineated tree crowns (Clinton et al., 2010).

Equation 2: Over segmentation equation model

$$\text{Over segmentation}_{ij} = 1 - \frac{\text{area}(X_i \cap Y_j)}{\text{area}(X_i)} \dots\dots\dots 2$$

Equation 3: Under segmentation equation model

$$\text{Under segmentation}_{ij} = 1 - \frac{\text{area}(X_i \cap Y_j)}{\text{area}(Y_j)} \dots\dots\dots 3$$

Where;

X<sub>i</sub>: Reference object manually segment crown (on screen digitized objects)

Y<sub>j</sub>: corresponding segmented object by e-Cognition  $\sqrt{\text{oversegmentation}^2 + u} + \text{under segmentation}$

Equation 4: Measures of goodness

$$D = \sqrt{\frac{\text{over segmenation}^2 + \text{under segmenation}^2}{2}} \dots\dots\dots 4$$

Where;

D; is closeness of fit or segmentation goodness

The value of over and under-segmentation lies within the range of 0 to 1, where 0, for both over and under-segmentation, means that training object is matching the segments (Clinton et al., 2010). The segmentation goodness or closeness of fit (D) is a measure of error in segmentation (equation 3). D value equals to zero (0) means the segmentation is perfect.

**TOWARDS A UAV BASED STANDALONE SYSTEM FOR ESTIMATING AND MAPPING  
ABOVEGROUND BIOMASS/ CARBON STOCK IN BERKELAH TROPICAL RAIN FOREST,  
MALAYSIA**

**3.3.8. CPA adjustment**

To complete the CPA of partially visible tree crowns a circularity measure was applied, assuming that a circle is a reasonable approximation of the real crown shape and size (see section 3.4). A circle was formed using the best fit of the circle with the arc of the outer boundary of the visible part of the crown of the lower trees on the segmented orthophoto. The lower tree crowns were identified with the help of the tree height derived from the UAV CHM.

After segmentation in e-Cognition, incomplete tree crowns of lower trees (Figure 19 A, B &C) were selected on the high-resolution ortho-photo, taking tree height into consideration (see section 3.8). In figure 19 the trees A, B and C are incomplete crowns while trees 1, 2 and 3 are the nearby higher trees where the crown is completely visible on the image. Tree A is shorter than tree number 1, tree B is shorter than tree number 2, and tree C is shorter than tree number 3 and tree B. All trees have their corresponding CPA derived from the segmented orthophoto, but, CPA of the incomplete tree crowns will be underestimated. The underestimation problem was minimized by replacing the original segment by the adjusted CPA (the red circles in Figure 19).

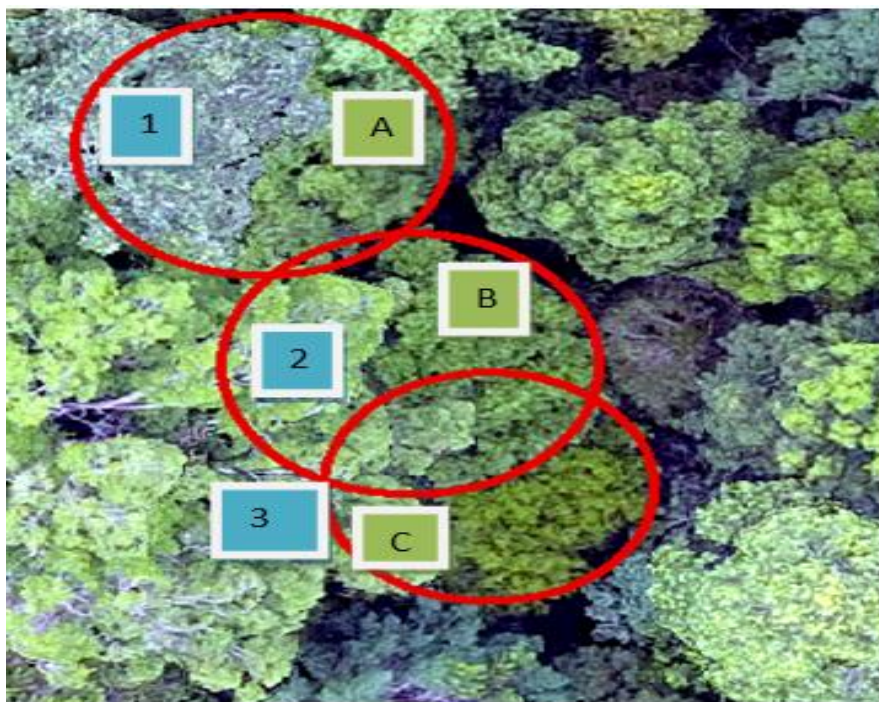


Figure 19: Illustration of CPA adjustment after segmentation.

Figure 19: shows 1, 2 and 3 are tall trees and A, B and C are short trees with partially visible crowns while the red circles are the adjusted CPA's of the incompletely visible crowns.

**3.3.9. Tree Height extraction from UAV and airborne LiDAR-CHM**

The allometric equation for aboveground biomass calculation used in this study requires DBH and tree height as input parameters (Chave et al., 2014). In this study, the extraction of tree height was done by overlaying the segmented shapefile on both the co-registered UAV-CHM and the airborne LiDAR-CHM in Arc Map and run the zonal statistics tool. The maximum values in the attribute of zonal statistics outputs were used as the tree heights.



**TOWARDS A UAV BASED STANDALONE SYSTEM FOR ESTIMATING AND MAPPING  
ABOVEGROUND BIOMASS/ CARBON STOCK IN BERKELAH TROPICAL RAIN FOREST,  
MALAYSIA**

**3.3.10. Individual tree Matching**

Appropriate field data collection and matching with its corresponding image information needs great attention. For this reason, the DBH data collected in the field needs to match with its corresponding tree height derived from UAV and airborne LiDAR-CHM. A spatial join function was used to match the segmented polygons and field DBH using the coordinates of the trees as recorded in the field in Arc Map. But, tree matching using tree location coordinate has a shift problem. Therefore, a circle with the radius of the field plot was placed in each plot and coordinates which were not inside the plot were matched manually through visual identification which segment belongs to which tree using the high-resolution orthophoto. Matching trees extracted from UAV-CHM and airborne LiDAR-CHM is not difficult since the segmented shapefile used to extract tree height from both CHM was the same. Trees which have height and DBH information in both data (extracted from UAV-CHM and airborne LiDAR-CHM) were considered for tree height and biomass accuracy assessment. In total 305 trees were matched in both UAV and airborne LiDAR-CHM.

**3.3.11. Data analysis**

Data analysis was performed using appropriate techniques of statistical analysis to test the hypothesis and achieve specific objectives. The main methods of statistical analysis which were applied in this study are descriptive statistics, regression, RMSE, the percentage of RMSE, correlation, F-test, paired t-test and independent t-test for two samples. Data normality was checked using SPSS software. The RMSE and percentage of RMSE were calculated using the equation used by Sherali et al., (2003) to compare the closeness of two parameters of the forest(Equation 5 &6).

Equation 5: Equation of RMSE computation

$$RMSE = \sqrt{\sum_{i=1}^n (y_i - \hat{Y})^2 / n} \dots\dots\dots 5$$

Equation 6: Equation of %RMSE computation

$$\%RMSE = RMSE * n * 100 / \sum Y_i \dots\dots\dots 6$$

Sources: (Sherali et al., 2003)

Where;

RMSE: Root mean square error

%RMSE: Percentage of RMSE

Y<sub>i</sub>; Original value of dependent variable

Ŷ; Predicted value of dependent variable and n is number of observations

**3.3.11.1. Comparison of actual and circularity measured CPA**

The inner, outer and intermediate circularity measures of CPA accuracy assessment before applying the method on incompletely visible tree crowns is important. Based on this principle, 76 fully visible tree crowns were delineated manually following the outer edge of individual tree crowns. And inner and outer circles were fitted to it in Arc Map. Since these selected trees were measured by fitting three rings (inner, outer and intermediate) it is time-consuming to delineate more than 76 trees. The area of the intermediate circle was calculated using equation1 (section 3.3.6). The mean difference between actual and circularity measured CPA's was tested using paired t-test since the CPA comparison is between the same tree measured by one hand. The RMSE and %RMSE were used to evaluate the deviation of the circularity measured CPA from the actual CPA.

**TOWARDS A UAV BASED STANDALONE SYSTEM FOR ESTIMATING AND MAPPING  
ABOVEGROUND BIOMASS/ CARBON STOCK IN BERKELAH TROPICAL RAIN FOREST,  
MALAYSIA**

**3.3.11. 2. Delineated and circularity measured CPA and DBH relationship**

A total of 55 fully visible tree crowns (55 trees) were manually delineated (onscreen digitizing) using Arc GIS on the orthophoto for preliminary analysis of the relationship between CPA and DBH. Similarly, a circularity measure was applied with the best fit circle. A linear regression analysis was performed, and the linear and power trend line was fitted to check the relationship between actual CPA and DBH as well as between circularity measured CPA and DBH.

**3.3.11.3. Relationship between DBH and CPA**

CPA obtained from segmentation result is an important variable to predict DBH (see section 1, 1.2 & 2.8). In this study, the linear and power models were proposed to assess the relationship between CPA and DBH. To do that, the area of the segmented shapefile was calculated in Arc GIS. Out of 305 matched tree 207 trees (matched trees in section 3.3.10) was used for relation. The DBH of matched trees were regressed with their corresponding DBH using linear regression. The scatter plot was plotted, and trend line was fitted. The root mean square error and percentage of root mean square error was calculated. The result of the relationship was observed and used to evaluate the relationship between adjusted CPA and DBH.

Incompletely visible tree crowns were selected and adjusted using the fittest circularity measure, and the adjusted CPA replaced the segmented CPA. Since the objective is to assess the relationship between CPA and DBH after incompletely visible tree crowns adjustment, the adjusted CPA and normal CPA were mixed. The mixed CPA hereafter called adjusted CPA. The adjusted CPA and DBH were regressed and the scatter plot and trend line was fitted. The root mean square error and percentage of root mean square error was calculated to evaluate the relationship.

The improvement in the relationship between CPA and DBH after CPA adjustment was observed and discussed. Based on the best model, DBH was predicted using 88 trees which were not used in the model development and the predicted DBH was validated using DBH measured in the field. The scatter plot was plotted, and the trend line was fitted to check if it is close to linear. Two sample t-test assuming equal variance was performed to test the significance of the mean difference between predicted and observed DBH.

**3.3.11.4. Comparison of UAV and airborne LiDAR derived tree height**

Altitudes from UAV derived DTM and airborne LiDAR-derived DTM were validated by altitudes from DGPS (differential global positioning system) to check the influence of DTM heights on absolute tree height estimation (Jensen & Mathews 2016). During the field data collection, 35 location coordinates were collected from 4 UAV flight plans using DGPS to generate and georeference orthophoto. Those collected data were used to test the deviation of UAV DTM and airborne LiDAR DTM from the ground truth. The UAV and LiDAR DTM heights were extracted from point locations where the ground truth Z-values (altitudes) was collected. The RMSE and percentage of RMSE were calculated, and the UAV derived DTM accuracy was observed and evaluated in the open land surface. The tree height derived from the UAV-CHM was compared to the tree height derived from the airborne LiDAR-CHM, using a two-sample assuming equal variance t-test for means of two samples. The tree height from airborne LiDAR CHM was considered as accurate since they are actual measurements (Jensen & Mathews 2016; Magar, 2014; Ruben, 2017; Patenaude et al., 2005; Balzter et al., 2007; Lafsky et al., 2002), while the UAV-CHM tree height is an approximation. Also, the two sample t-tests assuming equal variance, RMSE, and percentage of RMSE were performed to compare between tree heights derived from UAV derived CHM and airborne LiDAR-derived CHM.

**TOWARDS A UAV BASED STANDALONE SYSTEM FOR ESTIMATING AND MAPPING  
ABOVEGROUND BIOMASS/ CARBON STOCK IN BERKELAH TROPICAL RAIN FOREST,  
MALAYSIA**

**3.3.11.5. Aboveground Biomass estimation**

The most common nondestructive method of AGB estimation is applying allometric equation (Ketterings et al., 2001) which allows estimating AGB of large forest areas. The allometric equation uses structural forest parameters that can be regularly measured in the field as input. Even though there are numerous allometric equations for biomass estimation, environmental suitability should be undertaken into consideration in selecting the appropriate equation. In tropical rainforest which is endowed with species diversity, applying regional or local model is not recommended (Gibbs et al., 2007). A model which developed based on large trees enhances the precision of AGB estimation (Gibbs et al., 2007; Chave et al., 2005). Therefore, the AGB was assessed using the generic allometric equation developed by Chave et al., (2014) which is widely used in a tropical rainforest (Equation 7).

Equation 7: Allometric equation model

$$AGB = 0.0673 * [(p * D^2 * H)] ^ (0.976) \dots\dots\dots 7$$

Where;

AGB is the aboveground biomass in (kg)

D; is Diameter at Breast Height (DBH) (cm)

H; is tree height (m)

P; is tree specific wood density (g/cm<sup>3</sup>)

The carbon stock was calculated using the equation proposed by (Brown, 1997; Drake et al., 2002; Burrows et al., 2002; Houghton & Hackler, 2000), 50% of estimated biomass is carbon.

Equation 8: Carbon stock estimation

$$C = AGB \times CF \dots\dots\dots 8$$

Where:

C: is above ground carbon stock (Mg)

CF: is a fraction of aboveground biomass (0.5)

The above ground biomass estimation was tree based. Because the relationship between CPA and DBH depends on the number of matched trees and the model should be apply to the whole study area.

Therefore, it would be easy to estimate the total above ground biomass in the study area.

**3.3.11.6. Regression and model validation**

Regression analysis is a technique which determines the relationship between dependent and independent variables statistically. It determines the change in the dependent variable as the result of a change in the independent variable (Husch et al., 2003). This statistical method of analysis is important for modelling the relationship between remotely sensed and observed data (Popescu, 2007; Lim et al., 2003). Since the objective of this study is to estimate AGB/carbon stock from UAV derived forest parameters, regression is very important to develop the relationship between CPA from UAV derived orthophoto and DBH measured in the field. To assess the relationship between Circularity measured CPA and DBH measured in the field as well as the relationship between actual CPA and DBH measured in the field as preliminary analysis. In addition to that regression analysis was performed to develop the best model (linear or power) before segmented CPA adjustment and after adjustment to predict DBH. To assess the performance of the selected model RMSE was calculated using equation 5 (section 3.3.11)

**3.3.11.7. Comparison of AGB-UAV and AGB-field**

The above ground biomass of matched trees in both airborne LiDAR and UAV derived CHM was used for biomass accuracy assessment calculation using the allometric equation in section 3.3.11.4. The input parameters were the trees matched between UAV and airborne LiDAR-derived CHM and the field DBH.

**TOWARDS A UAV BASED STANDALONE SYSTEM FOR ESTIMATING AND MAPPING  
ABOVEGROUND BIOMASS/ CARBON STOCK IN BERKELAH TROPICAL RAIN FOREST,  
MALAYSIA**

To assess the accuracy of AGB-UAV 150 trees (75 adjusted CPA and 75 segmented not need adjustment) were selected. Since the objective is to estimate aboveground biomass based on segmentation and CPA adjustment, fifty-fifty sample supports to evaluate the impact of the adjusted CPA on biomass. The above ground biomass estimated from UAV (AGB-UAV) was used the tree height extracted from UAV-CHM and predicted DBH. The aboveground biomass estimated from field or field-based (AGB-field) was used tree height extracted from airborne LiDAR-CHM, and DBH measured in the field.

The calculated AGB-UAV and AGB-field was compared using scatter plot and RMSE. In addition to that, independent t-test (assuming equal variance) was applied to test if there is a significant difference between the AGB-UAV and AGB-field. Finally, the mean difference between AGB-UAV and AGB-field was evaluated.

**3.3.11.8. Carbon stock mapping**

Carbon stock mapping based on the UAV-AGB/carbon stock estimated from manually adjusted CPA for the entire study area is tedious work and needs time. In this study, as an example, the amount of carbon stock based on segmented CPA and tree height derived from UAV imagery was used and mapped. The estimated AGB/carbon stock is to show the possibility of carbon stock mapping using UAV imagery. The allometric equation for the tropical forest was used to calculate the carbon stock of each tree in UAV flight plan-2 (block2) of the study area. DBH and tree height were predicted and estimated from segmented CPA and UAV-CHM respectively. Carbon stock map of UAV flight block two was prepared in Arc Map 10.5 due to time limitation though the method could be applied to the whole study area.

## 4. RESULTS

### 4.1. DTM, DSM and CHM generation from airborne LiDAR data

Airborne LiDAR data was processed, and the DSM, DTM and CHM were produced (Figure 20). The extracted ground and first return points were interpolated, and the DTM and DSM were generated respectively (Figure 20 a & b). The CHM was produced by subtracting DTM from DSM (Figure 20 c).

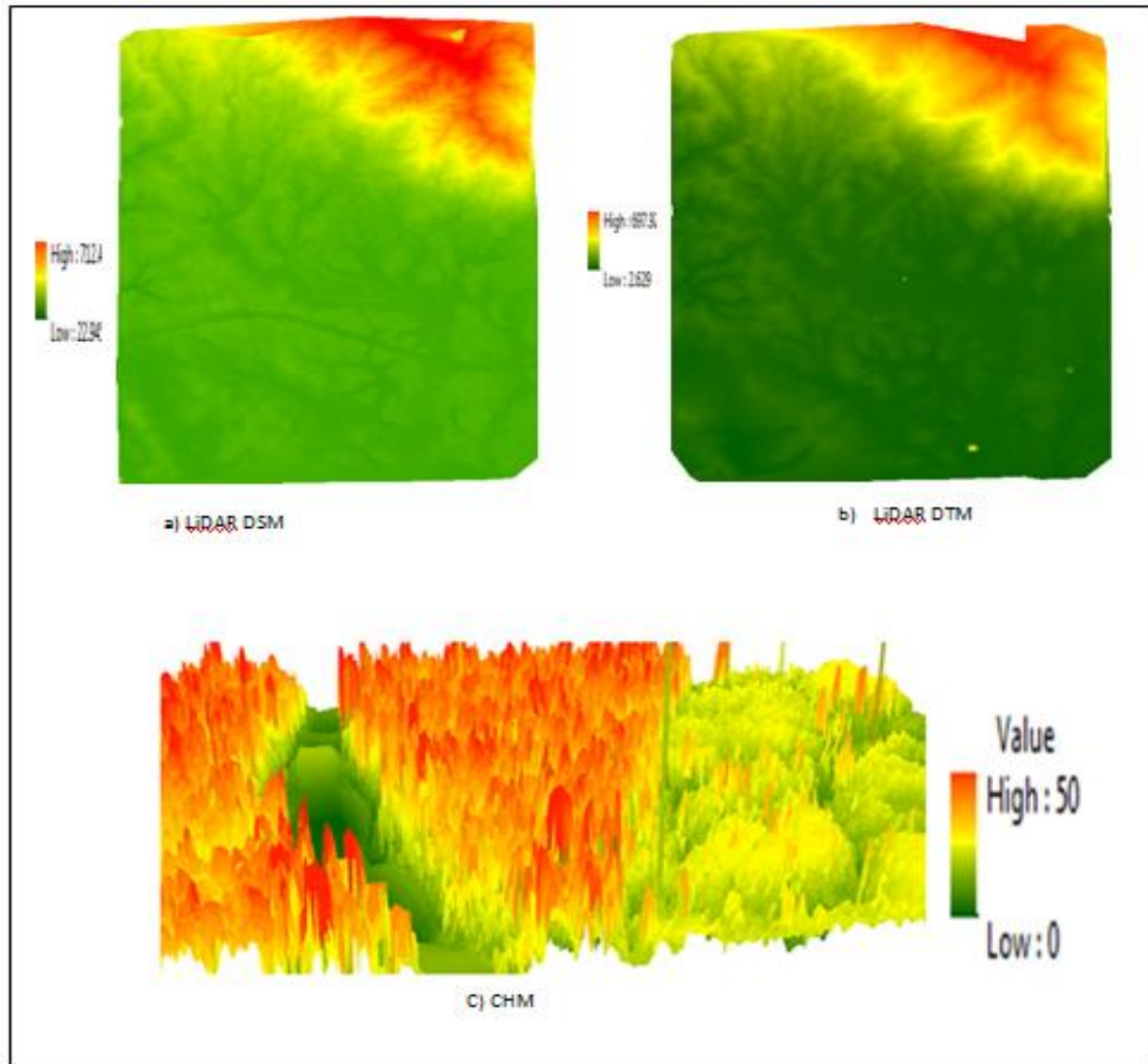


Figure 20: Airborne LiDAR-derived images (the top left DSM, top right DTM, and bottom CHM). Figure 20: shows the products of airborne LiDAR data process, the top left airborne LiDAR-derived DSM, the top right DTM and the bottom is a sample 3-D representation of the CHM based on airborne LiDAR data. Where minimum 0 m is ground surface and 50 m maximum canopy height after negative and above 50 m heights were removed.

**TOWARDS A UAV BASED STANDALONE SYSTEM FOR ESTIMATING AND MAPPING  
ABOVEGROUND BIOMASS/ CARBON STOCK IN BERKELAH TROPICAL RAIN FOREST,  
MALAYSIA**

**4.2. DSM, DTM , CHM, and orthophoto generation from photogrammetric image processing**

The photogrammetric image processing was done. The canopy height model was generated from the UAV 3-D point cloud (Figure 21). The dense point cloud was used as input for the DSM and DTM. After the dense point cloud was classified into the ground points and the rest, DTM and DSM were created (Figure 21 top left DSM, top right DTM). The orthophoto was generated from the dense point cloud automatically by selecting the build orthomosaic command from the work flow of the agisoft photo scan (Figure 21).

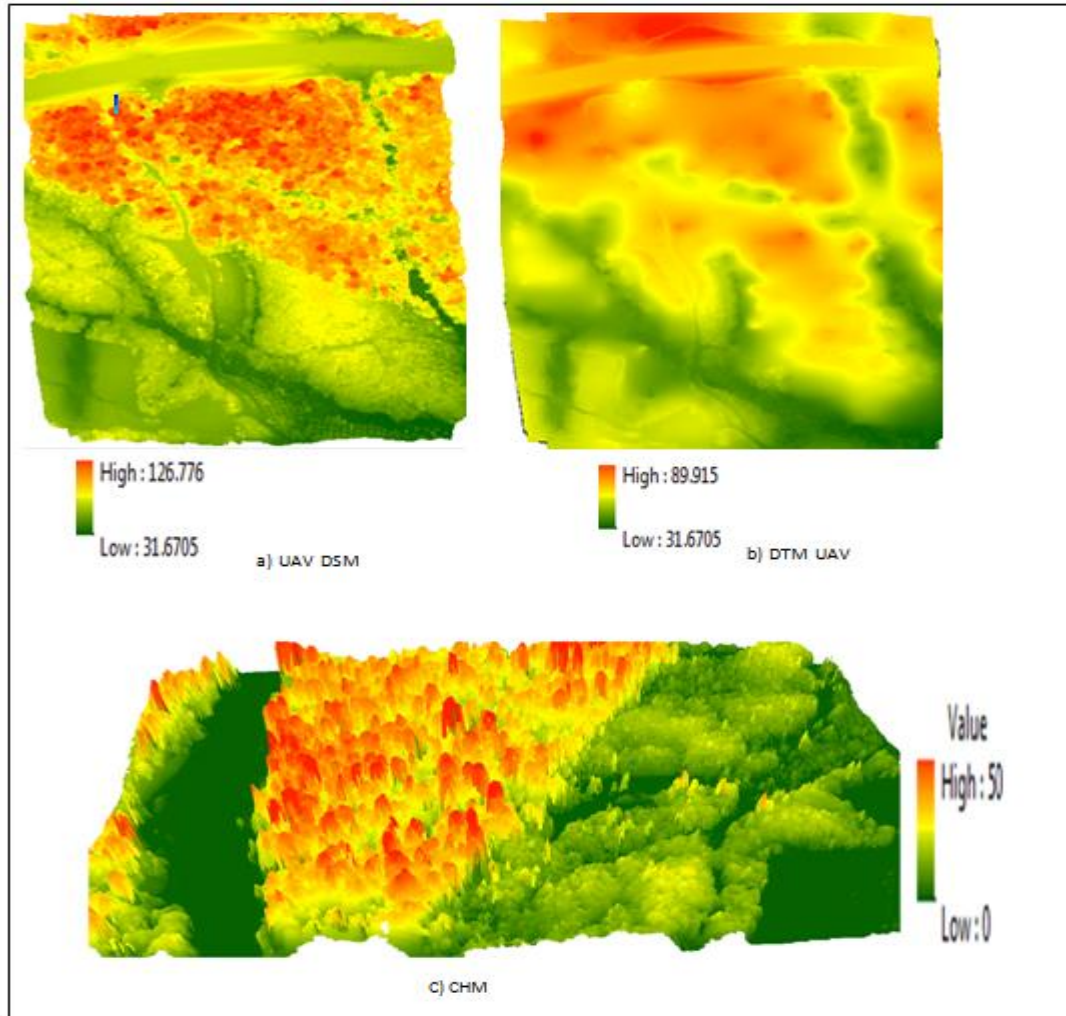


Figure 21: Agisoft UAV image processing results: DSM (a) DTM (b) CHM (c).

Figure: 21 showed the Agisoft photo scan UAV image processing results of flight block 2 (The top left DSM, the top right DTM, the bottom 3-Drepresentation of CHM after extreme heights removal).

The DSM height (Figure 21top left) ranges from 31.6 to 126.7m while the DTM (Figure 21 top right) ranges from 31.6 to 89.9 m. the DSM height is larger than the DTM height. The obtained CHM and DTM were used to assess UAV derived tree height accuracy assessment.



**TOWARDS A UAV BASED STANDALONE SYSTEM FOR ESTIMATING AND MAPPING ABOVEGROUND BIOMASS/ CARBON STOCK IN BERKELAH TROPICAL RAIN FOREST, MALAYSIA**

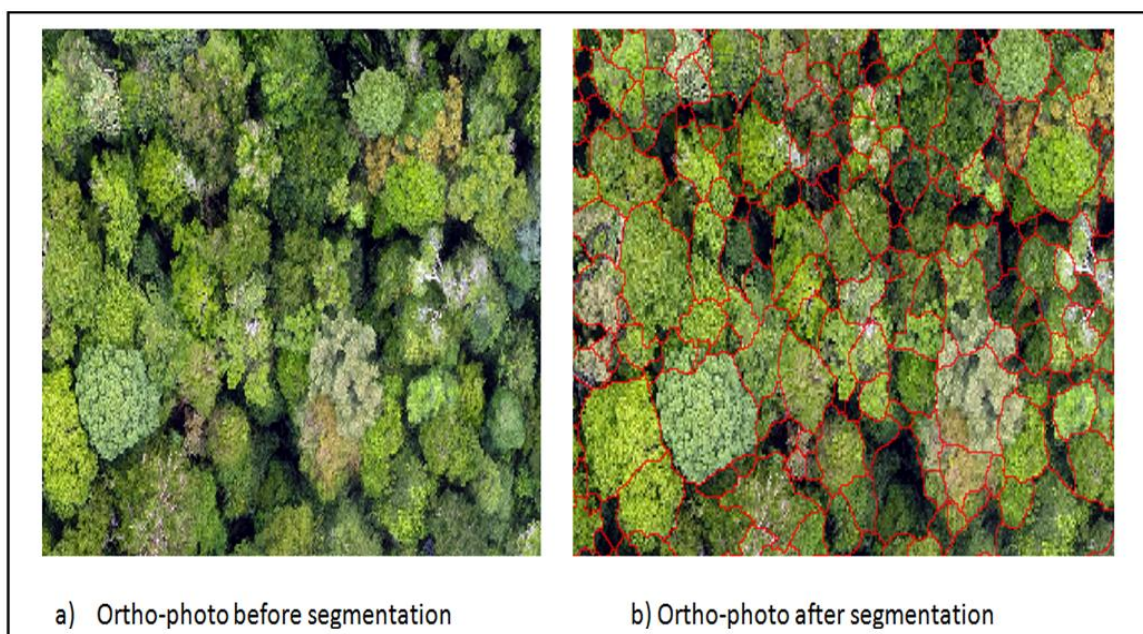


Figure 22 : Small part of orthophoto generated from UAV image.

Figure 22 shows an example of orthophoto generated in agisoft photo scan pro. The produced orthophoto is input for segmentation and manual delineation of tree crowns.

#### **4.3. Multiresolution segmentation**

In this study, multiresolution segmentation was done on the resampled 20 cm resolution orthophoto. The scale parameter, shape, and compactness which perform the best segmentation are 25, 0.8 and 0.5 respectively for flight blocks two and three while 25, 0.7 and 0.5 for flight blocks one and four (Figure 23).



a) Ortho-photo before segmentation

b) Ortho-photo after segmentation

**TOWARDS A UAV BASED STANDALONE SYSTEM FOR ESTIMATING AND MAPPING  
ABOVEGROUND BIOMASS/ CARBON STOCK IN BERKELAH TROPICAL RAIN FOREST,  
MALAYSIA**

Figure 23: Orthophoto before and after segmentation.

**4.4. segmentation accuracy**

The accuracy of segmentation was assessed by comparing with manually delineated crown polygons. Visible crowns were digitized manually on screen in Arc Map. Manually digitized polygons were then compared with automatically generated polygons of ortho photo as shown in Figure 24.

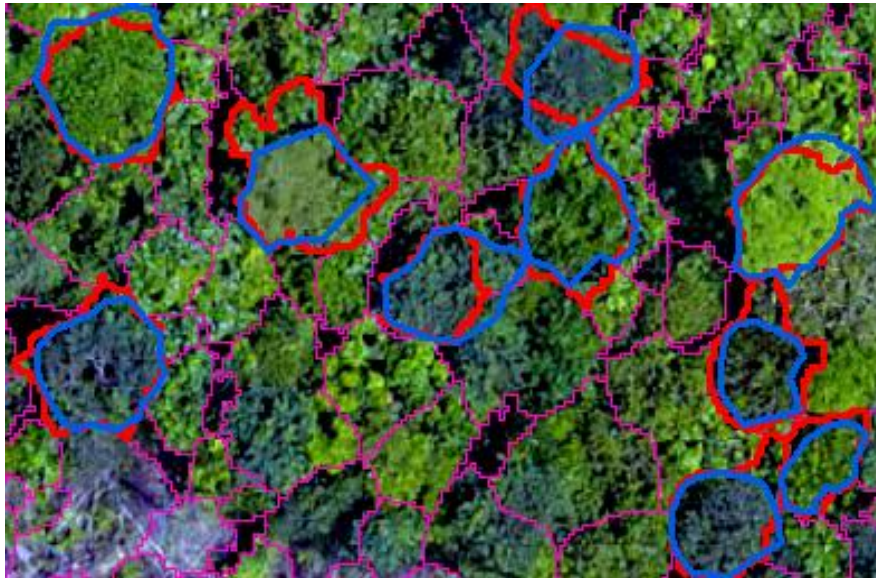


Figure 24: Manually delineated and segmented crowns for accuracy assessment.

Figure 24, the purple lines show the segmented shapefile and the blue lines are manually delineated tree crowns while the red lines are the segments corresponding with the manually delineated crowns.

The automatically segmented polygons were compared with manually delineated reference crowns and the over and under-segmentation errors were assessed. Accuracy assessment was done based on assessing segmentation goodness (D) (Equation 4). The segmentation error was 26.6% hence the segmentation accuracy was 73.4% while, using 1:1 manual matching of polygons resulted in 77% accuracy. The segmentation accuracy assessment result is summarized in Table 3

Table 3: Segmentation accuracy assessment result.

Total reference polygon	Total 1:1 matched polygon	Over-segmentation	Under-segmentation	Goodness of fit (D)
277	212	0.24	0.29	0.266
Accuracy (%)	77			73.4



**TOWARDS A UAV BASED STANDALONE SYSTEM FOR ESTIMATING AND MAPPING  
ABOVEGROUND BIOMASS/ CARBON STOCK IN BERKELAH TROPICAL RAIN FOREST,  
MALAYSIA**

**4.5. Descriptive statistics of field data**

The descriptive statistics result of collected DBH is shown in Table 4.

Table 4: Descriptive statistics of field DBH.

<b>Descriptive Statistics</b>						
	N	Minimum	Maximum	Mean	Std. Deviation	Variance
	Statistic	Statistic	Statistic	Statistic	Statistic	Statistic
DBH(cm)	1033	5.00	104.50	20.6171	12.48672	155.918

The normality of the collected data was checked in SPSS software and it was not normally distributed. The histogram and normal distribution curve of the data were as shown in figure 25. The Kolmogorov-Smirnov and Shapiro Wilk test are indicating not normally distributed data. The skewness value is less than one and skewed to the right.

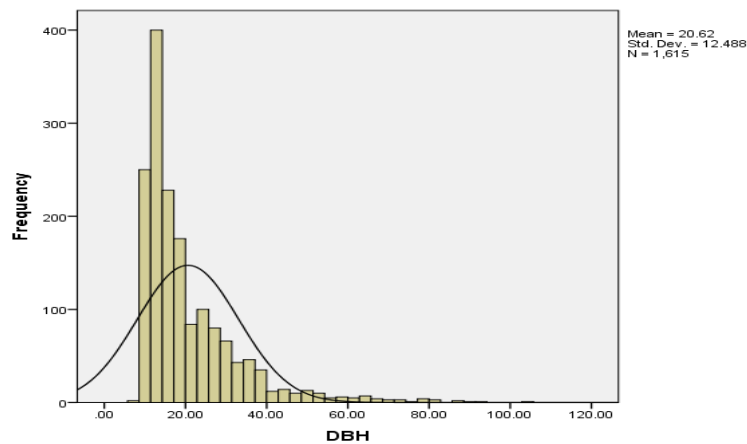


Figure 25: Histogram and normal distribution curve of DBH data.

**4.6. Circularity measured CPA accuracy**

The descriptive statistics are presented in Table 5. The scatter plot and t-test results are presented in Figure 26 and Table 6

Table 5: Descriptive statistics of actual and adjusted CPA (inner, outer and intermediate circles).

Statistics	Actual CPA(m <sup>2</sup> )	Outer circle CPA(m <sup>2</sup> )	Inner circle CPA(m <sup>2</sup> )	Intermediate circle CPA(m <sup>2</sup> )
Minimum	2.16	6.19	2	4.093951
Maximum	52.76	53.51	46.47	49.92796
Mean	21.95566	24.53737	19.09293421	21.65171
Standard Deviation	11.20297	11.15349	11.00144031	11.01117
Number of trees	76	76	76	76

TOWARDS A UAV BASED STANDALONE SYSTEM FOR ESTIMATING AND MAPPING ABOVEGROUND BIOMASS/ CARBON STOCK IN BERKELAH TROPICAL RAIN FOREST, MALAYSIA

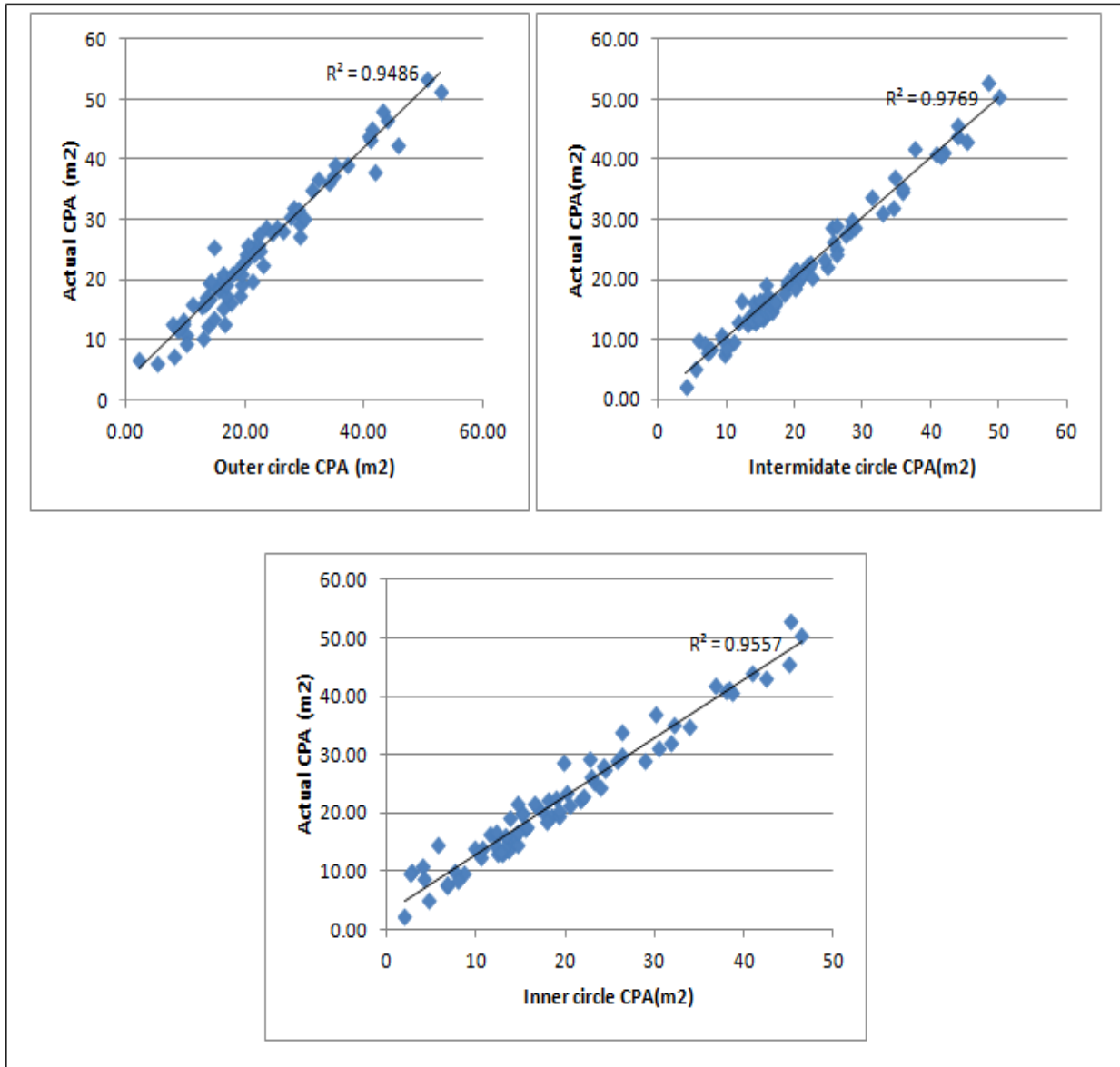


Figure 26: Scatter plot of actual and adjusted CPA (intermediate, inner & outer circles).

**TOWARDS A UAV BASED STANDALONE SYSTEM FOR ESTIMATING AND MAPPING  
ABOVEGROUND BIOMASS/ CARBON STOCK IN BERKELAH TROPICAL RAIN FOREST,  
MALAYSIA**

Table 6: Result summary of paired t-test between actual and adjusted CPA (inner, outer and intermediate circles).

	Actual CPA(m <sup>2</sup> )	inner circle CPA(m <sup>2</sup> )	Actual CPA(m <sup>2</sup> )	Intermediate circle (m <sup>2</sup> )	Actual CPA(m <sup>2</sup> )	outer circle CPA(m <sup>2</sup> )
Mean	21.95565789	19.09293421	21.95565789	21.65171288	21.95566	24.53737
Variance	125.5064356	121.031689	125.5064356	121.2459026	125.5064	124.4003
Observations	76	76	76	76	76	76
Pearson Correlation	0.977616731		0.988375839		0.973968	
Hypothesized Mean Difference	0		0		0	
df	75		75		75	
t Stat	10.58584869		1.554730794		-8.82255	
P(T<=t) one-tail	7.67351E-17		0.062110068		1.62E-13	
t Critical one-tail	1.665425374		1.665425374		1.665425	
P(T<=t) two-tail	1.5347E-16		0.124220135		3.24E-13	
t Critical two-tail	1.992102124		1.992102124		1.992102	

The calculated RMSE and %RMSE for the inner, intermediate and outer circles results are 2.34 m<sup>2</sup> (10.66%), 1.69 m<sup>2</sup> (7.7%) and 3.61m<sup>2</sup>(16.77%) respectively.

#### 4.7. Relation DBH and manual delineated CPA

To test the relation between DBH and CPA (actual and adjusted), 55 trees with a fully visible crown which were measured their DBH in the field were selected. Manual delineation and circularity measure using the fittest circle was done. The descriptive statistics is presented in table 6. Through the scatter plot a linear and power trend line was fitted.

Table 7: Descriptive statistics of delineated and adjusted CPA and field DBH.

<b>Statistics</b>	<b><i>Delineated CPA (m<sup>2</sup>)</i></b>	<b><i>Field DBH (cm)</i></b>	<b><i>Adjusted CPA (m<sup>2</sup>)</i></b>
Minimum	3.222696	10	4.216904
Maximum	75.14157	82	77.67953
Mean	18.43683	24.07455	20.06938
Standard Deviation	15.70804	14.01739	15.27549
Number of trees	55	55	55

The CPA and DBH data normality test were performed in SPSS software and the data was not normal. The adjusted CPA, actual CPA and the DBH were skewed. Figure 27 shows the histogram and the distribution curve of the data.

**TOWARDS A UAV BASED STANDALONE SYSTEM FOR ESTIMATING AND MAPPING ABOVEGROUND BIOMASS/ CARBON STOCK IN BERKELAH TROPICAL RAIN FOREST, MALAYSIA**

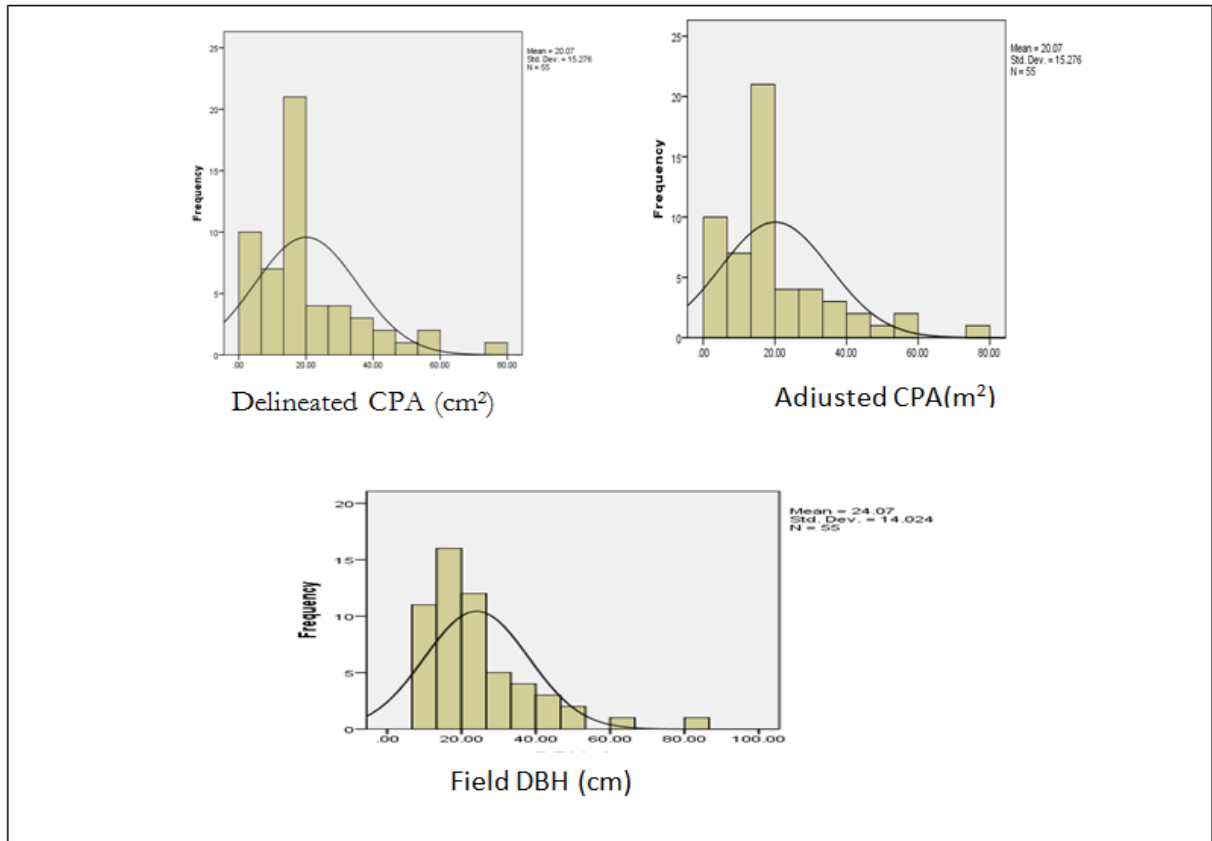


Figure 27: Histogram and normal distribution curve of actual CPA, adjusted CPA and DBH.

The scatter plot was plotted and the linear and power trend line was fitted (Figure 28). The regression result of the manually delineated fully visible crowns CPA and observed DBH are presented in Table 8.

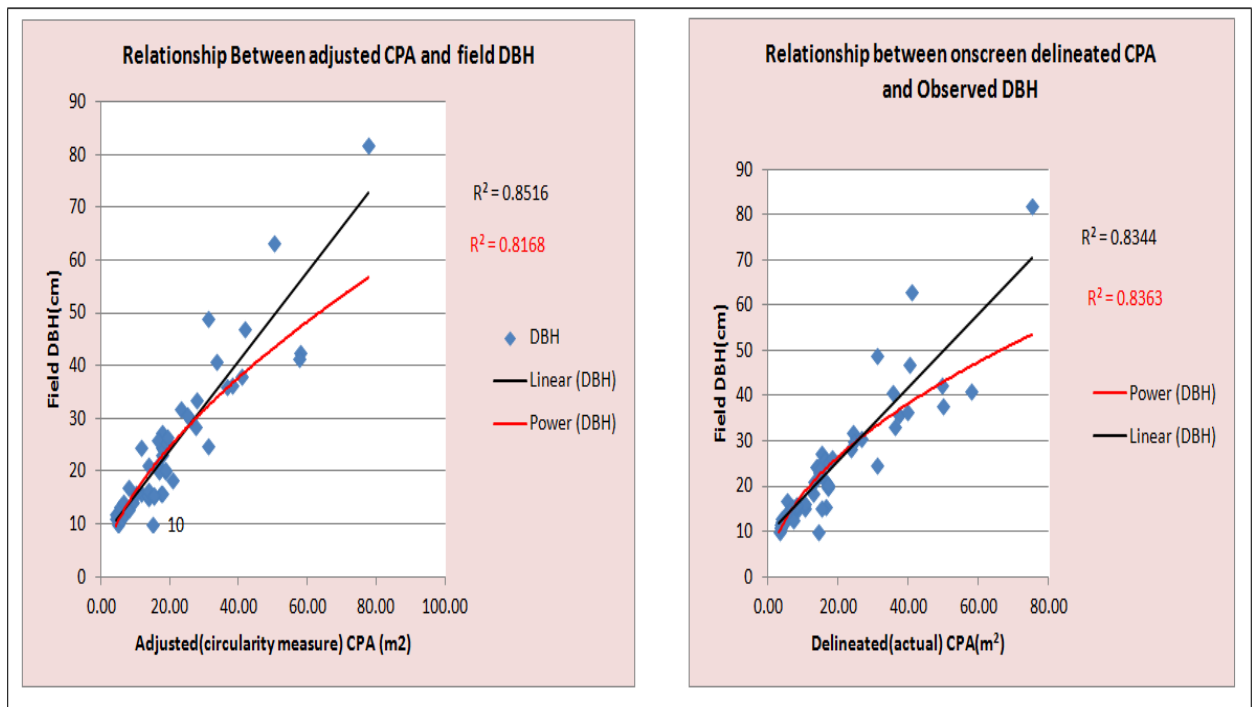


Figure 28: scatter plot of relationship between delineated CPA (actual CPA), adjusted CPA and field DBH.

**TOWARDS A UAV BASED STANDALONE SYSTEM FOR ESTIMATING AND MAPPING ABOVEGROUND BIOMASS/ CARBON STOCK IN BERKELAH TROPICAL RAIN FOREST, MALAYSIA**

The power function performs slightly better than the linear model as is shown in Table 8.

Table 8: Result summary of regression analysis between manually delineated CPA and Observed DBH.

Relationship	Model type	R(correlation determination coefficient)	R square(R <sup>2</sup> )	Adjusted R	Pearson correlation coefficient value
Actual CPA & DBH	Linear	0.913	0.834	0.831	0.914** (p< 0.01)
	Power	0.915	0.837	0.834	
Adjusted CPA & DBH	Linear	0.92	0.85	0.849	0.923** (p< 0.01)
	Power	0.904	0.81	0.81	

The Pearson correlation coefficient shows, a significant relationship between actual CPA and DBH in both the linear and power model and the results of this test justified to continue with (Appedix 3).

#### 4.8. Relation segmented CPA and DBH

The relationship between the segmented CPA (i.e. the result of OBIA with e-Cognition) and DBH measured in the field was assessed based 207 matched trees.

Table 9: Descriptive statistics of segmented CPA and field DBH.

Statistics	CPA_m2	DBH (cm)
Minimum	4.375116	10
Maximum	101.4573	90
Mean	21.49524	28.17681
Standard Deviation	17.49075	16.22092
Number of trees	207	207

The CPA and DBH data normality were tested and the histogram and normal distribution curve of the CPA and DBH data is presented in Figure 29. Since the DBH data is not normal. The CPA is also influenced by the DBH normality and both skewed to the right.

**TOWARDS A UAV BASED STANDALONE SYSTEM FOR ESTIMATING AND MAPPING ABOVEGROUND BIOMASS/ CARBON STOCK IN BERKELAH TROPICAL RAIN FOREST, MALAYSIA**

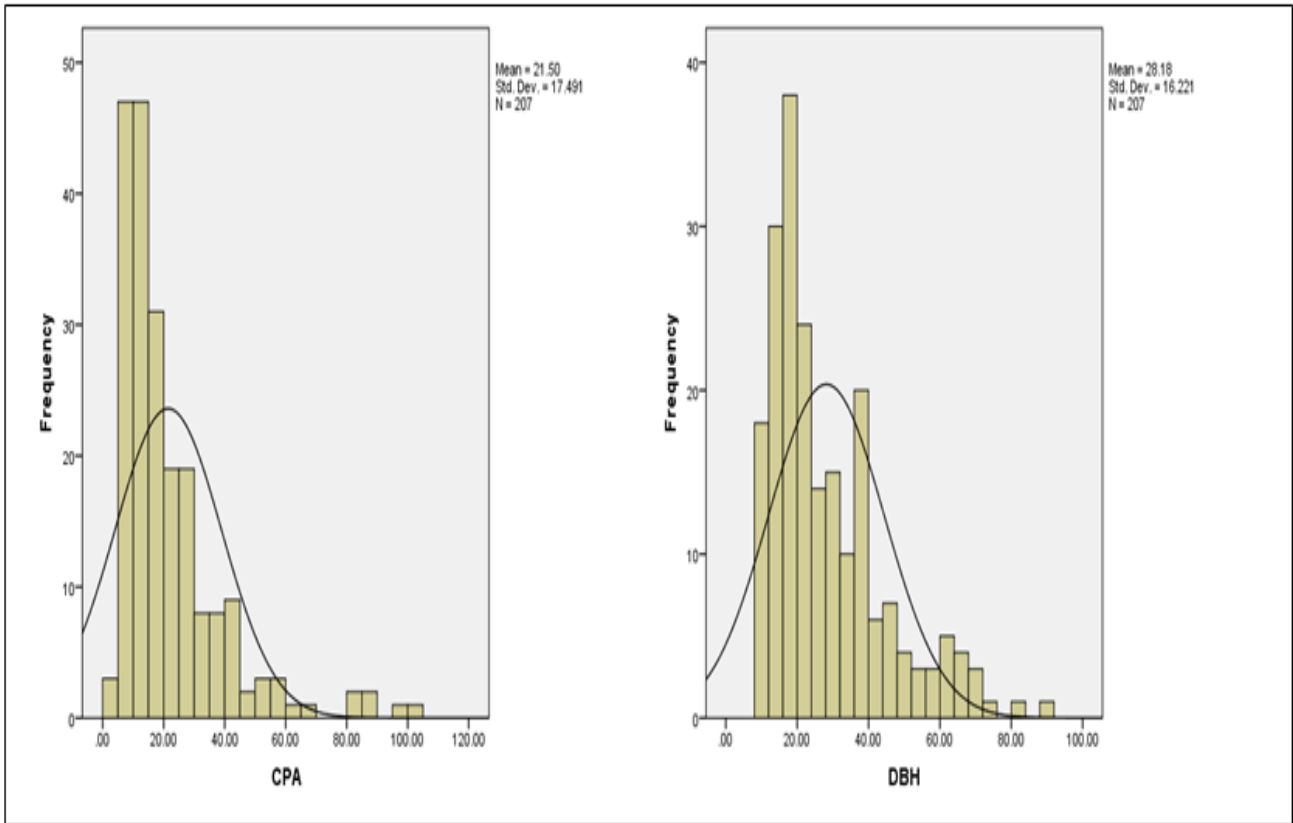


Figure 29: Histogram and normal distribution curve of CPA and DBH data.

The results of the regression analysis are presented in Figure 30 and Table 10.

**TOWARDS A UAV BASED STANDALONE SYSTEM FOR ESTIMATING AND MAPPING ABOVEGROUND BIOMASS/ CARBON STOCK IN BERKELAH TROPICAL RAIN FOREST, MALAYSIA**

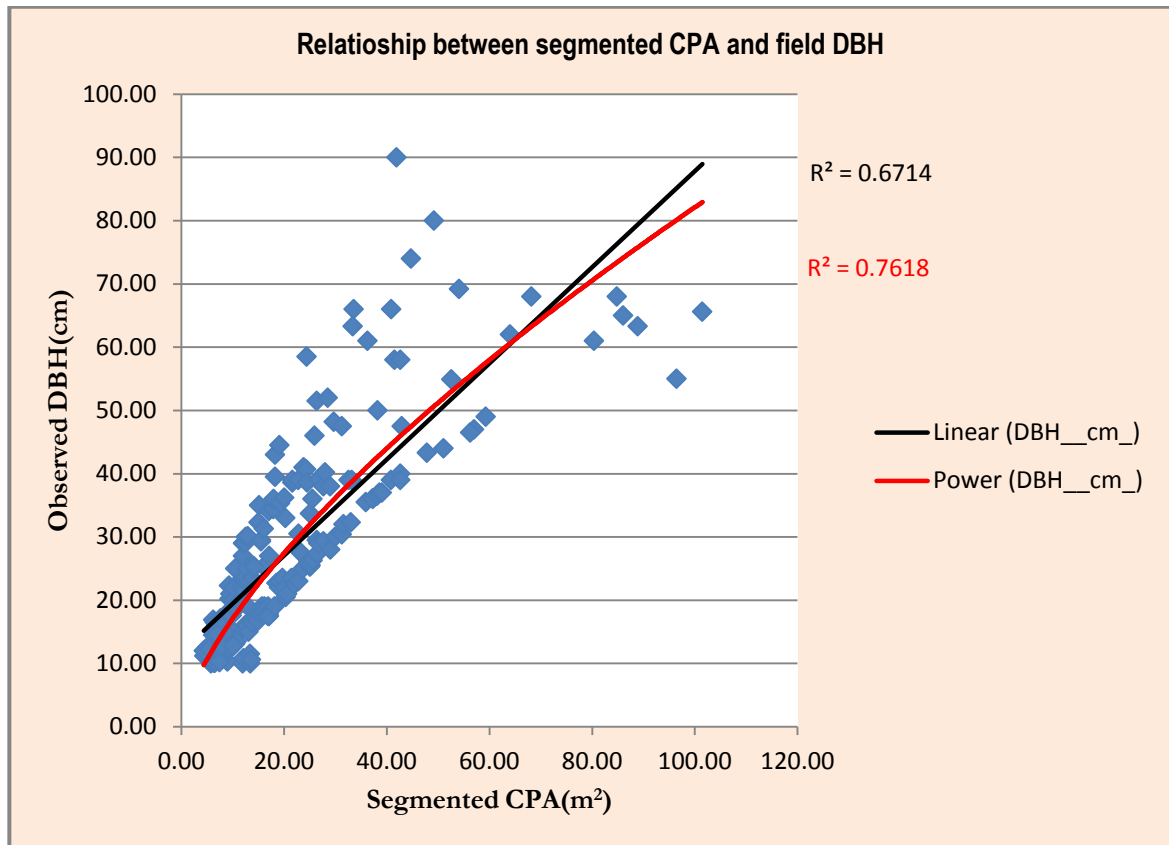


Figure 30: scatter plot of relationship between segmented CPA and observed DBH.

Table 10: Result summary of regression analysis between segmented CPA and Observed DBH.

Model type	R(correlation coefficient)	R <sup>2</sup>	Adjusted R	RMSE(cm)	RMSE (%)	Pearson correlation coefficient (value)
Linear	0.819	0.67	0.67	9.27	32.9	0.819** (p < 0.01)
Power	0.873	0.76	0.76	8.66	30	

The Pearson correlation value is less than 0.05 at 95% level of confidence (Appendix 3).

#### 4.9. Relation adjusted CPA and DBH

Trees with an incompletely visible crown in the segmented orthophoto were identified and the CPA's were adjusted with the help of UAV-CHM and extracted tree heights. 75 trees out of the 305 trees were identified and adjusted using the intermediate circularity measured CPA. These adjusted CPA substitute the incomplete corresponding CPA. The relationship between adjusted CPA and observed DBH was analysed using a linear regression with linear and power model. The descriptive statistics of adjusted CPA and observed DBH is presented in Table 11. The scatter plot and results of the regression and RMSE are shown in Figure 31 and Table 12.

**TOWARDS A UAV BASED STANDALONE SYSTEM FOR ESTIMATING AND MAPPING ABOVEGROUND BIOMASS/ CARBON STOCK IN BERKELAH TROPICAL RAIN FOREST, MALAYSIA**

Table 11: Descriptive statistics of the adjusted CPA and observed DBH.

<i>Statistics</i>	<i>CPA(m<sup>2</sup>)</i>	<i>DBH(cm)</i>
Mean	24.51382	28.17681
Minimum	4.375116	10
Maximum	101.4573	90
Standard Deviation	18.00577	16.22092
Number of trees	207	207

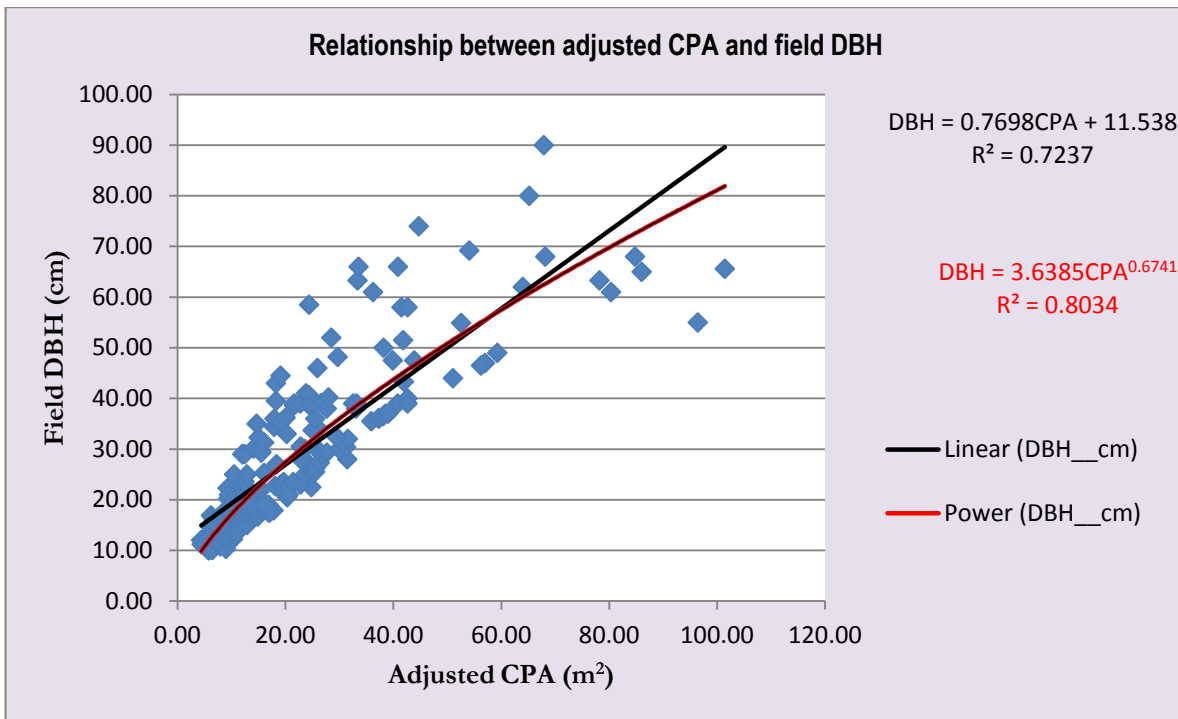


Figure 31: scatter plot that shows relationship between adjusted CPA and DBH.

Table 12: Result summary of regression analysis between adjusted CPA and Observed DBH.

Model type	R	R <sup>2</sup>	Adjusted R	RMSE (cm)	RMSE (%)	Pearson correlation coefficient value
Linear	0.85	0.724	0.722	8.54	29.45	0.851** (< 0.01)
Power	0.89	0.803	0.802	7.98	27.53	

CPA adjustment improves the relationship in both linear and power models. In the linear model, the error reduced from 33% to 29.4% and in the power from 30% to 27.5%. Compared to the segmented CPA, in the models using the adjusted CPA's the R<sup>2</sup> increases from 0.67 to 0.72 for the linear model and from 0.76 to 0.80 in the power model, indicating that the models with the adjusted CPA explain a higher percentage of the variation in the data. Based on the error of the relationship between adjusted CPA and DBH the model which has low error was selected for validation and DBH prediction.



**TOWARDS A UAV BASED STANDALONE SYSTEM FOR ESTIMATING AND MAPPING  
ABOVEGROUND BIOMASS/ CARBON STOCK IN BERKELAH TROPICAL RAIN FOREST,  
MALAYSIA**

Equation 9: Regression model

$$DBH = 3.36385CPA^{0.6741} \dots\dots\dots 9$$

Where;

DBH; Predicted diameter at breast height (cm)

CPA; Canopy projection area of individual trees after adjustment (m<sup>2</sup>) which includes the adjusted with circularity measured CPA and CPA which do not need adjustment.

Therefore, the 30% of matched trees (305 trees) which have been separated for validation were used to check the consistency of the model. DBH was predicted using 88 trees CPA. The descriptive statistics of the data is summarized in Table 13. The scatter plot was plotted and the RMSE was calculated. The results of the RMSE and the scatter plot are shown in Figure 32.

Table 13: Summary statistics of data used for validation.

	<i>CPA(m2)</i>	<i>Predicted DBH(cm)</i>	<i>DBH (cm)_</i>
Minimum	5.653241	11.69624	6
Maximum	76.11729	67.48858	55
Mean	19.41342	25.83043	22.15852
Standard Deviation	13.4	11.27035	10.7557
Number of trees	88	88	88

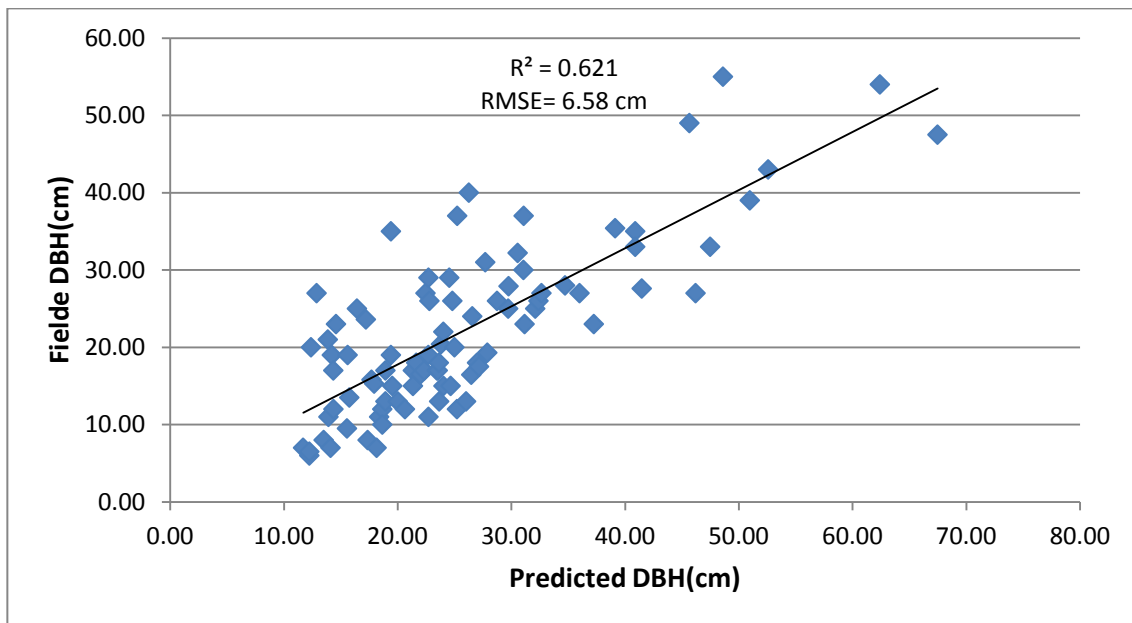


Figure 32: scatter plot of predicted and Observed DBH.

The result of the calculated RMSE is 6.58 cm (29.7%) as shown in the above figure 32. In addition to the RMSE, the mean difference between predicted and observed DBH was calculated using t-test. The result summary of the calculated t-test is shown in Table 14.

**TOWARDS A UAV BASED STANDALONE SYSTEM FOR ESTIMATING AND MAPPING  
ABOVEGROUND BIOMASS/ CARBON STOCK IN BERKELAH TROPICAL RAIN FOREST,  
MALAYSIA**

Table 14: Result summary of two-sample t-test between predicted and observed DBH of power model.

	predicted DBH(cm)	DBH (cm)
Mean	25.83043	22.15852
Variance	127.0207	115.6851
Observations	88	88
Pooled Variance	121.3529	
Hypothesized Mean Difference	0	
df	174	
t Stat	2.211024	
P(T<=t) one-tail	0.014169	
t Critical one-tail	1.653658	
P(T<=t) two-tail	0.028338	
t Critical two-tail	1.973691	

The P (T<=t) two-tailed t-test p-value is less than 0.05 at 95% level of confidence.

#### 4.10. UAV derived CHM accuracy

Before the absolute tree height derived from UAV and airborne LiDAR-CHM comparison, the UAV and airborne LiDAR DTM accuracy were checked as compared to ground truth (altitude from DGPS) using scatter plot and RMSE. In addition to that, comparison between UAV derived DTM and airborne LiDAR derived DTM was done. The result of calculated RMSE was used to evaluate the UAV-DTM accuracy compared to airborne LiDAR DTM in open land surface. Descriptive statistics of the data and scatter plots are shown in Table 15 and Figure 33 respectively.

Table 15: Descriptive statistics of UAV-DTM, airborne LiDAR-DTM and ground truth DTM.

Statistics	<i>airborne LiDAR</i>		
	<i>DGPs Altitude (m)</i>	<i>DTM(m)</i>	<i>UAV DTM(m)</i>
Minimum	38.611	40.52534	38.5793
Maximum	74.428	80.19007	74.47193
Mean	56.03152571	53.88073	56.26719
Standard Deviation	8.605524909	7.544805	8.402651
Number of pixels	35	35	35

**TOWARDS A UAV BASED STANDALONE SYSTEM FOR ESTIMATING AND MAPPING ABOVEGROUND BIOMASS/ CARBON STOCK IN BERKELAH TROPICAL RAIN FOREST, MALAYSIA**

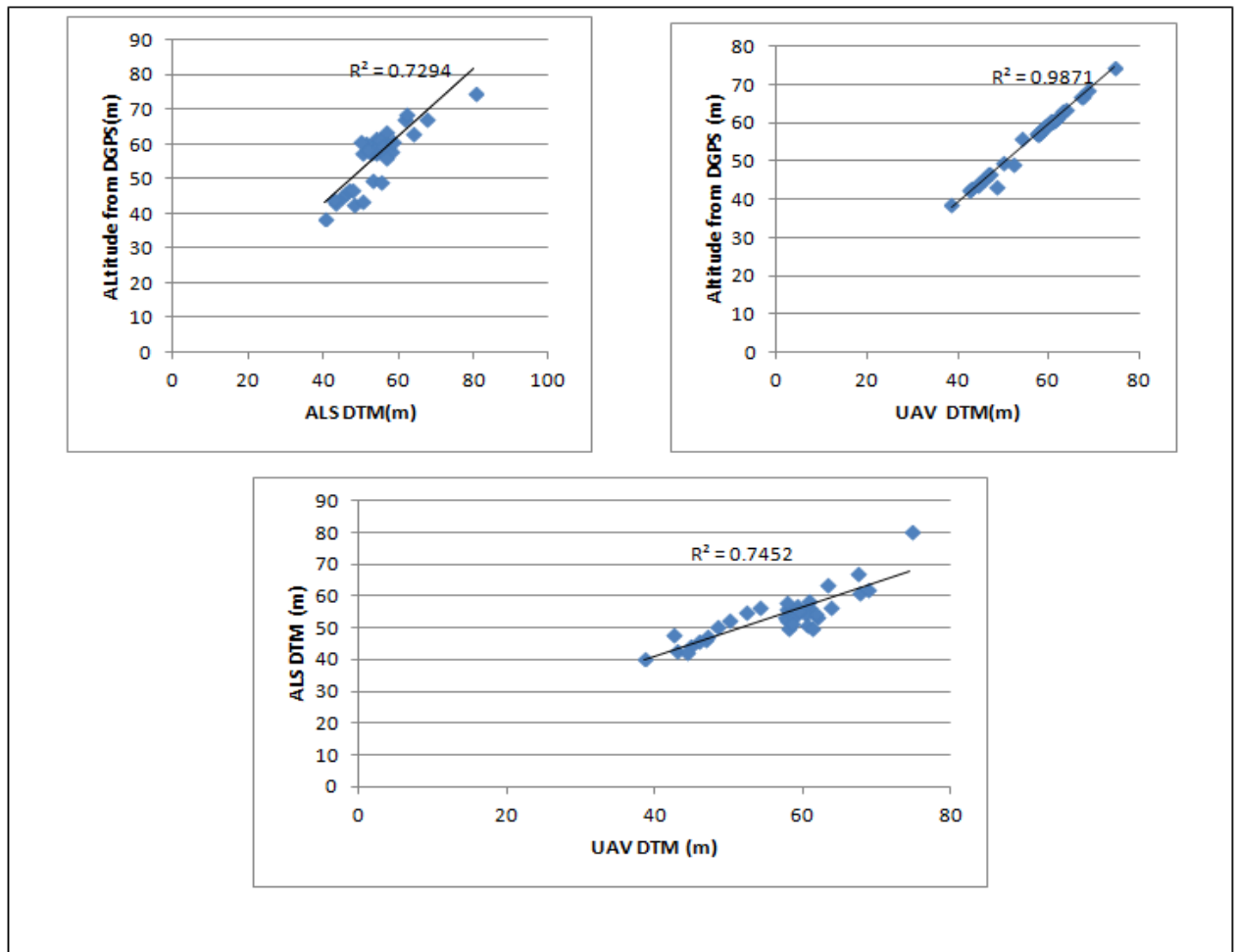


Figure 33: scatter plot UAV DM, airborne LiDAR DTM and DGPS altitude.

The RMSE between UAV DTM and airborne LiDAR DTM, UAV DTM and DGPS altitude and airborne LiDAR DTM and DGPS altitude was calculated and the obtained results are summarized in Table 16.

Table 16: Result summary of RMSE of UAV DTM, airborne LiDAR DTM, and altitude from DGPS.

	<i>DGPS &amp; UAV Altitude(m)</i>	DGPS & airborne LiDAR Altitude(m)	UAV and airborne LiDAR DTM (m)
RMSE(m)	0.96	4.4	3.75
RMSE (%)	1.7	7.8	6.9

Following the DTM comparison, CHM comparison was done using two-sample t-test assuming equal variance, scatter plot and RMSE. The descriptive statistics of the trees height used for t-test analysis are presented in Table 17.

**TOWARDS A UAV BASED STANDALONE SYSTEM FOR ESTIMATING AND MAPPING ABOVEGROUND BIOMASS/ CARBON STOCK IN BERKELAH TROPICAL RAIN FOREST, MALAYSIA**

Table 17: Descriptive statistics of tree heights derived from UAV-CHM and airborne LiDAR-CHM.

Statistics	airborne LiDAR derived height(m)	UAV derived height(m)
Minimum	3.141674	4.51844
Maximum	43.86	42.3515
Mean	22.52421	23.39252
Standard Deviation	8.794501	9.748218
Number of trees	292	292

The two sample t-test assuming equal variance was done. The scatter plot and t-test result shown in figure 34 and Table 18.

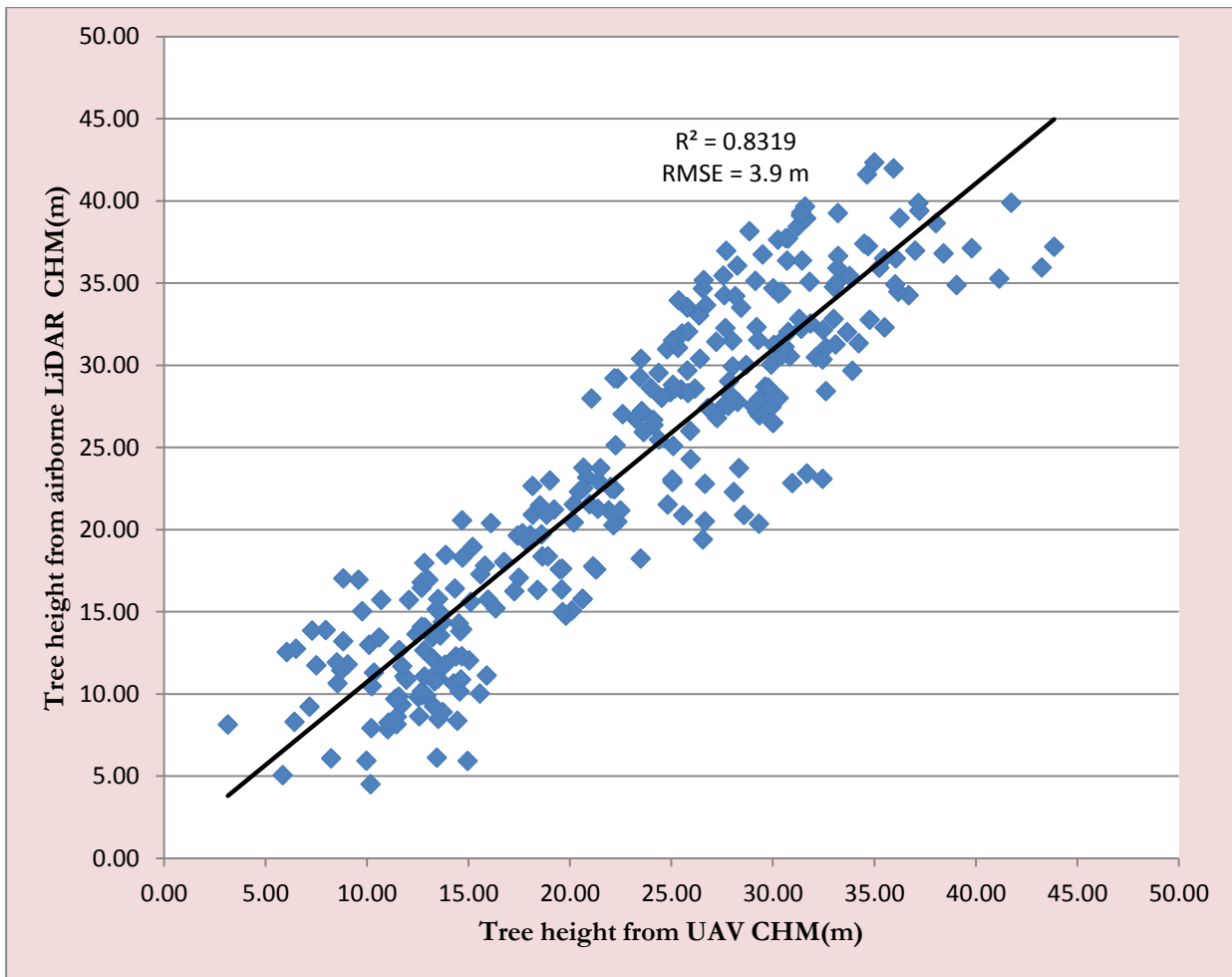


Figure 34: Scatter plot of UAV and airborne LiDAR CHM.

The RMSE was calculated and the result is 3.9 m (17%).

**TOWARDS A UAV BASED STANDALONE SYSTEM FOR ESTIMATING AND MAPPING  
ABOVEGROUND BIOMASS/ CARBON STOCK IN BERKELAH TROPICAL RAIN FOREST,  
MALAYSIA**

Table 18: Two-sample assuming equal variances t-test for means of tree heights from UAV and airborne LiDAR CHM.

	UAV derived CHM (m)	Airborne LiDAR derived CHM(m)
Mean	23.39252367	22.52421264
Variance	95.02775065	77.34324488
Observations	292	292
Pooled Variance	86.18549777	
Hypothesized Mean Difference	0	
df	582	
t Stat	1.130146254	
P(T<=t) one-tail	0.129440069	
t Critical one-tail	1.647475985	
P(T<=t) two-tail	0.258880138	
t Critical two-tail	1.964048309	

The p (T<=t) two-tailed t-test p-value is greater than 0.05.

#### 4.11. Comparison of AGB-UAV and AGB-field

The descriptive statistics of the tree parameters used to compare AGB-UAV and AGB-field in the analysis are presented in Table 19.

Table 19: Descriptive statistics of CPA, tree height and DBH data for AGB/carbon stock estimation.

Statistics	DBH(cm)	Airborne LiDAR derived CHM		Predicted DBH(cm)	UAV derived CHM (m)
		(m)	CPA(m <sup>2</sup> )		
Minimum	10	3.14	5.65	11.7	4.52
Maximum	45.4	47.74	45.2	47.49	38.97
Mean	18.62667	21.1756	16.31093	23.36507	21.49553
Standard Deviation	8.122325	9.442017	7.915917	7.330822	9.446079
Number of trees	150	150	150	150	150

The AGB-UAV and AGB-field was calculated and the mean difference between AGB-UAV and AGB-field were compared using two samples t-test assuming equal variance. The scatter plot and t-test results are showed in Figure 35 and Table 20.

**TOWARDS A UAV BASED STANDALONE SYSTEM FOR ESTIMATING AND MAPPING ABOVEGROUND BIOMASS/ CARBON STOCK IN BERKELAH TROPICAL RAIN FOREST, MALAYSIA**

Table 20: Results summary of UAV-based and field-based AGB

Statistics	AGB_UAV (Kg)	AGB_field (Kg)
Minimum	44.94307318	14.69149319
Maximum	2223.204622	2258.938004
Mean	424.3533072	309.9441478
Standard Deviation	380.5347567	385.8138741
Sum	63652.99608	46491.62217
Number of trees	150	150

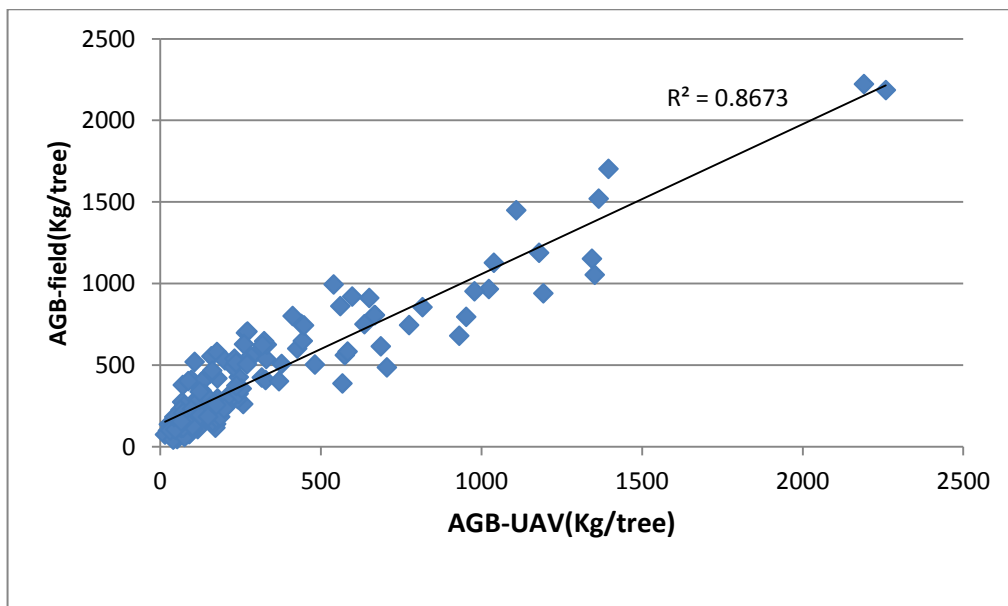


Figure 35: scatter plot between AGB-UAV and AGB-field

Table 21: Result summary of two sample t-test assuming equal variance between AGB-UAV and AGB-field.

	AGB-field(Kg)	AGB-UAV(Kg)
Mean	424.3533	309.9441
Variance	144806.7	148852.3
Observations	150	150
Pooled Variance	146829.5	
Hypothesized Mean Difference	0	
df	298	
t Stat	2.585739	
P(T<=t) one-tail	0.005096	
t Critical one-tail	1.649983	
P(T<=t) two-tail	0.010192	
t Critical two-tail	1.967956	

**TOWARDS A UAV BASED STANDALONE SYSTEM FOR ESTIMATING AND MAPPING ABOVEGROUND BIOMASS/ CARBON STOCK IN BERKELAH TROPICAL RAIN FOREST, MALAYSIA**

The P ( $T \leq t$ ) two-tail value is 0.01. The calculated RMSE and %RMSE are 138.7355 Kg and 32.69% respectively.

**4.12. Carbon stock map**

AGB/carbon stock estimation using predicted DBH and UAV derived CHM was done for UAV flight plan-2 (block2). The CPA from segmentation (i.e., OBIA in e-cognition) was used to predict DBH. A total of 1204796.603Kg AGB was estimated from the 33.35-hectare area of block-2 equivalent to 180.62 Mgha<sup>-1</sup>. The tree level carbon stock map of flight block-2 is demonstrated in Figure 36.

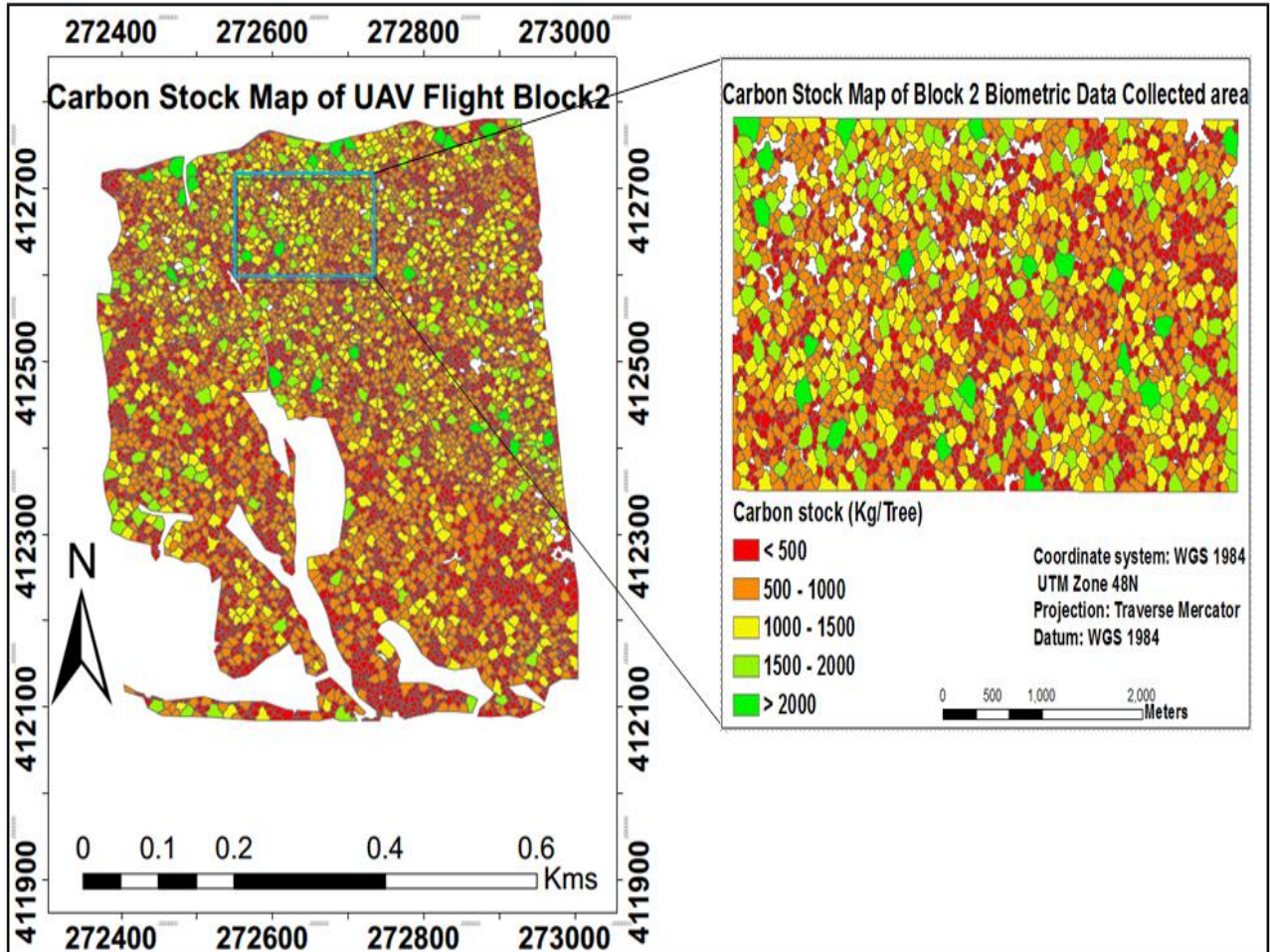


Figure 36: Carbon stock map of UAV flight block 2 based on UAV imagery.

The amount of carbon stock per tree varies from less than 500 Kg to more than 2000 Kg/tree. The variation in carbon stock per tree was inspected and the trees with large CPA have large carbon stock.



## 5. DISCUSSION

### 5.1. Distributions of DBH data

The distribution of 1033 DBH collected in the field showed high skewness. The result indicates lopsidedness of data distribution as it tilts to the right of the middle point of the distribution curve( Cam & Cam, 2017). In a probability distribution, the data which is not normal can be positively or negatively skewed(Doane & Seward, 2011) (Figure 37). In case of this study, the DBH data is skewed to the right (long-tailed in the positive direction). The possible reason for high skewness could be that measurement was taken for trees with a DBH greater than 5cm (since these with less than 5cm DBH have invisible crowns in the image) and if trees with less than 5cm DBH would have been measured, the distribution would be close to normal.

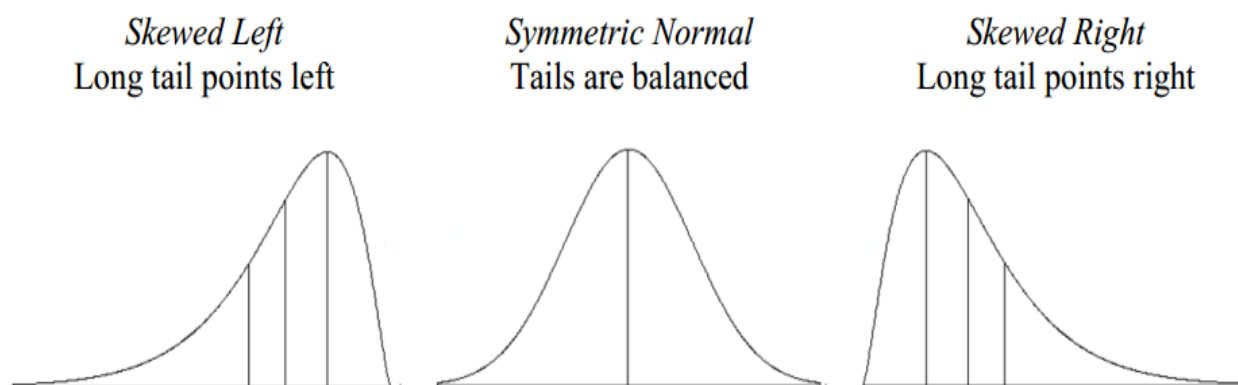


Figure 37: Graphs showing data skewness position[source: (Doane & Seward, 2011)].

### 5.2. Accuracy of circularity measured CPA

The potential of this study is incomplete CPA adjustment. The inner, outer and intermediate circles accuracy assessment was done using 76 fully visible trees. Even though this new method of incomplete CPA adjustment has no related literature, the obtained results discussion is crucial. The obtained  $R^2$  value of inner circle is 0.95 and RMSE is 2.3 m<sup>2</sup> (10.6%). The obtained result shows, applying inner circle to adjust incompletely visible tree crowns deviates by 10.6% from the actual CPA. The obtained result of the intermediate circle was  $R^2$  of 0.97 and RMSE of 1.69 m<sup>2</sup> (7.7%). The obtained result of the outer circle is  $R^2$  of 0.94 and RMSE of 3.6m<sup>2</sup> (16.7%). The CPA obtained from these circles was compared to the actual CPA in order to select the best circle close to the actual CPA. Thus, paired t-test and RMSE was used as factors to select the best fit. The circularity measure with an intermediate circle has the smallest error. In addition to that, the result of paired t-test showed insignificant difference compared to the actual. Therefore, fitting the intermediate circle was found the best method.

### 5.3. Relationship of delineated and circularity measured CPA and DBH

In this study, testing the relationship between actual CPA and field DBH was done. 55 trees which were matched with field DBH were manually delineated, and the best fit circle was used to calculate its CPA. The reason to take the small number of trees is due to the field measured DBH restriction, and the selected tree must have fully visible crowns. The regression result of the linear and power model showed a relationship with a coefficient of determination 85% and 81% respectively in the circularity measured CPA while in the actual CPA were 83.3% and 83.6% respectively. The calculated Pearson correlation coefficient

**TOWARDS A UAV BASED STANDALONE SYSTEM FOR ESTIMATING AND MAPPING  
ABOVEGROUND BIOMASS/ CARBON STOCK IN BERKELAH TROPICAL RAIN FOREST,  
MALAYSIA**

indicates, there is a statistically significant relationship between CPA and DBH in both CPA types (actual and circularity measured, see appendix 3).

The obtained result of the circularity measured CPA explains more variation in DBH in the linear model while in the actual CPA shows in the power model. The possible reason to obtain high  $R^2$  value could be due to the delineated tree crowns variations and CPA measurement precision. The manually delineated CPA restricted by the DBH measured in field hence number of trees and distribution was not considered. The selected data (DBH, circularity measured CPA and delineated CPA) normality was tested, and it was not normally distributed.

The obtained result of this preliminary analysis is comparable to the result obtained by Dubravac et al., (2013)  $R^2$  of 0.80 (Figure 38 left side graph). The study was done in natural regeneration of beech forest and the method was experimental field based while CPA measurement in this study was by manual delineation and circularity measure technique. A research conducted by Malinovski et al., (2016) with Eucalyptus plantation was revealed 0.87 correlation coefficient and linear relationship with  $R^2$  of 0.76 (Figure 38 right side graph). Since the aim of this section was to check if there is a relation between DBH and CPA in the fully visible tree crowns, the obtained result encourages continuing with.

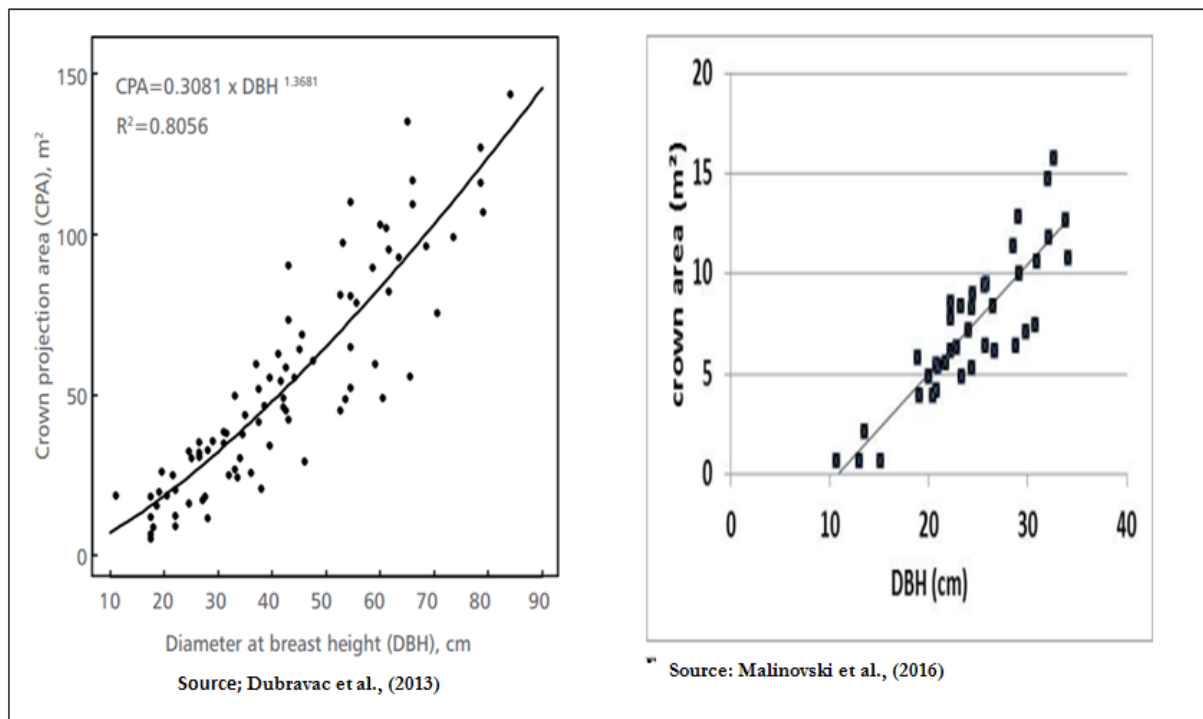


Figure 38: Relationship between field DBH and CPA.

Errors in the GPS measurements of the coordinates of the individual trees in the field hamper identification of the corresponding tree crown in the segmented orthophoto. This may have negatively influenced the relation between DBH and CPA.

**TOWARDS A UAV BASED STANDALONE SYSTEM FOR ESTIMATING AND MAPPING  
ABOVEGROUND BIOMASS/ CARBON STOCK IN BERKELAH TROPICAL RAIN FOREST,  
MALAYSIA**

#### **5.4. Relationship of adjusted CPA and DBH**

The relationship between segmented CPA and DBH was used to evaluate the contribution of adjusted CPA in the relationship. The regression determination coefficient of the model ( $R^2$ ) indicates the independent variable explaining potential of the dependent variable. In the regression the independent variable was CPA, and the dependent variable was DBH.

The obtained  $R^2$  value of DBH before CPA adjustment is 0.67 and RMSE of 9.27cm (32.9%) with the linear model while with the power model is  $R^2$  of 0.76 and RMSE of 8.66 cm (30%). The result of the linear model is lower than the result obtained by Malinovski et al., (2016)  $R^2$  of 0.76 with the leaner model (see figure 38 right side graph). The study was done in plantation forest while this study is in the tropical forest before CPA adjustment. Thus, the observed difference is expected. The possible reason of tropical forest to show the weak relationship between CPA and DBH is either species variation or the effect of the vertically multilayered canopy on segmentation.

The obtained result with the power model before CPA adjustment is lower than the result obtained by Malinovski et al., (2016)  $R^2$  of 0.79 with power model. Relatively power model shows a small difference compared to the linear model. Bautista, (2012) stated that power model is more consistent than the linear model.. The correlation result indicates a significant relationship between CPA and DBH (see appendix 3). The obtained  $R^2$  value of DBH after CPA adjustment is 0.724 and RMSE of 8.54 cm (29.4%) with the linear model while with the power model is  $R^2$  of 0.80 and RMSE of 7.9 cm (27.5%). A result obtained by Shah et al., (2011) who study in subtropical forest based on selected species was  $R^2$  range from 0.62-0.74 in the linear model which is comparable to the linear model result of this study. The result indicates the CPA adjustment in multilayer forest canopy can predict DBH comparable to the DBH predicted in simple forests.

The power model explains the variation in DBH better than the linear model. Adjusted CPA showed an increase in CPA with constant DBH made the relation close to power. Thus, the relationship with power model raises from 0.76 before adjustment to 0.80 after CPA adjusted. Similarly, Sium (2015) obtained a non-linear but close to a linear relationship between CPA and DBH in tropical forest with  $R^2$  of 0.79 using a Worldview-2 high-resolution satellite image. This study obtained comparable result after CPA adjustment with the power model. Moreover, Shimano, (2000) revealed that power function fits DBH class distribution in natural broadleaved forests.

The calculated RMSE was used as the best parameter to select the best model which has a smaller error. The RMSE of the relationship before and after CPA adjustment in the linear model were 32% and 29% respectively while in the power model were 30% and 27% respectively. In all the relationships the power model has a smaller error as compared to linear. Based on the RMSE values before and after CPA adjustment the best model which has a small error is power model. The adjusted CPA explains the field DBH better in the power model up to 80%.

The better relation with power model could be due to variation in the age of the trees. The young trees can prepare enough food using their green leaves and show a high rate of increase in DBH while the old trees could not prepare enough food as leaves could shade. As the branches of a tree increase, food competition between the stem and branches increase and the rate of stem size increment slow.

A similar result obtained by Iizuka et al., (2017) who study on Cypress forest in Japan heterogeneous micro-topography using UAV imagery with power model  $R^2$  of 0.79 (Figure 39b). The method of segmentation used to compute CPA was watershed Algorithm of SAGA-GIS (System for Automated Geoscientific Analyses) while this study was used multiresolution segmentation in e-Cognition. Even though this study was done in the multilayered forest canopy, CPA adjustment helps to obtain similar results. A study done by Herney et al., (2005) revealed a linear relationship between crown diameter and DBH with a determination coefficient of  $R^2 > 0.8$  in major broad-leaved tree species (example beech trees  $R^2 = 0.92$ ). Iizuka et al., (2017) also obtained a significant relationship between crown diameter and DBH

**TOWARDS A UAV BASED STANDALONE SYSTEM FOR ESTIMATING AND MAPPING ABOVEGROUND BIOMASS/ CARBON STOCK IN BERKELAH TROPICAL RAIN FOREST, MALAYSIA**

with  $R^2$  of 0.77. The relationship between DBH and crown diameter could be a good indicator of the relationship between CPA and DBH since CPA is a function of crown diameter. So, this result could be a robust result.

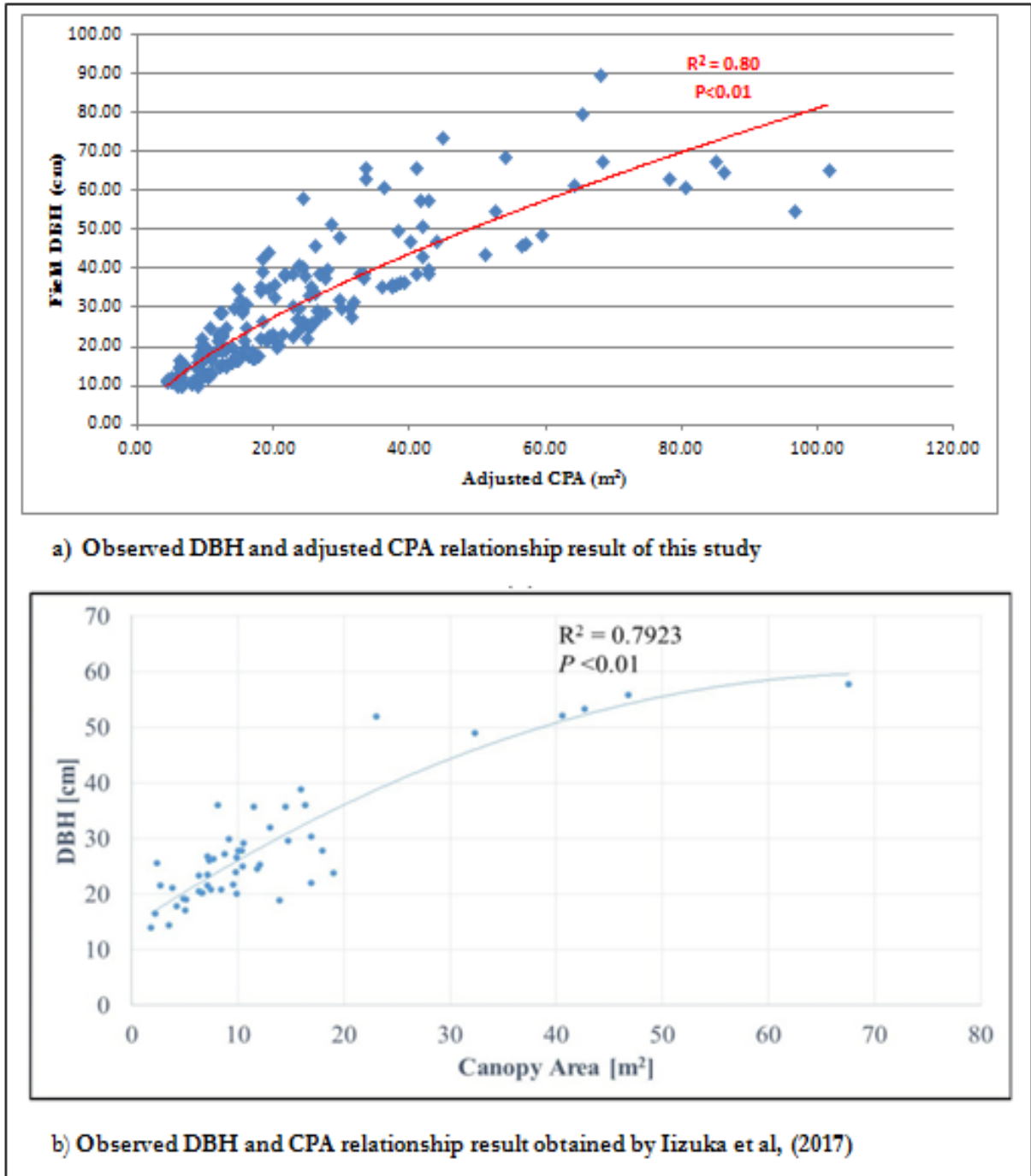


Figure 39: Scatter plot of a relationship between CPA and DBH in compare to another research result.

In Figure 39, the top (a) shows the  $R^2$  value of DBH in this study while the bottom (b) shows the  $R^2$  value of DBH and scatter plot obtained by Iizuka et al., (2017).

The correlation coefficient of the power model in this study was 89% which is comparable with the result revealed by Bautista, (2012) which was 85% in the subtropical forest using airborne LiDAR.

**TOWARDS A UAV BASED STANDALONE SYSTEM FOR ESTIMATING AND MAPPING  
ABOVEGROUND BIOMASS/ CARBON STOCK IN BERKELAH TROPICAL RAIN FOREST,  
MALAYSIA**

In order to validate the power model, other trees (30% of the matched) which are not used during model development were used for DBH prediction. A scatter plot was plotted using predicted DBH as independent and field DBH as dependent variables. The obtained  $R^2$  is 0.62 and RMSE is 6.58 cm (29%). The result shows predicted DBH can explain 62% of field DBH. Except for the uncertainty of GPS measurement of the coordinates of individual trees which may have negatively influenced the relation between DBH and CPA, still the relationship achieves a robust result.

In order to compare the mean DBH of predicted and observed DBH, two-sample t-test assuming equal variance was performed and the result shows a significant difference. The result indicates, the mean predicted DBH deviates from the observed. But, the result of the t-test does not mean the relationship is not valid. The test was done only to check how the mean predicted DBH deviated from the observed. The possible reason not significant could be because of the segmentation error. The over segmentation leads to larger predicted DBH since the mean predicted DBH showed greater than DBH measured in the field.

### **5.5. Accuracy of UAV derived tree height**

The UAV and airborne LiDAR DTM heights accuracy assessment using altitude from the ground truth (DGPS) is crucial and the first step to assess the accuracy of tree height derived from UAV 3-D point cloud and airborne LiDAR data. The accuracy of UAV and airborne LiDAR DTM height was compared to the ground truth heights which were collected using DGPS. The obtained RMSE between UAV derived DTM, and DGPS altitude is 0.96 m (1.7%) with  $R^2$  value of 0.98 while from airborne LiDAR DTM is 3.75 m (6.9%) with  $R^2$  of 0.74. The result indicates the UAV DTM deviate by 0.96 m from the ground truth and 3.75 m from the airborne LiDAR.

A similar study by Ruben (207) obtained RMSE of 2.53 to 6.32 m and % RMSE ranges from 6.6% to 13% and  $R^2$  range from 0.14 to 0.94. The RMSE between the altitude derived from airborne LiDAR and ground truth was 3.86 m (7.8%). The altitude from UAV derived DTM has smaller error compared to the ground truth while the altitude from airborne LiDAR-DTM has a larger error. The closeness of heights from UAV derived DTM to the ground truth could be the ground control points used during dense point cloud generation to georeference the orthophoto and point cloud density/m<sup>2</sup>. The UAV 3-D point cloud has more points per m<sup>2</sup> than the airborne point density, and the interpolation distance is smaller in open land surface.

A similar study by Ruben (2017) obtained  $R^2$  of 0.99 with heights from airborne LIDAR derived DTM and 0.96 with heights from UAV derived DTM. The height from UAV derived DTM is close to the outcome obtained in this study. But, the height derived from airborne LiDAR derived DTM deviates from the result of this study. The reason for the difference in the airborne LiDAR result could be due to the place where ground control points placed. If the ground control points located close to cracks and narrow valleys, the airborne LiDAR laser pulse could pass through that and obtain information of the most in-depth sites. UAV imagery cannot pass through such sites, and the data could be similar to DGPS. The accuracy of the UAV imagery processing has a direct impact on the quality of UAV derived DTM. If the GCPS are not placed in the centre of markers during the dense point cloud generation, there would be positional errors in X, Y or Z positions.

A similar study was done by Jensen & Mathews (2016) that compare height from UAV derived DTM and airborne LiDAR derived DTM using height from GPS. The result revealed that height from UAV derived DTM and height from GPS with  $R^2$  of 98.8% while with airborne LiDAR derived DTM was 99%. The obtained  $R^2$  value of height from UAV derived DTM of this study supports the result obtained by Jensen & Mathews (2016). But, the obtained  $R^2$  value of height from airborne LiDAR derived DTM of this study is lower than their result from airborne LiDAR-height. The result of this research indicates height from

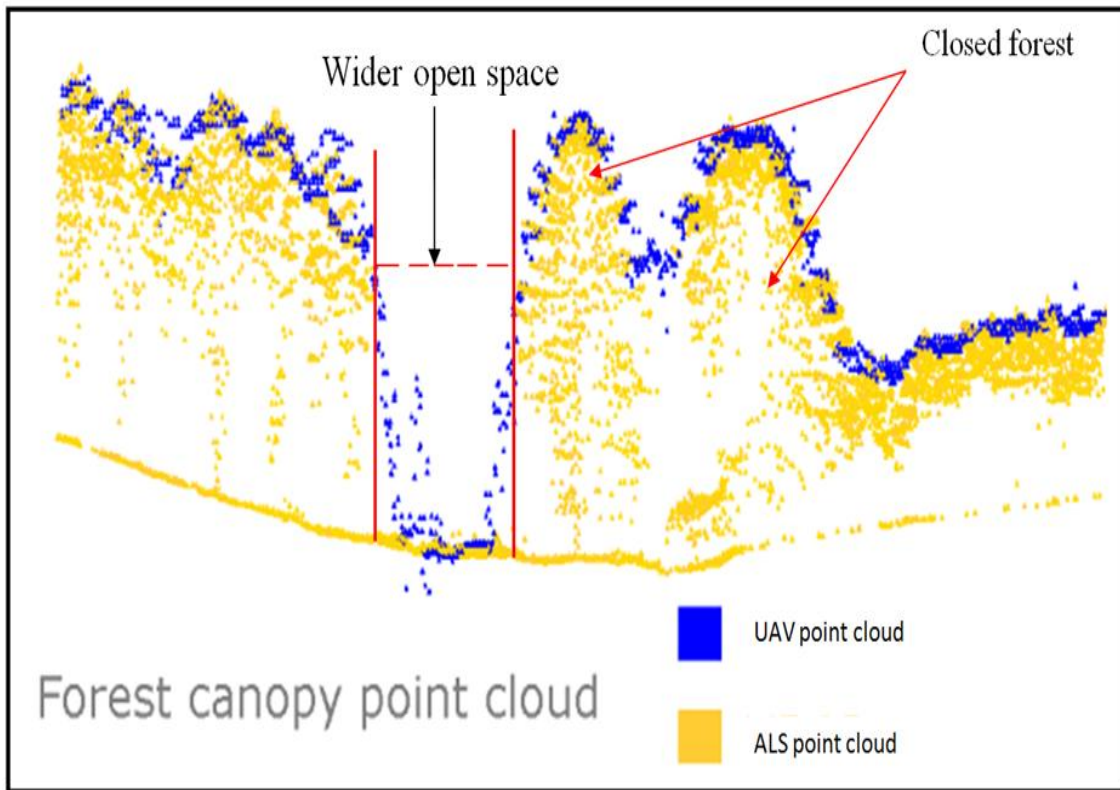
**TOWARDS A UAV BASED STANDALONE SYSTEM FOR ESTIMATING AND MAPPING  
ABOVEGROUND BIOMASS/ CARBON STOCK IN BERKELAH TROPICAL RAIN FOREST,  
MALAYSIA**

UAV derived DTM is much closer to the ground truth. The reason could be due to topographic characteristics of the study area and airborne LiDAR data point density difference. In addition to that, the GPS used by Jensen & Mathews (2016) for recording ground truth height might have similar accuracy with the airborne LiDAR GPS.

In order to assess the accuracy of tree height from UAV derived CHM and airborne LiDAR derived CHM scatter plot was plotted and RMSE was calculated. The obtained  $R^2$  value is 0.83. The CHM from UAV deviates from airborne CHM by 3.9m (17.05%). The  $R^2$  obtained in this study supports the  $R^2$  obtained by Ruben (2017). A similar study by Dandois & Ellis (2013) obtained RMSE 2.3 m stating that the two sensors were characterizing the canopy with a similar degree of precision. The obtained result has small error compared to the RMSE obtained in this study. The difference between RMSE of this study and the Dandois & Ellis (2013) could be the difference in topographic characteristics, airborne LiDAR data point density and time of data acquisition between the two sensors. The average point density of airborne LiDAR data in this study was 6 points/m<sup>2</sup> while Dandois & Ellis (2013) was used 78 points/m<sup>2</sup>). A study by Birdal et al., (2017) who compare tree height estimated from UAV-CHM and field-measured tree height in an open forest obtained  $R^2$  value of 0.94 and RMSE was 28 cm. The result is better compared to the result obtained in this study. In a sparse forest, tree height measured in the field is comparable to tree height derived from airborne LiDAR-CHM. thus, the possible reason for the lower result obtained in this study could be the available open land surface in the open forest than the tropical forest.

The minimum and maximum tree heights estimated from UAV derived CHM were 4.5 m and 42.3 m while the tree heights from airborne LiDAR derived CHM were 3.1m and 43.8 m respectively. The shortest and tallest estimated tree height was obtained from airborne LiDAR derived CHM. Relatively airborne LiDAR laser pulse can pass through the small opening of the forest canopy and can acquire ground information. The airborne LiDAR laser pulse reached the forest floor reduces the ground interpolation distance (Lisein et al., 2013). UAV derived CHM has an accuracy close to airborne LiDAR in sparse forest canopy since DTM generation is georeferenced. Lisein et al., (2013) stated that in dense forest airborne LiDAR point cloud could pass through forest openings and take ground information and it is better than UAV point cloud (Figure 40).

**TOWARDS A UAV BASED STANDALONE SYSTEM FOR ESTIMATING AND MAPPING ABOVEGROUND BIOMASS/ CARBON STOCK IN BERKELAH TROPICAL RAIN FOREST, MALAYSIA**



[Source: Lisein et al (2013) modified].

Figure 40: Illustration of UAV point cloud and airborne LiDAR point cloud in the forest canopy.

In Figure 40, the yellow colour shows the airborne LiDAR point cloud in the dense forest while blue colour shows the UAV point cloud. In the dense forest, the airborne LiDAR point cloud shows higher distribution compared to the UAV point cloud which needs more abundant open space.

The mean tree heights derived from UAV 3-D point cloud and airborne LiDAR data were 23.39 m and 22.52 m respectively, and the t-test result indicates, the mean tree height estimated from UAV derived CHM, and airborne LiDAR derived CHM has no significant difference. The possible reason for this result could be due to the open space available on the roads inside the forest and the small altitude difference between the dense forest location and nearby open area (Figure 41).



**TOWARDS A UAV BASED STANDALONE SYSTEM FOR ESTIMATING AND MAPPING  
ABOVEGROUND BIOMASS/ CARBON STOCK IN BERKELAH TROPICAL RAIN FOREST,  
MALAYSIA**

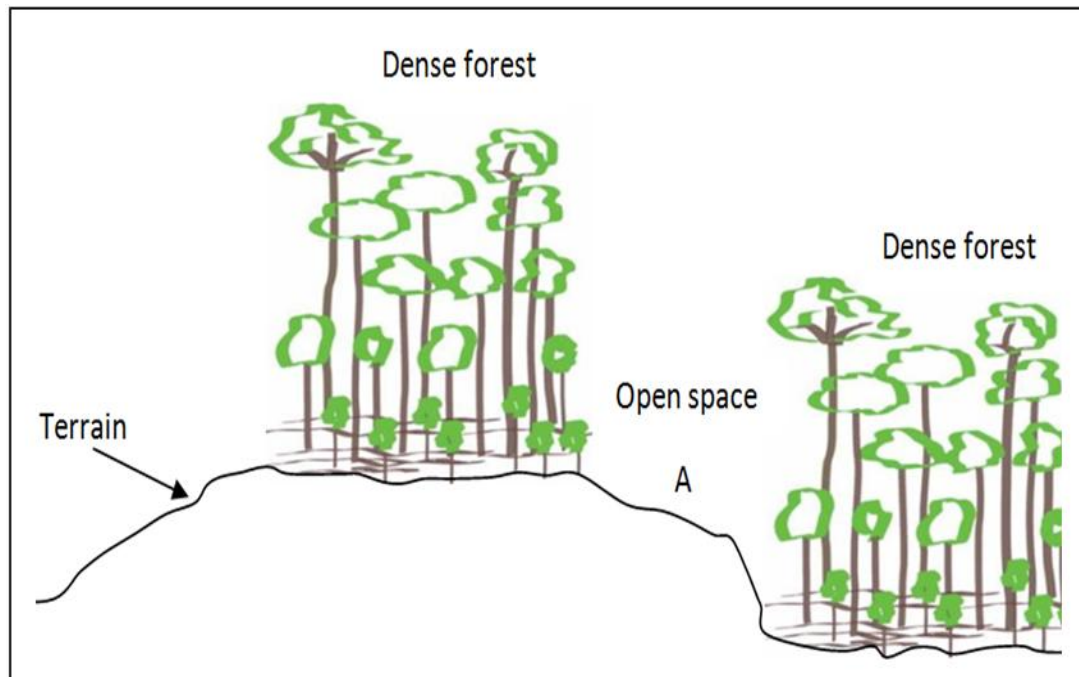


Figure 41: Illustration of open land surface location effect in DTM interpolation.

Figure 41 shows, the dense forest to the left locates at a higher altitude than location point (a) hence height estimated from UAV derived CHM is overestimated. The dense forest to the right locates at a lower altitude than the altitude of location point (a) and tree height could be underestimated.

In my opinion, there are three UAV based estimated tree height accuracy conditions depending on the forest location altitude compared to the nearby open surface location altitude.

1. When the forest is located at a higher altitude than the open land surface location (left side) of (a) Figure 41, the UAV derived CHM is overestimated since DTM interpolation starts at a lower altitude.
2. When the forest is located at a lower altitude than the open land surface location (left side) of (a) Figure 41, the UAV derived CHM is underestimated since DTM interpolation starts at higher altitude.
3. When the forest is located at the same altitude with the open land surface location, the estimated tree height is close to accurate.

### **5. 6. AGB/ Carbon stock accuracy**

In this study, UAV-based and field-based aboveground biomass/carbon stock was estimated from 150 trees using a general allometric equation. The minimum, maximum, mean and total field-based estimated aboveground biomass was 14.69, 3164.29, 395.36 and 69585 Kg respectively while UAV-based was 44.94, 4768.82, 604.12 and 106325.46 Kg respectively. Half of the obtained result is carbon stock. The AGB-UAV was larger than field-based. The calculated RMSE obtained 138.55 Kg and %RMSE 32.6%. The RMSE indicates the mean deviation of AGB-UAV from AGB-field. The obtained result is comparable to the result obtained by Ediriweera et al., (2014) who obtained  $R^2$  of 0.81 by combining airborne and multi-spectral data in subtropical eucalyptus forest area. The result is also in the range of the result obtained by Karna et al., (2015) for the reforested tropical forest that obtained  $R^2$  ranging from 0.78 to 94% using a combination of Worldview-2 high-resolution satellite image and airborne LiDAR. The highest result obtained could be due to the use of the same height values to estimate both the modelled and field-based

**TOWARDS A UAV BASED STANDALONE SYSTEM FOR ESTIMATING AND MAPPING  
ABOVEGROUND BIOMASS/ CARBON STOCK IN BERKELAH TROPICAL RAIN FOREST,  
MALAYSIA**

AGB/carbon stock while this study, uses airborne LiDAR derived height and field DBH as a standard. The result is lower than the study of Lawas, (2016) for tropical rainforest that obtained  $R^2$  of 0.98 AGB/carbon stock estimation through the integration of airborne LiDAR and TLS. The possible reason for the difference in  $R^2$  could be the use of the same height values to estimate both the modelled and field-based AGB/carbon stock.

To check the mean difference in biomass of the AGB-UAV and AGB-field t-test was done and the obtained result shows, there is a significant difference between the mean AGB-UAV and AGB-field. The reason for the significant difference between AGB-UAV and AGB-field result is due to the error created during DBH prediction and CHM generation (error-multiplication).

### **5.7. AGB/Carbon stock of the study area**

The amount of aboveground biomass in UAV flight plan-2 (block-2) of the study area was estimated using the segmented CPA (which is not adjusted). Even though the estimated result is not based on the adjusted CPA, comparing the obtained result with other literature is crucial.

The amount of aboveground biomass in UAV flight block-2 of the study area was estimated to be  $361.2583\text{Mgha}^{-1}$  that is,  $180.63\text{Mgha}^{-1}$  of carbon stock. The estimated amount of carbon stock is similar to the result revealed by Laumonier et al.(2010) in hill *Dipterocarp* old-growth tropical rainforest of the south and central Sumatra. They revealed a range of  $135\text{-}240\text{ Mgha}^{-1}$  of carbon stock with a mean of  $180\text{ Mgha}^{-1}$  using a universal allometric equation. In addition to that, a result obtained by Sium (2015) who study in the tropical forest of the same country (Malaysia), but the different site was revealed  $185\text{ Mgha}^{-1}$  of carbon stock based on a model developed using CPA from the Worldview-2 high-resolution image. The reason to obtain more significant result than the result of this study could be the method of the model development. The model was developed using CPA and carbon relationship directly while in this study the model is a generic allometric equation which uses modelled DBH and estimated tree height from UAV-CHM. Dirocco (2012) revealed  $146\text{ Mgha}^{-1}$  of carbon in a similar site of Temenger forest reserve which is lower than the result of this study. Even though variation observed in the results of different studies, the result of this study is not outside the range of aboveground biomass in the tropical rainforest of Asia which is  $120\text{-}680\text{ Mgha}^{-1}$  (Aalde et al., 2006). Sium (2015) stated that the environmental condition of the study area, the allometric equation used, Sensor types used, forest management and methods applied could result in carbon stock estimation variations.

Even though, the estimated AGB of the study area per hectare has comparable result with the other researchers, the amount of estimated carbon is not as expected. If the whole area was manageable to adjust incomplete CPA with the limited time the estimated biomass would have been better than the obtained result.

## 6. CONCLUSION AND RECOMMENDATION

### 6.1. Conclusion

This study investigated the possibilities of accurate assessment of AGB/carbon stock of the tropical rainforest in Berkelah, Malaysia using UAV imagery stand alone. A generic allometric equation used to estimate AGB/carbon stock input parameters (DBH and height) were derived from UAV 3-D point cloud. AGB/carbon stock of the multilayered forest made use of incompletely visible CPA adjustment after segmentation to derive a robust result of DBH through linear regression and the modelled DBH achieved  $R^2$  of 0.80 in the power model. UAV derived height compared to airborne derived height showed no significant difference at 95% level of confidence in the study area. The UAV height and modelled DBH was applied to estimate the AGB/carbon stock using the generic allometric equation and compared to the AGB/carbon stock estimated from field DBH and airborne LiDAR height using t-test. The result shows a significant difference due to error multiplication during DBH prediction, and UAV derived CHM generation. Based on the obtained result, the following conclusions made to address research questions.

**1. Is there a significant relationship between adjusted CPA (after segmentation) and DBH measured in the field?**

The adjusted CPA and DBH measured in the field were correlated as the correlation coefficient was 89%. Similarly, the regression determination coefficient of the relationship was 80% with power model. Test of Pearson correlation indicated that the relationship is significant ( $p < 0.01$ ). Power model showed a better relationship between CPA and DBH, and it is better to follow it for DBH prediction. There was a significant relationship between adjusted CPA and DBH measured in the field at 95% level of confidence. Hence, the null hypothesis which state there is no significant relationship was rejected.

**2. Is there a significant difference between tree height estimated from UAV 3-D point cloud and airborne LiDAR data?**

Tree height derived from UAV 3-D point cloud deviated from airborne LiDAR derived CHM by 3.9 m (17%). The  $p$  ( $T \leq t$ ) two-tailed t-test  $p$ -value was 0.258 which is greater than 0.05. Hence, there is no a significant difference between the mean of tree heights derived from UAV 3-D point cloud and ALS data at 95% level of confidence in the study area. Thus, the null hypothesis which state there is no significant difference was not rejected.

**3. Is there a significant difference between estimated AGB/carbon stock-UAV-based and field-based/airborne LiDAR?**

The calculated RMSE between UAV-based and field-based estimated AGB/carbon stock obtained 138.55 Kg (32.6%). In addition, the estimated AGB-UAV was compared to AGB-field using t-test and the obtained result shows there is a statistically significant difference at 95% level of confidence. Hence, the null hypothesis which state there is no significant difference was rejected.

**4. What is the estimated amount of carbon-stock in the study area?**

A total of 6023981.603Kg carbon-stock equivalent to 180.18Mgha<sup>-1</sup> was estimated in UAV flight block-2 of the study area.

**TOWARDS A UAV BASED STANDALONE SYSTEM FOR ESTIMATING AND MAPPING  
ABOVEGROUND BIOMASS/ CARBON STOCK IN BERKELAH TROPICAL RAIN FOREST,  
MALAYSIA**

**6.2. Recommendation**

Use of UAV imagery and object-based image analysis with CPA adjustment improves the relationship between CPA and DBH in the power model though; the estimated AGB/carbon stock shows a significant difference due to error multiplication from predicted DBH and estimated height thus, it is recommended to integrate UAV imagery with other promising remote sensing tools to implement REDD+MRV program in tropical rainforest, Malaysia. However, some recommendations are listed for further research.

1. Automatic CPA adjustment technique is strongly recommended to apply this technique in a large area and an algorithm should be developed to save time and energy.
2. Further research can be done in AGB/carbon stock estimation using tree height from UAV-DSM and airborne LiDAR-DTM integration as DTM is not changing abruptly. Once the forest area is surveyed by airborne LiDAR a regular carbon stock assessment using UAV combing with the existed DTM from ALS.
3. The UAV and airborne LiDAR data acquisition time should be at the same time to validate tree height estimation using UAV standalone by airborne LiDAR.

**TOWARDS A UAV BASED STANDALONE SYSTEM FOR ESTIMATING AND MAPPING  
ABOVEGROUND BIOMASS/ CARBON STOCK IN BERKELAH TROPICAL RAIN FOREST,  
MALAYSIA**

## LIST OF REFERENCES

- Aalde, H., Gonsalez, P., Gytarsky, M., Krug, T., Kurz, W. A., Lasco, R. D., ... Verchot, L. (2006). Forest land. *2006 IPCC Guidelines for National Greenhouse Gas Inventories.*, 4(2), 4.1-4.83.  
<http://doi.org/10.1016/j.phrs.2011.03.002>
- Abegg, M., Kükenbrink, D., Zell, J., Schaepman, M., & Morsdorf, F. (2017). Terrestrial Laser Scanning for Forest Inventories—Tree Diameter Distribution and Scanner Location Impact on Occlusion. *Forests*, 8(6), 184. <http://doi.org/10.3390/f8060184>
- Ahamed, T., Tian, L., Zhang, Y., & Ting, K. C. (2011). A review of remote sensing methods for biomass feedstock production. *Biomass and Bioenergy*, 35(7), 2455–2469.  
<http://doi.org/10.1016/j.biombioe.2011.02.028>
- Andersen, H. E., McGaughey, R. J., & Reutebuch, S. E. (2005). Estimating forest canopy fuel parameters using LIDAR data. *Remote Sensing of Environment*, 94(4), 441–449. <http://doi.org/10.1016/j.rse.2004.10.013>
- Ansell, F. A., Edwards, D. P., & Hamer, K. C. (2011). Rehabilitation of Logged Rain Forests: Avifaunal Composition, Habitat Structure, and Implications for Biodiversity-Friendly REDD+. *Biotropica*, 43(4), 504–511. <http://doi.org/10.1111/j.1744-7429.2010.00725.x>
- Balzter, H., Rowland, C. S., & Saich, P. (2007). Forest canopy height and carbon estimation at Monks Wood National Nature Reserve, UK, using dual-wavelength SAR interferometry. *Remote Sensing of Environment*, 108(3), 224–239. <http://doi.org/10.1016/j.rse.2006.11.014>
- Barizan, R., Sulaiman, R., & Sciences, M. (1997). Studies on the Early Establishment of Dipterocarp, (February).
- Basuki, T. M., van Laake, P. E., Skidmore, A. K., & Hussin, Y. A. (2009). Allometric equations for estimating the above-ground biomass in tropical lowland Dipterocarp forests. *Forest Ecology and Management*, 257(8), 1684–1694. <http://doi.org/10.1016/j.foreco.2009.01.027>
- Bautista, L. A. A. (2012). Biomass carbon estimation and mapping in the subtropical forest of Chitwan, Nepal : a comparison between VHR geo-eye satellite images and airborne LIDAR data, 57. Retrieved from [http://www.itc.nl/library/papers\\_2012/msc/nrm/lopezbautista.pdf](http://www.itc.nl/library/papers_2012/msc/nrm/lopezbautista.pdf)
- Benz, U. C., Hofmann, P., Willhauck, G., Lingenfelder, I., & Heynen, M. (2004). Multi-resolution, object-oriented fuzzy analysis of remote sensing data for GIS-ready information. *ISPRS Journal of Photogrammetry and Remote Sensing*, 58(3–4), 239–258. <http://doi.org/10.1016/j.isprsjprs.2003.10.002>
- Birdal, A. C., Avdan, U., & Trk, T. (2017). Estimating tree heights with images from an unmanned aerial vehicle. *Geomatics, Natural Hazards and Risk*, 5705(January 2018), 1–13.  
<http://doi.org/10.1080/19475705.2017.1300608>
- Blaschke, T. (2010). Object based image analysis for remote sensing. *ISPRS Journal of Photogrammetry and Remote Sensing*, 65(1), 2–16. <http://doi.org/10.1016/j.isprsjprs.2009.06.004>
- Blaschke, T., Burnett, C., & Pekkarinen, A. (2004). Image segmentation methods for object-based analysis and classification. In *Remote Sensing Image Analysis: Including the Spatial Domain*, 211–236(December), 359. <http://doi.org/10.1007/978-1-4020-2560-0>

**TOWARDS A UAV BASED STANDALONE SYSTEM FOR ESTIMATING AND MAPPING  
ABOVEGROUND BIOMASS/ CARBON STOCK IN BERKELAH TROPICAL RAIN FOREST,  
MALAYSIA**

- Bragg, D. C. (2001). A Local Basal Area Adjustment for Crown Width Prediction. *Northern Journal of Applied Forestry*, 18(1), 22–28(7). Retrieved from <http://www.ingentaconnect.com/content/saf/njaf/2001/00000018/00000001/art00004>
- Brovkina, O., Novotny, J., Cienciala, E., Zemek, F., & Russ, R. (2017). Mapping forest aboveground biomass using airborne hyperspectral and LiDAR data in the mountainous conditions of Central Europe. *Ecological Engineering*, 100, 219–230. <http://doi.org/10.1016/j.ecoleng.2016.12.004>
- Brown, S. (2002). Measuring carbon in forests: Current status and future challenges. *Environmental Pollution*, 116(3), 363–372. [http://doi.org/10.1016/S0269-7491\(01\)00212-3](http://doi.org/10.1016/S0269-7491(01)00212-3)
- Brown, S., Pearson, T., Slaymaker, D., Ambagis, S., Moore, N., Novelo, D., & Sabido, W. (2005). Creating a virtual tropical forest from three-dimensional aerial imagery to estimate carbon stocks. *Ecological Applications*, 15(3), 1083–1095. <http://doi.org/10.1890/04-0829>
- Bujotzek, A. (2007). Allometric Scaling Laws In Nature pt. 1, (July).
- Burrows, W. H., Henry, B. K., Back, P. V., Hoffmann, M. B., Tait, L. J., Anderson, E. R., ... McKeon, G. M. (2002). Growth and carbon stock change in eucalypt woodlands in northeast Australia: Ecological and greenhouse sink implications. *Global Change Biology*, 8(8), 769–784. <http://doi.org/10.1046/j.1365-2486.2002.00515.x>
- Calders, K., Verbesselt, J., Bartholomeus, H. M., Herold, M., & Others. (2011). Applying terrestrial LiDAR to derive gap fraction distribution time series during bud break. *Proceedings SilviLaser 2011, 11th International LiDAR Forest Applications Conference, 16--20 Oct. 2011, Tasmania Hobart, Tasmania*, (May 2016), 1–9.
- Cam, L. Le, & Cam, L. Le. (2017). Maximum Likelihood : An Introduction Maximum Likelihood : An Introduction, 58(2), 153–171.
- Carleer, A. P., Debeir, O., & Wolff, E. (2005). Assessment of very high spatial resolution satellite image segmentations. *Photogrammetric Engineering and Remote Sensing*, 71(11), 1285–1294. <http://doi.org/10.1117/12.511027>
- Chave, J., Réjou-Méchain, M., Búrquez, A., Chidumayo, E., Colgan, M. S., Delitti, W. B. C., ... Vieilledent, G. (2014). Improved allometric models to estimate the aboveground biomass of tropical trees. *Global Change Biology*, 20(10), 3177–3190. <http://doi.org/10.1111/gcb.12629>
- Chubey, M. S., Franklin, S. E., & Wulder, M. a. (2006). Object-based analysis of Ikonos-2 imagery for extraction of forest inventory parameters. *Photogrammetric Engineering and Remote Sensing*, 72(4), 383–394. <http://doi.org/10.14358/PERS.72.4.383>
- Clark, D. A., Brown, S., Kicklighter, D. W., Chambers, J. Q., Thomlinson, J. R., Ni, J., & Holland, E. A. (2001). Net primary production in tropical forests: An evaluation and synthesis of existing field data. *Ecological Applications*, 11(2), 371–384. [http://doi.org/10.1890/1051-0761\(2001\)011\[0371:NPPITF\]2.0.CO;2](http://doi.org/10.1890/1051-0761(2001)011[0371:NPPITF]2.0.CO;2)
- Clinton, N., Holt, A., Scarborough, J., Yan, L., & Gong, P. (2010). Accuracy Assessment Measures for Object-based Image Segmentation Goodness. *Photogrammetric Engineering and Remote Sensing*, 76(3), 289–299. <http://doi.org/10.14358/PERS.76.3.289>
- Colomina, I., Blázquez, M., Molina, P., Parés, M. E., & Wis, M. (2008). Towards A New Paradigm for High-Resolution Low-Cost Photogrammetry and Remote Sensing. *XXIst ISPRS Congress: Technical*

**TOWARDS A UAV BASED STANDALONE SYSTEM FOR ESTIMATING AND MAPPING  
ABOVEGROUND BIOMASS/ CARBON STOCK IN BERKELAH TROPICAL RAIN FOREST,  
MALAYSIA**

- Commission I, XXXVII Par*, 1201. Retrieved from  
[http://www.isprs.org/proceedings/XXXVII/congress/1\\_pdf/205.pdf](http://www.isprs.org/proceedings/XXXVII/congress/1_pdf/205.pdf)
- Colomina, I., & Molina, P. (2014). Unmanned aerial systems for photogrammetry and remote sensing: A review. *ISPRS Journal of Photogrammetry and Remote Sensing*, 92, 79–97.  
<http://doi.org/10.1016/j.isprsjprs.2014.02.013>
- Coops, N. C., Hilker, T., Wulder, M. A., St-Onge, B., Newnham, G., Siggins, A., & Trofymow, J. A. (2007). Estimating canopy structure of Douglas-fir forest stands from discrete-return LiDAR. *Trees - Structure and Function*, 21(3), 295–310. <http://doi.org/10.1007/s00468-006-0119-6>
- Culvenor, D. S. (2002). TIDA: An algorithm for the delineation of tree crowns in high spatial resolution remotely sensed imagery. *Computers and Geosciences*, 28(1), 33–44. [http://doi.org/10.1016/S0098-3004\(00\)00110-2](http://doi.org/10.1016/S0098-3004(00)00110-2)
- Dandois, J. P., & Ellis, E. C. (2013). High spatial resolution three-dimensional mapping of vegetation spectral dynamics using computer vision. *Remote Sensing of Environment*, 136, 259–276.  
<http://doi.org/10.1016/j.rse.2013.04.005>
- Derivaux, S., Forestier, G., Wemmert, C., & Lefvre, S. (2010). Supervised image segmentation using watershed transform, fuzzy classification and evolutionary computation. *Pattern Recognition Letters*, 31(15), 2364–2374. <http://doi.org/10.1016/j.patrec.2010.07.007>
- Dirocco, T. L. (2012). A Thorough Quantification of Tropical Forest Carbon Stocks in Malaysia. *Carbon Stocks of Tropical Forests*, 1–18.
- Doane, D. P., & Seward, L. E. (2011). Measuring Skewness: A Forgotten Statistic? *Journal of Statistics Education*, 19(2), 1–18. <http://doi.org/10.1.1.362.5312>
- Dowman, I. J. (2004). Integration of LIDAR and IFSAR for Mapping. *International Archives of Photogrammetry and Remote Sensing*, 35(September), 90–100. Retrieved from  
<http://discovery.ucl.ac.uk/55564/>
- Drăguț, L., Tiede, D., & Levick, S. R. (2010). ESP: A tool to estimate scale parameter for multiresolution image segmentation of remotely sensed data. *International Journal of Geographical Information Science*, 24(6), 859–871. <http://doi.org/10.1080/13658810903174803>
- Drake, J. B., Dubayah, R. O., Clark, D. B., Knox, R. G., Blair, J. B., Hofton, M. A., ... Prince, S. (2002). Estimation of tropical forest structural characteristics, using large-footprint lidar. *Remote Sensing of Environment*, 79(2–3), 305–319. [http://doi.org/10.1016/S0034-4257\(01\)00281-4](http://doi.org/10.1016/S0034-4257(01)00281-4)
- Drake, J. B., Dubayah, R. O., Knox, R. G., Clark, D. B., & Blair, J. B. (2002). Sensitivity of large-footprint lidar to canopy structure and biomass in a neotropical rainforest. *Remote Sensing of Environment*, 81(2–3), 378–392. [http://doi.org/10.1016/S0034-4257\(02\)00013-5](http://doi.org/10.1016/S0034-4257(02)00013-5)
- Drake, J. B., Knox, R. G., Dubayah, R. O., Clark, D. B., Condit, R., Blair, J. B., & Hofton, M. (2003). Above-ground biomass estimation in closed canopy Neotropical forests using lidar remote sensing: Factors affecting the generality of relationships. *Global Ecology and Biogeography*, 12(2), 147–159.  
<http://doi.org/10.1046/j.1466-822X.2003.00010.x>
- Dubravac, T., Dekanić, S., & Novotny, V. (2013). Natural Regeneration of Beech Forests in the Strict Protected Area of the Plitvice Lakes National Park. *South-East European Forestry*, 4(2), 95–103.



**TOWARDS A UAV BASED STANDALONE SYSTEM FOR ESTIMATING AND MAPPING  
ABOVEGROUND BIOMASS/ CARBON STOCK IN BERKELAH TROPICAL RAIN FOREST,  
MALAYSIA**

- Ediriweera, S., Pathirana, S., Danaher, T., & Nichols, D. (2014). Estimating above-ground biomass by fusion of LiDAR and multispectral data in subtropical woody plant communities in topographically complex terrain in North-eastern Australia. *Journal of Forestry Research*, 25(4), 761–771. <http://doi.org/10.1007/s11676-014-0485-7>
- Ene, L. T., Næsset, E., Gobakken, T., Mauya, E. W., Bollandsås, O. M., Gregoire, T. G., ... Zahabu, E. (2016). Large-scale estimation of aboveground biomass in miombo woodlands using airborne laser scanning and national forest inventory data. *Remote Sensing of Environment*, 186, 626–636. <http://doi.org/10.1016/j.rse.2016.09.006>
- Erikson, M. (2004). Species classification of individually segmented tree crowns in high-resolution aerial images using radiometric and morphologic image measures. *Remote Sensing of Environment*, 91(3–4), 469–477. <http://doi.org/10.1016/j.rse.2004.04.006>
- Evans, J. S., Hudak, A. T., Faux, R., & Smith, A. M. S. (2009). Discrete return lidar in natural resources: Recommendations for project planning, data processing, and deliverables. *Remote Sensing*, 1(4), 776–794. <http://doi.org/10.3390/rs1040776>
- Fritz, a., Kattenborn, T., & Koch, B. (2013). UAV-Based Photogrammetric Point Clouds – Tree Stem Mapping in Open Stands in Comparison to Terrestrial Laser Scanner Point Clouds. *ISPRS - International Archives of the Photogrammetry, Remote Sensing and Spatial Information Sciences*, XL-1/W2(September), 141–146. <http://doi.org/10.5194/isprsarchives-XL-1-W2-141-2013>
- Gartner, G., Meng, L., & Peterson, M. P. (2010). *Lecture Notes in Geoinformation and Cartography. Technology*. <http://doi.org/10.1007/978-3-540-88183-4>
- Getzin, S., Wiegand, K., & Schöning, I. (2012). Assessing biodiversity in forests using very high-resolution images and unmanned aerial vehicles. *Methods in Ecology and Evolution*, 3(2), 397–404. <http://doi.org/10.1111/j.2041-210X.2011.00158.x>
- Gibbs, H. K., Brown, S., Niles, J. O., & Foley, J. A. (2007). Monitoring and estimating tropical forest carbon stocks: making REDD a reality. *Environmental Research Letters*, 2(4), 45023. <http://doi.org/10.1088/1748-9326/2/4/045023>
- Goetz, S. J., Hansen, M., Houghton, R. A., Olander, L. P., Gibbs, H. K., Steininger, M., ... Federici, S. (2012). and methods Reporting carbon losses from tropical deforestation with Pan-tropical biomass maps.
- Graham, V., Laurance, S. G., Grech, A., & Venter, O. (2017). Spatially explicit estimates of forest carbon emissions, mitigation costs and REDD+ opportunities in Indonesia. *Environmental Research Letters*, 12(4), 44017. <http://doi.org/10.1088/1748-9326/aa6656>
- Grenzdörffer, G. J., Engel, A., & Teichert, B. (2008). The Photogrammetric Potential of Low-Cost UAVs in Forestry and Agriculture. *The International Archives of the Photogrammetry, Remote Sensing and Spatial Information Sciences*, Vol. XXXVII, 31(B3), 1207–2014. <http://doi.org/10.2747/1548-1603.41.4.287>
- Gschwantner, T., Schadauer, K., Vidal, C., Lanz, A., Tomppo, E., Di Cosmo, L., ... Lawrence, M. (2009). Common tree definitions for national forest inventories in Europe. *Silva Fennica*, 43(2), 303–321. <http://doi.org/10.14214/sf.463>
- Harding, D. J., & Carabajal, C. C. (2005). ICESat waveform measurements of within-footprint topographic relief and vegetation vertical structure. *Geophysical Research Letters*, 32(21), 1–4.

**TOWARDS A UAV BASED STANDALONE SYSTEM FOR ESTIMATING AND MAPPING  
ABOVEGROUND BIOMASS/ CARBON STOCK IN BERKELAH TROPICAL RAIN FOREST,  
MALAYSIA**

<http://doi.org/10.1029/2005GL023471>

- Harding, D. J., Lefsky, M. A., Parker, G. G., & Blair, J. B. (2001). Laser altimeter canopy height profiles methods and validation for closed-canopy, broadleaf forests. *Remote Sensing of Environment*, 76(3), 283–297. [http://doi.org/10.1016/S0034-4257\(00\)00210-8](http://doi.org/10.1016/S0034-4257(00)00210-8)
- Hay, G. J., Castilla, G., Wulder, M. A., & Ruiz, J. R. (2005). An automated object-based approach for the multiscale image segmentation of forest scenes. *International Journal of Applied Earth Observation and Geoinformation*, 7(4), 339–359. <http://doi.org/10.1016/j.jag.2005.06.005>
- Hemery, G. E., Savill, P. S., & Pryor, S. N. (2005). Applications of the crown diameter-stem diameter relationship for different species of broadleaved trees. *Forest Ecology and Management*, 215(1–3), 285–294. <http://doi.org/10.1016/j.foreco.2005.05.016>
- Hirata, Y., Tsubota, Y., & Sakai, A. (2009). Allometric models of DBH and crown area derived from QuickBird panchromatic data in *Cryptomeria japonica* and *Chamaecyparis obtusa* stands. *International Journal of Remote Sensing*, 30(19), 5071–5088. <http://doi.org/10.1080/01431160903022977>
- Hopkinson, C., Chasmer, L., Young-Pow, C., & Treitz, P. (2004). Assessing forest metrics with a ground-based scanning lidar. *Canadian Journal of Forest Research*, 34(3), 573–583. <http://doi.org/10.1139/x03-225>
- Horcher, A., & Visser, R. J. M. (2004). Unmanned Aerial Vehicles: Applications for Natural Resource Management and Monitoring. *Machines and People, The Interface*, 5.
- Houghton, R. A., & Hackler, J. L. (2000). Changes in terrestrial carbon storage in the United States. 1: The roles of agriculture and forestry. *Global Ecology and Biogeography*, 9(2), 125–144. <http://doi.org/10.1046/j.1365-2699.2000.00166.x>
- Iizuka, K., Yonehara, T., Itoh, M., & Kosugi, Y. (2017). Estimating Tree Height and Diameter at Breast Height (DBH) from Digital Surface Models and Orthophotos Obtained with an Unmanned Aerial System for a Japanese Cypress (*Chamaecyparis obtusa*) Forest. *Remote Sensing*, 10(1), 13. <http://doi.org/10.3390/rs10010013>
- IPCC. (2007). IPCC, 2007: Summary for Policymakers. In: *Climate Change 2007: The Physical Science Basis. Contribution of Working Group I to the Fourth Assessment Report of the Intergovernmental Panel on Climate Change* [Solomon, S., D. Qin, M. Manning, Z. Chen, M. Marqu. *New York Cambridge University Press*, 996. <http://doi.org/10.1038/446727a>
- Jensen, J. L. R., & Mathews, A. J. (2016). Assessment of image-based point cloud products to generate a bare earth surface and estimate canopy heights in a woodland ecosystem. *Remote Sensing*, 8(1). <http://doi.org/10.3390/rs8010050>
- JungleBoy. (2013). Gunung Pulai in Johor - Rainforest Journal. Retrieved July 5, 2017, from <https://www.rainforestjournal.com/gunung-pulai-in-johor/>
- Kankare, V., Holopainen, M., Vastaranta, M., Puttonen, E., Yu, X., Hyyppä, J., ... Alho, P. (2013). Individual tree biomass estimation using terrestrial laser scanning. *ISPRS Journal of Photogrammetry and Remote Sensing*, 75, 64–75. <http://doi.org/10.1016/j.isprsjprs.2012.10.003>
- Karna, Y. K., Hussin, Y. A., Gilani, H., Bronsveld, M. C., Murthy, M. S. R., Qamer, F. M., ... Baniya, C. B. (2015). Integration of WorldView-2 and airborne LiDAR data for tree species level carbon stock mapping in Kayar Khola watershed, Nepal. *International Journal of Applied Earth Observation and*

**TOWARDS A UAV BASED STANDALONE SYSTEM FOR ESTIMATING AND MAPPING  
ABOVEGROUND BIOMASS/ CARBON STOCK IN BERKELAH TROPICAL RAIN FOREST,  
MALAYSIA**

*Geoinformation*, 38, 280–291. <http://doi.org/10.1016/j.jag.2015.01.011>

- Ketterings, Q. M., Coe, R., Van Noordwijk, M., Ambagau, Y., & Palm, C. A. (2001). Reducing uncertain in the use of allometric biomass equation for predciting above-ground tree biomass in mixed secondary forests. *Forest Ecology and Management*, 146, 199–209. <http://doi.org/Reducing uncertain in the use of allometric biomass equation for predciting above-ground tree biomass in mixed secondary forests>
- Kim, M., Madden, M., & Warner, T. A. (2009). Forest T ype Mapping using Object-specific Texture Measur es fr om Multispectral Ikonos Imagery : Segmentation Quality and Image Classification Issues, 75(7), 819–829.
- Köhl, M., Baldauf, T., Plugge, D., & Krug, J. (2009). Reduced emissions from deforestation and forest degradation (REDD): a climate change mitigation strategy on a critical track. *Carbon Balance and Management*, 4, 10. <http://doi.org/10.1186/1750-0680-4-10>
- Kuuluvainen, T. (1991). Relationships between crown projected area and components of above-ground biomass in Norway spruce trees in even-aged stands: Empirical results and their interpretation. *Forest Ecology and Management*, 40(3–4), 243–260. [http://doi.org/10.1016/0378-1127\(91\)90043-U](http://doi.org/10.1016/0378-1127(91)90043-U)
- Kwak, D.-A. A., Lee, W.-K. K., Lee, J.-H. H., Biging, G. S., & Gong, P. (2007). Detection of individual trees and estimation of tree height using LiDAR data. *Journal of Forest Research*, 12(6), 425–434. <http://doi.org/10.1007/s10310-007-0041-9>
- Laumonier, Y., Edin, A., Kanninen, M., & Munandar, A. W. (2010). Landscape-scale variation in the structure and biomass of the hill dipterocarp forest of Sumatra: Implications for carbon stock assessments. *Forest Ecology and Management*, 259(3), 505–513. <http://doi.org/10.1016/j.foreco.2009.11.007>
- Lawas, C. J. C. (2016). Complementary use of Airborne Lidar and Terrestrial Laser Scanner to Assess Above Ground Biomass / Carbon in Ayer Hitam tropical rain forest reserve. Retrieved from [http://www.itc.nl/library/papers\\_2016/msc/nrm/lawas.pdf](http://www.itc.nl/library/papers_2016/msc/nrm/lawas.pdf)
- Leberl, F., Irschara, A., Pock, T., Meixner, P., Gruber, M., Scholz, S., & Wiechert, A. (2010). Point Clouds : Lidar versus 3D Vision, 76(10), 1123–1134.
- Lefsky, M. A., Cohen, W. B., Parker, G. G., & Harding, D. J. D. (2002). Lidar Remote Sensing for Ecosystem Studies. *BioScience*, 52(1), 19–30. [http://doi.org/10.1641/0006-3568\(2002\)052\[0019:LRSFES\]2.0.CO;2](http://doi.org/10.1641/0006-3568(2002)052[0019:LRSFES]2.0.CO;2)
- Lefsky, M. A., Turner, D. P., Guzy, M., & Cohen, W. B. (2005). Combining lidar estimates of aboveground biomass and Landsat estimates of stand age for spatially extensive validation of modeled forest productivity. *Remote Sensing of Environment*, 95(4), 549–558. <http://doi.org/10.1016/j.rse.2004.12.022>
- Liang, X., Hyyppe, J., Kukko, A., Kaartinen, H., Jaakkola, A., & Yu, X. (2014). The Use of a Mobile Laser Scanning System for Mapping Large Forest Plots. *IEEE Geoscience and Remote Sensing Letters*, 11(9), 1504–1508. <http://doi.org/10.1109/LGRS.2013.2297418>
- Lim, K. S., & Treitz, P. M. (2004). Estimation of above ground forest biomass from airborne discrete return laser scanner data using canopy-based quantile estimators. *Scandinavian Journal of Forest Research*, 19(6), 558–570. <http://doi.org/10.1080/02827580410019490>
- Lisein, J., Pierrot-Deseilligny, M., Bonnet, S., & Lejeune, P. (2013). A photogrammetric workflow for the creation of a forest canopy height model from small unmanned aerial system imagery. *Forests*, 4(4), 922–944. <http://doi.org/10.3390/f4040922>

**TOWARDS A UAV BASED STANDALONE SYSTEM FOR ESTIMATING AND MAPPING  
ABOVEGROUND BIOMASS/ CARBON STOCK IN BERKELAH TROPICAL RAIN FOREST,  
MALAYSIA**

- Lovell, J. L., Jupp, D. L. B., Culvenor, D. S., & Coops, N. C. (2003). Using airborne and ground-based ranging lidar to measure canopy structure in Australian forests. *Canadian Journal of Remote Sensing*, 29(5), 607–622. <http://doi.org/10.5589/m03-026>
- Lu, D. (2005). Aboveground biomass estimation using Landsat TM data in the Brazilian Amazon. *International Journal of Remote Sensing*, 26(12), 2509–2525. <http://doi.org/10.1080/01431160500142145>
- Lu, D. (2006). The potential and challenge of remote sensing-based biomass estimation. *International Journal of Remote Sensing*, 27(7), 1297–1328. <http://doi.org/10.1080/01431160500486732>
- Luo, S., Wang, C., Xi, X., Pan, F., Peng, D., & Zou, J. (2017). Fusion of airborne LiDAR data and hyperspectral imagery for aboveground and belowground forest biomass estimation. *Ecological Indicators*, 73, 378–387. <http://doi.org/10.1016/j.ecolind.2016.10.001>
- Magar, A. T. (2014). Estimation and mapping of forest biomass and carbon using point-clouds derived from airborne LiDAR and from 3D photogrammetric matching of aerial images. The University of Twente, Faculty of Geo-information and Earth Observation Science (ITC) MSc thesis. Ret, 79. Retrieved from [http://www.itc.nl/library/papers\\_2014/msc/gem/thapamagar.pdf](http://www.itc.nl/library/papers_2014/msc/gem/thapamagar.pdf)
- Magnussen, S., & Boudewyn, P. (1998). Derivations of stand heights from airborne laser scanner data with canopy-based quantile estimators. *Canadian Journal of Forest Research*, 28(7), 1016–1031. <http://doi.org/10.1139/x98-078>
- Malinowski, R. A., Nutto, L., Wiese, W. S., & Brunsmeier, M. (2016). Non-destructive analysis of the root system and tree growth parameters. *Revista Árvore. Sociedade de Investigações Florestais.*, 40, 289–295.
- Matese, A., Toscano, P., Di Gennaro, S. F., Genesio, L., Vaccari, F. P., Primicerio, J., ... Gioli, B. (2015). Intercomparison of UAV, aircraft and satellite remote sensing platforms for precision viticulture. *Remote Sensing*, 7(3), 2971–2990. <http://doi.org/10.3390/rs70302971>
- Mayr, W. (2011). Unmanned Aerial Systems in Use for Mapping at Blom. *53rd Photogrammetric Week, Institute for Photogrammetry*, 125–134.
- Messinger, M., Asner, G. P., & Silman, M. (2016a). Rapid assessments of amazon forest structure and biomass using small unmanned aerial systems. *Remote Sensing*, 8(8), 1–15. <http://doi.org/10.3390/rs8080615>
- Messinger, M., Asner, G. P., & Silman, M. (2016b). Rapid Assessments of Amazon Forest Structure and Biomass Using Small Unmanned Aerial Systems. *Remote Sensing Article*, 1–15. <http://doi.org/10.3390/rs8080615>
- Mohren, G. M. J., Hasenauer, H., Köhl, M., & Nabuurs, G. J. (2012). Forest inventories for carbon change assessments. *Current Opinion in Environmental Sustainability*, 4(6), 686–695. <http://doi.org/10.1016/j.cosust.2012.10.002>
- Naesset, E. (1997). Determination of mean tree height of forest stands using airborne laser scanner data. *ISPRS Journal of Photogrammetry and Remote Sensing*, 52(2), 49–56. [http://doi.org/10.1016/S0924-2716\(97\)83000-6](http://doi.org/10.1016/S0924-2716(97)83000-6)
- Naesset, E., Bollandsas, O. M., & Gobakken, T. (2005). Comparing regression methods in estimation of biophysical properties of forest stands from two different inventories using laser scanner data. *Remote Sensing of Environment*, 94(4), 541–553. <http://doi.org/10.1016/j.rse.2004.11.010>
- Næsset, E., & Økland, T. (2002). Estimating tree height and tree crown properties using airborne scanning laser

**TOWARDS A UAV BASED STANDALONE SYSTEM FOR ESTIMATING AND MAPPING  
ABOVEGROUND BIOMASS/ CARBON STOCK IN BERKELAH TROPICAL RAIN FOREST,  
MALAYSIA**

in a boreal nature reserve. *Remote Sensing of Environment*, 79(1), 105–115. [http://doi.org/10.1016/S0034-4257\(01\)00243-7](http://doi.org/10.1016/S0034-4257(01)00243-7)

- Nelson, R., Margolis, H., Montesano, P., Sun, G., Cook, B., Corp, L., ... Prisley, S. (2017). Lidar-based estimates of aboveground biomass in the continental US and Mexico using ground, airborne, and satellite observations. *Remote Sensing of Environment*, 188, 127–140. <http://doi.org/10.1016/j.rse.2016.10.038>
- Nilsson, M. (1996). Estimation of tree heights and stand volume using an airborne lidar system. *Remote Sensing of Environment*, 56(1), 1–7. [http://doi.org/10.1016/0034-4257\(95\)00224-3](http://doi.org/10.1016/0034-4257(95)00224-3)
- Nonami, K. (2007). Prospect and Recent Research & Development for Civil Use Autonomous Unmanned Aircraft as UAV and MAV. *Journal of System Design and Dynamics*, 1(2), 120–128. <http://doi.org/10.1299/jsdd.1.120>
- Nonami, K., Kendoul, F., Suzuki, S., Wang, W., & Nakazawa, D. (2010). Autonomous flying robots: Unmanned aerial vehicles and micro aerial vehicles. *Autonomous Flying Robots: Unmanned Aerial Vehicles and Micro Aerial Vehicles*, 1–329. <http://doi.org/10.1007/978-4-431-53856-1>
- Okojie, J. (2017). Assessment of Forest Tree Structural Parameter Extractability From Optical Imaging Uav Datasets , in Ahaus. Germany. The University of Twente, Faculty of Geo-information and Earth Observation Science(ITC) MSc thesis. R.
- Pan, Y., Birdsey, R. A., Fang, J., Houghton, R., Kauppi, P. E., Kurz, W. A., ... Hayes, D. (2011). A Large and Persistent Carbon Sink in the World's Forests. *Science*, 333(6045). Retrieved from <http://science.sciencemag.org/content/333/6045/988/tab-pdf>
- Pasgaard, M., Sun, Z., Møller, D., & Mertz, O. (2016). Challenges and opportunities for REDD+: A reality check from perspectives of effectiveness, efficiency and equity. *Environmental Science and Policy*, 63, 161–169. <http://doi.org/10.1016/j.envsci.2016.05.021>
- Patenaude, G., Milne, R., & Dawson, T. P. (2005). Synthesis of remote sensing approaches for forest carbon estimation: reporting to the Kyoto Protocol. *Environmental Science and Policy*, 8(2), 161–178. <http://doi.org/10.1016/j.envsci.2004.12.010>
- Paustian, K., Six, J., Elliott, E., & Hunt, H. (2000). Management options for reducing CO<sub>2</sub> emissions from agricultural soils. *Biogeochemistry*, 48, 147–163. <http://doi.org/10.1007/s10584-005-5951-y>
- Peltoniemi, M., Palosuo, T., Monni, S., & Mäkipää, R. (2006). Factors affecting the uncertainty of sinks and stocks of carbon in Finnish forests soils and vegetation. *Forest Ecology and Management*, 232(1–3), 75–85. <http://doi.org/10.1016/j.foreco.2006.05.045>
- Pfeifer, N., Gorte, B., & Winterhalder, D. (2004). Automatic reconstruction of single trees from terrestrial laser scanner data. *ISPRS XX ISPRS Congress, Commission , I–VII, XXXV-A*.
- Phua, M.-H., Su Wah, H., Ioki, K., Hashim, M., Bidin, K., Musta, B., ... Maycock, C. R. (2016). Estimating Logged-Over Lowland Rainforest Aboveground Biomass in Sabah , Malaysia Using Airborne LiDAR Data. *Terrestrial Atmospheric and Oceanic Sciences*, 27(September), 481–489. [http://doi.org/10.3319/TAO.2016.01.06.02\(ISRS\)1](http://doi.org/10.3319/TAO.2016.01.06.02(ISRS)1).
- Pollock, R. (1996). The automatic recognition of individual trees in aerial images of forests based on a synthetic tree crown image model. <http://doi.org/10.14288/1.0051597>
- Popescu, S. C., Wynne, R. H., & Nelson, R. F. (2003). Measuring individual tree crown diameter with lidar and

**TOWARDS A UAV BASED STANDALONE SYSTEM FOR ESTIMATING AND MAPPING  
ABOVEGROUND BIOMASS/ CARBON STOCK IN BERKELAH TROPICAL RAIN FOREST,  
MALAYSIA**

- assessing its influence on estimating forest volume and biomass. *Canadian Journal of Remote Sensing*, 29(5), 564–577. <http://doi.org/10.5589/m03-027>
- Pouliot, D. A., King, D. J., & Pitt, D. G. (2005). Development and evaluation of an automated tree detection–delineation algorithm for monitoring regenerating coniferous forests. *Canadian Journal of Forest Research*, 35(10), 2332–2345. <http://doi.org/10.1139/x05-145>
- Ravindranath, N. H., & Ostwald, M. (2008). Carbon Pools and Measurement Frequency. *Carbon Inventory Methods: Handbook for Greenhouse Gas Inventory, Carbon Mitigation and Roundwood Production Projects.*, 31–44.
- Remondino, F., Barazzetti, L., Nex, F., Scaioni, M., & Sarazzi, D. (2011). UAV photogrammetry for mapping and 3d modeling–current status and future perspectives. *The International Archives of the Photogrammetry, Remote Sensing and Spatial Information Sciences*, 38–1/C22, 25–31. <http://doi.org/10.5194/isprsarchives-XXXVIII-1-C22-25-2011>
- Reuben, J. (2017). The Accuracy of Tree Height Drieved from Point Clouds of UAV Compared to Airborne LiDAR and its Effect on Estimating Biomass and Carbon Stock in Part of Tropical Forest in Malaysia. University of Twente Faculty of Geo-Information and Earth Observation (IT. Retrieved from <http://stacks.iop.org/1748-9326/12/i=4/a=044017?key=crossref.969b6ca7c50dd7aa01dc8119235e7322>
- Riggan & Weih. (2009). Riggan, N. D. Jr. and Weih, Robert C. Jr. (2009) “Comparison of Pixel-based versus Object-based Land Use/Land Cover Classification Methodologies,” *Journal of the Arkansas Academy of Science*: Vol. 63 , Article 18. Available at: <http://scholarworks.uark.edu/j>, 63.
- Saatchi, S. S., Harris, N. L., Brown, S., Lefsky, M., Mitchard, E. T. A., Salas, W., ... Morel, A. (2011). Benchmark map of forest carbon stocks in tropical regions across three continents. *Proceedings of the National Academy of Sciences*, 108(24), 9899–9904. <http://doi.org/10.1073/pnas.1019576108>
- Sampaio, E., Gasson, P., Baracat, A., Cutler, D., Pareyn, F., & Lima, K. C. (2010). Tree biomass estimation in regenerating areas of tropical dry vegetation in northeast Brazil. *Forest Ecology and Management*, 259(6), 1135–1140. <http://doi.org/10.1016/j.foreco.2009.12.028>
- Shah, S. K., Hussin, Y. A., van Leeuwen, L. M., & Al.], ... [et. (2011). Modelling the relationship between tree canopy projection area and above ground carbon stock using high resolution geoeeye satellite images. *ACRS 2011 : Proceedings of the 32nd Asian Conference on Remote Sensing : Sensing for Green Asia*, 3-7 October 2011, Taipei, Taiwan, 6.
- Sherali, H. D., Narayanan, A., & Sivanandan, R. (2003). Estimation of origin-destination trip-tables based on a partial set of traffic link volumes. *Transportation Research Part B: Methodological*, 37(9), 815–836. [http://doi.org/10.1016/S0191-2615\(02\)00073-5](http://doi.org/10.1016/S0191-2615(02)00073-5)
- Shimano, K. (1997). Analysis of the Relationship between DBH and Crown Projection Area Using a New Model. *Journal of Forest Research*, 2(4), 237–242. <http://doi.org/10.1007/BF02348322>
- Shimano, K. (2000). A power function for forest structure and regeneration pattern of pioneer and climax species in patch mosaic forests. *Plant Ecology*, 146(2), 207–220. <http://doi.org/10.1023/a:1009867302660>
- Sium, M. T. (2015). Estimating Carbon Stock Using Very High Resolution Imagery and Terrestrial Laser Scanning in Tropical Rain Forest of Royal Belum, Malaysia February, 2015. The University of Twente, Faculty of Geo-information and Earth Observation Science(ITC) MSc thesis. R.

**TOWARDS A UAV BASED STANDALONE SYSTEM FOR ESTIMATING AND MAPPING  
ABOVEGROUND BIOMASS/ CARBON STOCK IN BERKELAH TROPICAL RAIN FOREST,  
MALAYSIA**

- Smith. (2015). Search | Britannica.com. Retrieved December 22, 2017, from [https://www.britannica.com/search?query=Smith%2C 2015 tropical rainforest](https://www.britannica.com/search?query=Smith%2C%202015%20tropical%20rainforest)
- Soares-Filho, B., Moutinho, P., Nepstad, D., Anderson, A., Rodrigues, H., Garcia, R., ... Maretti, C. (2010). Role of Brazilian Amazon protected areas in climate change mitigation. *Proceedings of the National Academy of Sciences*, 107(24), 10821–10826. <http://doi.org/10.1073/pnas.0913048107>
- Song, C., Dickinson, M. B., Su, L., Zhang, S., & Yaussey, D. (2010). Estimating average tree crown size using spatial information from Ikonos and QuickBird images: Across-sensor and across-site comparisons. *Remote Sensing of Environment*, 114(5), 1099–1107. <http://doi.org/10.1016/j.rse.2009.12.022>
- Sumerling, G. (2011). Lidar Analysis in ArcGIS ® 10 for Forestry Applications. *ESRI White Paper*, (January), 53. Retrieved from <http://www.esri.com/library/whitepapers/pdfs/lidar-analysis-forestry.pdf>
- Torres-Sánchez, J., López-Granados, F., Serrano, N., Arquero, O., & Peña, J. M. (2015). High-throughput 3-D monitoring of agricultural-tree plantations with Unmanned Aerial Vehicle (UAV) technology. *PLoS ONE*, 10(6), 1–20. <http://doi.org/10.1371/journal.pone.0130479>
- Torresan, C., Berton, A., Carotenuto, F., Di Gennaro, S. F., Gioli, B., Matese, A., ... Wallace, L. (2017). Forestry applications of UAVs in Europe: a review. *International Journal of Remote Sensing*, 38(8–10), 2427–2447. <http://doi.org/10.1080/01431161.2016.1252477>
- Turner, D., Lucieer, A., & Watson, C. (2012). An automated technique for generating georectified mosaics from ultra-high resolution Unmanned Aerial Vehicle (UAV) imagery, based on Structure from Motion (SFM) point clouds. *Remote Sensing*, 4(5), 1392–1410. <http://doi.org/10.3390/rs4051392>
- Wang, C. (2006). Biomass allometric equations for 10 co-occurring tree species in Chinese temperate forests. *Forest Ecology and Management*, 222(1–3), 9–16. <http://doi.org/10.1016/j.foreco.2005.10.074>
- Westoby, M. J., Brasington, J., Glasser, N. F., Hambrey, M. J., & Reynolds, J. M. (2012). “Structure-from-Motion” photogrammetry: A low-cost, effective tool for geoscience applications. *Geomorphology*, 179, 300–314. <http://doi.org/10.1016/j.geomorph.2012.08.021>
- Yao, T., Yang, X., Zhao, F., Wang, Z., Zhang, Q., Jupp, D., ... Strahler, A. (2011). Measuring forest structure and biomass in New England forest stands using Echidna ground-based lidar. *Remote Sensing of Environment*, 115(11), 2965–2974. <http://doi.org/10.1016/j.rse.2010.03.019>
- Yuen, J. Q., Fung, T., & Ziegler, A. D. (2016). Review of allometric equations for major land covers in SE Asia: Uncertainty and implications for above- and below-ground carbon estimates. *Forest Ecology and Management*, 360, 323–340. <http://doi.org/10.1016/j.foreco.2015.09.016>
- Zhang, J., Hu, J., Lian, J., Fan, Z., Ouyang, X., & Ye, W. (2016). Seeing the forest from drones: Testing the potential of lightweight drones as a tool for long-term forest monitoring. *Biological Conservation*, 198, 60–69. <http://doi.org/10.1016/j.biocon.2016.03.027>
- Zhang, L. &. (2009). Li, H., Zhang, X., 2009 Segmentation of forest terrain laser scanner data. *science*, 47-54. [doi.org/10.1145/1900179.1900188](http://doi.org/10.1145/1900179.1900188). *Image and Vision Computing*, 27(8), 1223–1227. <http://doi.org/10.1016/j.imavis.2008.09.008>



**TOWARDS A UAV BASED STANDALONE SYSTEM FOR ESTIMATING AND MAPPING  
ABOVEGROUND BIOMASS/ CARBON STOCK IN BERKELAH TROPICAL RAIN FOREST,  
MALAYSIA**

## APPENDICES

Appendix 1: Field data collection sheet form

COLLECTION SHEET (BERKELAH FOREST RESERVE MALAYSIA 2017)						
Recorder:		Plot Number:	plot radius:	Date:		
Plot center:	Latitude		Slope (%)			
	Longitude		Crown cover (%)			
Photograph number:			Photographer Name:			
Tree No.	Latitude	Longitude	Diameter /DBH(cm)	Species	Crown diameter(m)	Remark
1						
2						
3						
4						
5						
6						
7						
8						
9						
10						
11						
12						
13						
14						
15						
16						
17						
18						
19						
20						
21						
22						
23						
24						
25						
26						
27						
28						
29						
30						
31						
32						
33						
34						
35						

**TOWARDS A UAV BASED STANDALONE SYSTEM FOR ESTIMATING AND MAPPING  
ABOVEGROUND BIOMASS/ CARBON STOCK IN BERKELAH TROPICAL RAIN FOREST,  
MALAYSIA**

Appendix 2: Sample calculated adjusted CPA using intermediate circle

Outer circle Area m <sup>2</sup>	Inner circle Area m <sup>2</sup>	outer circle radius (R) (m)	Inner Circle radius (r) (m)	(R-r)/2	r+(R-r)/2	New CPA(m <sup>2</sup> )
7.90444000000	5.08283700000	1.586611981	1.272296309	0.157157836	1.429454145	6.416084942
9.94979000000	3.46682000000	1.780090708	1.050753445	0.364668632	1.415422077	6.290737718
8.48602000000	4.99500800000	1.643944689	1.261256072	0.191344308	1.45260038	6.625550297
19.55140000000	4.65088700000	2.495307698	1.217035005	0.639136347	1.856171352	10.81846835
15.16720000000	5.61989600000	2.197798551	1.337825024	0.429986763	1.767811788	9.812997744
24.91270000000	5.95392500000	2.816732307	1.377009244	0.719861532	2.096870776	13.80616254
15.92770000000	7.36172500000	2.252224661	1.531175499	0.360524581	1.89170008	11.23658166
33.82010000000	4.27996200000	3.281879413	1.167495277	1.057192068	2.224687345	15.54059408
17.00810000000	9.41075800000	2.327357376	1.731200938	0.298078219	2.029279157	12.93043804
19.09760000000	12.67515100000	2.46617887	2.009147156	0.228515857	2.237663013	15.72240628
50.72230000000	7.62886000000	4.019153981	1.55870884	1.230222571	2.788931411	24.42335462
42.84060000000	10.04622800000	3.693711302	1.78869664	0.952507331	2.741203971	23.59458552
18.13050000000	10.58819400000	2.402924174	1.836310515	0.28330683	2.119617344	14.10732193
21.05810000000	9.42580900000	2.58967204	1.732584774	0.428543633	2.161128407	14.66529461
27.29780000000	11.19721200000	2.948485523	1.888383193	0.530051165	2.418434358	18.36530969
87.33140000000	12.88157200000	5.273760307	2.025441054	1.624159626	3.64960068	41.8234973
51.77720000000	18.58384800000	4.060733202	2.432780905	0.813976149	3.246757053	33.10009448
64.06610000000	21.44525800000	4.516991981	2.613369473	0.951811254	3.565180727	39.91101275
64.36350000000	27.31360000000	4.527463963	2.949338693	0.789062635	3.738401328	43.8835237
85.19730000000	71.54188600000	5.20892485	4.773263048	0.217830901	4.991093949	78.22059905
10.60930000000	3.36595300000	1.83813981	1.035354796	0.401392507	1.436747303	6.481722434
13.16250000000	6.28663700000	2.047407869	1.414960669	0.3162236	1.731184269	9.410576773
14.31640000000	6.92805300000	2.135266507	1.485390961	0.324937773	1.810328734	10.29069099
14.07720000000	8.32943500000	2.117353233	1.628706943	0.244323145	1.873030088	11.01587897
21.89260000000	6.23199100000	2.640485865	1.40879754	0.615844163	2.024641703	12.87140644
20.20200000000	15.56096100000	2.536485356	2.226144664	0.155170346	2.38131501	17.80587609
19.32860000000	10.53663000000	2.481049192	1.831833685	0.324607754	2.156441439	14.60175259
20.89710000000	12.05824300000	2.579753358	1.959644043	0.310054657	2.269698701	16.17581108

**TOWARDS A UAV BASED STANDALONE SYSTEM FOR ESTIMATING AND MAPPING  
ABOVEGROUND BIOMASS/ CARBON STOCK IN BERKELAH TROPICAL RAIN FOREST,  
MALAYSIA**

Appendix 3: Correlation between CPA and DBH results

<b>Correlation result between segmented CPA and DBH</b>		
	CPA	DBH
CPA	Pearson Correlation	1
	Sig. (2-tailed)	.819**
	N	207
DBH	Pearson Correlation	.819**
	Sig. (2-tailed)	1
	N	207

\*\* . Correlation is significant at the 0.01 level (2-tailed).

<b>Correlation result between adjusted CPA and DBH</b>		
	CPA	DBH
CPA	Pearson Correlation	1
	Sig. (2-tailed)	.851**
	N	207
DBH	Pearson Correlation	.851**
	Sig. (2-tailed)	1
	N	207

\*\* . Correlation is significant at the 0.01 level (2-tailed).

<b>Correlation result between circularity measured CPA and DBH</b>		
	CPA	DBH
CPA	Pearson Correlation	1
	Sig. (2-tailed)	.923**
	N	55
DBH	Pearson Correlation	.923**
	Sig. (2-tailed)	1
	N	55

\*\* . Correlation is significant at the 0.01 level (2-tailed).

<b>Correlation result between actual CPA and DBH</b>		
	CPA	DBH
CPA	Pearson Correlation	1
	Sig. (2-tailed)	.914**
	N	55
DBH	Pearson Correlation	.914**
	Sig. (2-tailed)	1
	N	55

\*\* . Correlation is significant at the 0.01 level (2-tailed).



**TOWARDS A UAV BASED STANDALONE SYSTEM FOR ESTIMATING AND MAPPING ABOVEGROUND BIOMASS/ CARBON STOCK IN BERKELAH TROPICAL RAIN FOREST, MALAYSIA**

Appendix 4 : Field photos

